

**EVALUATING THE EFFECT OF NANOCLAY AND
NANOSILICA ON THE PROPERTIES OF WATER-BASED
DRILLING FLUID**

BY
Fahd Saeed Alakbari

A Thesis Presented to the
DEANSHIP OF GRADUATE STUDIES

KING FAHD UNIVERSITY OF PETROLEUM & MINERALS

DHAHRAN, SAUDI ARABIA

In Partial Fulfillment of the
Requirements for the Degree of

MASTER OF SCIENCE

In

PETROLEUM ENGINEERING

January, 2017

KING FAHD UNIVERSITY OF PETROLEUM & MINERALS

DHAHRAN- 31261, SAUDI ARABIA

DEANSHIP OF GRADUATE STUDIES

This thesis, written by **Fahd Saeed Alakbari** under the direction his thesis advisor and approved by his thesis committee, has been presented and accepted by the Dean of Graduate Studies, in partial fulfillment of the requirements for the degree of **MASTER OF SCIENCE IN PETROLEUM ENGINEERING**.

Salaheldin Elkatatny

Dr. Salaheldin Elkatatny
(Advisor)

497

Dr. Abdullah S. Sultan
Department Chairman

Mohamed Mahmoud

Dr. Mohamed Mahmoud
(Member)

[Signature]

Dr. Salam A. Zummo
Dean of Graduate Studies



Rahul Gajbhiye

Dr. Rahul Gajbhiye
(Member)

5/1/2017
Date

© Fahd Saeed Alakbari

2017

Dedication

This thesis is dedicated to my beloved parents, my wife, my son (Malk)
and all my family

Whose prayers and perseverance led to this success

ACKNOWLEDGMENTS

In the name of Allah, Most Gracious, Most Merciful. All praise is to Almighty Allah who gave me courage, knowledge and ability to complete this work and blessing of Allah be upon his prophet Mohammed.

I really appreciate and thank Dr. Salaheldin Elkatatny, thesis advisor, Dr. Mohamed Mahmoud, Dr. Rahul Gajbhiye, committee members for providing their invaluable help and guidance through my thesis work.

Acknowledgment is due to King Fahd University of Petroleum & Minerals to give me a chance to complete my master degree. I would like to express my appreciation to all faculty and staff of the Petroleum Engineering Department for the contribution to my thesis work.

I also thank Mr. AbdulSamad Iddrius, Mr. Abdulrahim Muhammadain, for their priceless in PETE Department laboratories.

Special thanks are due to all my colleagues and friends who help me in my work. Finally, I am indebted to Eng. A. A. Bugshan & HEFHD for their extreme moral support throughout my master program career and also for their encouragement.

TABLE OF CONTENTS

ACKNOWLEDGMENTS	V
TABLE OF CONTENTS.....	VI
LIST OF TABLES.....	VIII
LIST OF FIGURES.....	IX
ABSTRACT	XI
ملخص الرسالة	XII
CHAPTER1.....	1
INTRODUCTION	1
CHAPTER 2.....	6
LITERATURE REVIEW	6

CHAPTER 3.....	15
MATERIALS AND EXPERIMENTS	15
CHAPTER 4.....	25
4.1 Results of the Stability of the Drilling Fluid	25
4.2 Results of the rheological properties and gel strength of the drilling fluid	43
4.3 Filtration measurements of drilling fluid	76
4.4 Removal efficiency measurements of the drilling fluid.....	77
CHAPTER 5.....	78
CONCLUSIONS AND RECOMMENDATION	78
REFERENCES.....	80
VITAE.....	85

LIST OF TABLES

Table 1: Barite with different particle size	26
Table 2: XRF and electronegativity for barite	27
Table 3: Barite with nanosilica	29
Table 4: XRF and electronegativity for nanosilica	30
Table 5: Functional groups of nanosilica.....	31
Table 6: Barite with nanoclay	32
Table 7: XRF and electronegativity for nanoclay	33
Table 8: Functional groups of nanoclay.....	34
Table 9: CaCO ₃ with nanoparticles.....	35
Table 10: Ilmenite with nanoparticles.....	37
Table 11: XRF and electronegativity for ilmenite	38
Table 12: XRF and electronegativity for KCl and NaCl and CaCO ₃	41
Table 13: XRF and electronegativity for bentonite	42
Table 14: Drilling fluid formula for lab scale	44
Table 15: Drilling fluid formulation for the based case.....	47
Table 16: Drilling fluid formulation for different concentrations of bentonite	54
Table 17: Drilling fluid formulation for different concentrations of nanoclay.....	62
Table 18: Drilling fluid formulation for different concentrations of nanosilica.....	70

LIST OF FIGURES

Figure 1: Electronegativity of elements	14
Figure 2: Shaker	17
Figure 3: Zetal Pals machine.....	17
Figure 4: XRF machine.....	18
Figure 5: FTIR machine.....	19
Figure 6: NMR machine	20
Figure 7: HPHT Rheometer	22
Figure 8: HPHT filter press.....	23
Figure 9: Zeta potential measurements for barite (less 75 micr. m and 75-95 micr. m)...	28
Figure 10: Zeta potential measurements for barite with nanosilica.....	30
Figure 11: FTIR for nanosilica	31
Figure 12: Zeta potential measurements for nanoclay with barite.....	33
Figure 13: FTIR for nanoclay	34
Figure 14: Zeta potential measurements for CaCO ₃ and nanoparticles	36
Figure 15: Zeta potential measurements for ilmenite with nanoclay and nanosilica.....	38
Figure 16: Zeta potential measurements for nanosilica with KCl and Nacl	39
Figure 17: Zeta potential measurements for nanoclay with KCl and NaCl	40
Figure 18: Zeta potential measurements of bentonite	42
Figure 19: Based fluid behavior at 85 °F with different applied pressure.....	48
Figure 20: The gel strength of based drilling fluid	48
Figure 21: Based fluid behavior at 120 °F with different applied pressure.....	49
Figure 22: Based fluid behavior at 150 °F with different applied pressure.....	49
Figure 23: Based fluid behavior at 200 °F with different applied pressure.....	50
Figure 24: The plastic viscosity of based drilling fluid	50
Figure 25: The yield point of based drilling fluid.....	51
Figure 26: Different concentrations of bentonite with drilling fluid behavior at 85 °F	55
Figure 27: The gel strength of different concentrations of bentonite with drilling fluid at 85 °F	55
Figure 28: Different concentrations of bentonite with drilling fluid behavior at 120 °F ..	56
Figure 29: The gel strength of different concentrations of bentonite with drilling fluid at 120 °F	56
Figure 30: Different concentrations of bentonite with drilling fluid behavior at 150 °F ..	57
Figure 31: The gel strength of different concentrations of bentonite with drilling fluid at 150 °F	57
Figure 32: Different concentrations of bentonite with drilling fluid behavior at 200 °F ..	58
Figure 33: The gel strength of different concentrations of bentonite with drilling fluid at 200 °F	58
Figure 34: The plastic viscosity of different concentrations of bentonite with drilling fluid.....	59

Figure 35: The yield point of different concentrations of bentonite with drilling fluid ...	59
Figure 36: Different concentrations of nanoclay with drilling fluid behavior at 85 °F.....	63
Figure 37: The gel strength of different concentrations of nanoclay with drilling fluid at 85 °F	63
Figure 38: Different concentrations of nanoclay with drilling fluid behavior at 120 °F...	64
Figure 39: The gel strength of different concentrations of nanoclay with drilling fluid at 120 °F	64
Figure 40: Different concentrations of nanoclay with drilling fluid behavior at 150 °F...	65
Figure 41: The gel strength of different concentrations of nanoclay with drilling fluid at 150 °F	65
Figure 42: Different concentrations of nanoclay with drilling fluid behavior at 200 °F...	66
Figure 43: The gel strength of different concentrations of nanoclay with drilling fluid at 200 °F	66
Figure 44: The plastic viscosity of different concentrations of nanoclay with drilling fluid.....	67
Figure 45: The yield point of different concentrations of nanoclay with drilling fluid....	67
Figure 46: Different concentrations of nanosilica with drilling fluid behavior at 85 °F...	71
Figure 47: The gel strength of different concentrations of nanosilica with drilling fluid at 85 °F	71
Figure 48: Different concentrations of nanosilica with drilling fluid behavior at 120 °F.....	72
Figure 49: The gel strength of different concentrations of nanosilica with drilling fluid at 120 °F	72
Figure 50: Different concentrations of nanosilica with drilling fluid behavior at 150 °F.....	73
Figure 51: The gel strength of different concentrations of nanosilica with drilling fluid at 150 °F	73
Figure 52: Different concentrations of nanosilica with drilling fluid behavior at 200 °F.....	74
Figure 53: The gel strength of different concentrations of nanosilica with drilling fluid at 200 °F	74
Figure 54: The plastic viscosity of different concentrations of nanosilica with drilling fluid.....	75
Figure 55: The yield point of different concentrations of nanosilica with drilling fluid ..	75
Figure 56: Filtration measurements of drilling fluid.....	76
Figure 57: Filter cake thickness of the drilling fluid.....	77

ABSTRACT

Full Name : [Fahd Saeed Alakbari]

Thesis Title : [Evaluating the Effect of Nanoclay and Nanosilica on the Properties of Water-Based Drilling Fluid]

Major Field : [Petroleum Engineering]

Date of Degree : [January, 2017]

Drilling fluid constitutes an important part of the drilling operations. Drilling mud is circulated into the wellbore to minimize the formation damage, transport cuttings from the bottom to the top of the well, cool and lubricate the bit, and maintain the stability of shale formations. Also drilling fluids should be safe, environmentally friendly, and pumpable. Currently nanoparticles are introduced as new drilling fluid-additives to enhance the drilling fluid efficiency. The mechanisms of drilling fluid enhancement due to nanoparticles were not fully investigated in the literature.

In previous studies nanoparticles were used with different percentages in the drilling fluid to obtain the required properties. In this study, we will thoroughly investigate the fundamentals of adding nanoparticles to water based drilling fluid by evaluating stability, rheological and filtration properties.

The base formulation of calcium carbonate water-based drilling fluid has a serious issue of gel strength stability at 200 °F, to solve this issue, nanosilica was used. It was found that using 7.5 wt % of nanosilica improved the gel strength at 200 °F after 30 min. Using nanoclay did not enhance the drilling fluid rheological properties. Adding nanoclay to the based drilling fluid decreased the rheological properties. The nanosilica can be used with the drilling fluid to stabilize the gel strength at 200 °F and at this temperature the base drilling fluid was not stable.

ملخص الرسالة

الاسم الكامل: فهد سعيد عبد الله العكبري

عنوان الرسالة: تقييم تأثير نانوكلاي و نانوسيليكا على خصائص مانع الحفر ذو الأساس المائي

التخصص: هندسة بترول

تاريخ الدرجة العلمية: 2017

تشكل سوائل الحفر جزءا هاما من عمليات الحفر. وطین الحفر يستعمل في حفر البئر النفطي لتقليل الضرر خلال عملية حفر البئر. كما يجب أن تكون سوائل الحفر آمنة، صديقة للبيئة، وسهلة للضخ. حاليا أدخلت المواد المتناهية الصغر كمواد اضافية لسوائل الحفر التي تساعد سائل الحفر في تعزيز خصائصه. في الدراسات السابقة استخدمت المواد المتناهية الصغر مع سوائل الحفر بنسب مختلفة لتحسين خصائص سوائل الحفر.

سائل الحفر ذو الأساس المائي و الكالسيوم كربون عندما يستخدم في درجات الحرارة العالية مثلا 200 درجة حرارة فهداين يفقد خصائصه مثلا خاصية الجل . عندما يفقد السائل خاصية الجل سوف يتراكم في البئر و يسبب مشكلة الالتصاق لانابيب. و لتغلب على هذه المشكلة لقد تم اضافة عدة نسب من المواد المتناهية الصغر مثلا المواد المتناهية الصغر ذو الأساس الرملي و الأساس الطفلي. و قد عطى المواد المتناهية الصغر ذو الأساس الرملي نتائج جيدة. إضافة 7.5 نسبة المواد المتناهية الصغر ذو الأساس الرملي الى سائل الحفر تقدر تتغلب على مشكلة ترسيب سائل الحفر في درجة الحرارة العالية 200 درجة حرارة فهداين.

CHAPTER1

INTRODUCTION

Drilling fluid is an essential part of the drilling operations. Drilling fluids have many functions in the drilling operation. These functions are cleaning well, controlling formation pressure, suspension of the cuttings, sealing permeable formations, keep the stability of wellbore, decreasing the damage of formation, cooling, lubrication and supporting the bit and drilling assembly, transferring hydraulic energy to tools and bit, confirming adequate formation evaluation, inhibiting corrosion, reduction of environment effect and simplifying cementing and completion. There are several categories of drilling fluids due to the features of the base fluid. These types are; water based mud (WBM), oil base mud (OBM) or invert emulsions fluid and gas fluid such as foams. Water base mud can be suitable for low-pressure and low-temperature conditions. Water base mud is cheaper and less problematic to maintain than oil muds. Oil based mud is used in high pressure and high temperature (HPHT) conditions due to their stability in these conditions [1]. High-pressure high-temperature conditions can be defined as a condition when the pressure is more than 10,000 psi and the temperature is more than 300 °F [2]. The properties of drilling fluid include, density, rheology properties, fluid loss, pH, alkalinity, salt content, oil-water ratio, sand content, solid content, hardness, electrical stability and other properties must be controlled. Drilling fluid density is the significant property and it should be maintained to the specified value. Increasing the density of the mud can be achieved by using additives such as barite and calcium carbonate (CaCO_3). Ilmenite can be used to increase the mud density due to the high specific gravity [3]. Rheological properties include; viscosity, gel strength, and

yield point. The viscosity of drilling fluids is an important property in the drilling operation. It is known as the measurement of resistance to flow. Fluids can be classified into two types; Newtonian fluids and non-Newtonian fluids. In non-Newtonian fluids, the viscosity depends on shear rate such as drilling fluids. In Newtonian fluids, the viscosity is not function of shear rate such as water. Apparent viscosity is the shear stress of the fluid divided by the shear rate of the fluid; it is constant for Newtonian fluids. The apparent viscosity increases with increasing shear stress with independent time is called dilatant fluid [4]. The apparent viscosity reduces with increasing of the shear stress with independent time is known pseudoplastic fluid [5]. The reduction of the apparent viscosity on the growth of time with independent shear stress is named thixotropic fluid [6]. The material that looks an inelastic form at low stresses but can be as a viscous fluid at high stress is Bingham plastic [7]. Plastic viscosity is the measure of the internal resistance to flow based on type, amount, and size of solids in the fluid. Yield point (YP) is the minimum value of stress that is required to move the fluid or the attractive force between internal particles in the fluids. Another property of rheology is the gel strength that is the ability of the drilling fluids to suspend cuttings when circulation is stopped. Fluid loss or filtration is another issue in the drilling operation. Fluid loss occurs when the mud pressure is greater than the formation pressure. Two types of filtration can be used which are dynamic and static filtration. Dynamic filtration occurs when the drilling mud is circulated and static when the drilling mud is stopped. The pH indicates the alkalinity or acidity of the drilling fluid, a pH equals seven is neutral, a pH is less than seven is acidic and a pH is more than seven is alkaline. The pH is essential in the drilling fluid to control the corrosion and the bacterial growth that might degrade the additives of polymer and creates H_2S . The pH

affects some additives of drilling mud such as viscosifiers. Alkalinity can be obtained by using HCO_3^- , CO_3^{2-} and OH^- . Several additives (viscosifiers) of the drilling mud can be affected by alkalinity. Salt content in drilling mud is important due to its effects on the drilling fluids additives such as viscosifiers. Other properties can be used in particular cases such as the glycol content, KCl and corrosion inhibitors. Drilling mud contains of an excessively complex chemistry based on the use of the drilling fluids. These drilling fluids are usually consisted of water and viscosifier. When the wells are drilled deeper, more additives are added to the drilling fluids to improve the properties of the mud to control the problems such as fluid loss. In the past, many additives were used in the drilling fluids such as bentonite, barite, and calcium carbonate but with these additives the mud still needs to develop its properties. Currently, nanomaterial in drilling mud become a new generation of the drilling mud. Nanomaterial has small particles (around 1-100 nanometers). Nanoparticles was used to decrease the formation damage, differential sticking problem and frictional resistance between the borehole wall and the pipe. Drilling mud with nanoparticles is safe to the environment [8]. The wellbore stability can be enhanced by using nanoparticles. In shale formation with tight permeability, nanomaterials was used to reduce the fluid loss [9]. The additives in the drilling fluid should be dispersed and stable when mixed with the compositions of drilling fluids. Drilling fluids with nanoparticles is more stable due to light particles of nanomaterials. This study was planned to understand the stability of the additives drilling fluids with nanoparticles. Nanomaterials invade between the large particles and block the flow through them. Nanoparticles can be used to improve the rheological properties of the mud such as viscosity. The study was arranged

to evaluate the rheological properties of drilling mud with nanoparticles. The loss of drilling fluid is the major problem of the drilling operations due to the cost.

1.1 Problem Statement

The mechanisms of drilling fluid properties enhancement due to nanoparticles were not fully investigated in the literature. In previous studies they used nanoparticles with different percentages in the drilling fluid to obtain the required properties. In this study, we will investigate the fundamentals of adding nanoparticles to water based drilling fluid by evaluating stability, rheological, and filtration properties. The essential goal will be to assess which type, and concentration of the nanoparticles are more stable in the drilling mud, evaluate the rheological properties and develop the reduction of the drilling fluid loss. Laboratory experiments were performed using different combinations of the drilling additives and nanomaterials with varying concentrations to obtain the optimum stability of the drilling fluids. The laboratory measurements included measuring pH, zeta potential, the compositions, viscosity, yield point, gel strength, and filtration test of the additives and nanomaterials.

1.2 Research Objectives

The main objective is to evaluate the effect of adding nanomaterials (nanoclay and nanosilica) to calcium carbonate water-based drilling fluid. The specific objectives are as following:

- 1- Study the stability of the drilling fluids with nanomaterials by using zeta potential.
- 2- Assess the rheological properties of the drilling fluids with nanoparticles by using HPHT rheometer.
- 3- Evaluate the possibility of formation damage by measuring the removal efficiency and retained permeability of the drilling fluid by using HPHT filter press.

CHAPTER 2

LITERATURE REVIEW

2.1 Nanoparticles in drilling fluid

The drilling fluids provide plenty of opportunities for these nanoparticles to be utilized. The performance of drilling fluids in high-temperature high pressure can be improved by adding nanoparticles to the fluids [10]. The viscosity of the drilling mud can be increased by adding nanoparticles such as iron oxide. Iron oxide has particle sizes less than three nm that makes the fluid more viscous. Baird and Walz [10] used different concentrations of nanosilica with water based drilling fluid to improve the rheological properties. Smaller particles disperse more than the large particles. Therefore, smaller particles have big surface area makes bridges between bentonite particles and promotes the gelation of the bentonite particle [11]. Adding nanoparticles to the drilling mud includes infusion and intercalation methods [12]. Infusion is the method that extracts chemical compounds in a solvent. Intercalation is the exclusion of a molecule to compounds with a layered structure. Drilling fluid with added nanoparticles of zinc oxide eliminates 100 % of hydrogen sulfide from water-based muds in fifteen minutes, however without nanoparticles of zinc oxide eliminates just 2.5 % after 90 minutes [13].

Invert emulsion drilling mud can be stabilized by adding both nanoclay and nanosilica in high pressure and high temperature (HPHT) conditions. Nanoclay has stability in the phase of oil, it exhibits better gel formation capacity. Nanoparticles effect on plastic viscosity,

yield stress, and gel strength [14]. Agarwal et al. [14] used 2 wt % nanoclay with oil based drilling fluid to improve the rheological properties.

Adding silicon nanoparticles to the drilling fluid helped form integrated filter cake with low permeability and small thickness [15]. This ideal filter cake prevented the loss of the drilling fluid into the formation and hence prevent differential sticking. stated that there is no side effect on the environmental when using silicon nanoparticles, which is thermally stable up to 250°F. Javeri et al. [15] concluded that the use of silicon nanoparticles, which are generally available in the required volumes, will reduce the drilling problems (loss of circulation and differential sticking) and provide an environmental solution to these problems.

It is very difficult to form homogenous, physically stable, and functionally valuable drilling fluids based on water or salt water. Amanullah et al. [16] mentioned that adding nanoparticles to water-based drilling fluid would develop a fluid system with the desirable rheological and filtration properties. They stated that nano-based drilling fluids had a higher yield point, which provides a better dynamic suspension of cuttings and efficient borehole cleaning while drilling. In addition, nano-based drilling fluids had a flat type gel strength, which requires lower circulation pressure to restart the drilling operation. These properties of the nano-based drilling fluid will reduce the common problems associated with the drilling operations such as loss of circulation and hole cleaning problems.

Formation damage associated with stimulation fluid (polymer based) and paraffin blocks can be treated using stabilized nanoparticle dispersions, which contain silica (diameter of 4-20 nm). The structural arrays of the three-phase interface of the particles helped in lifting

the damage and stimulate the reservoir. Mcelfresh et al. [17] concluded that the aqueous nanoparticle dispersions have a force called disjoining pressure, which causes the particles to force themselves between a rock and organic matter and hence separate the organic matter from the rock surface. Mcelfresh et al. [17] added 10 wt % nanosilica to water based drilling fluid to decrease filter cake.

Filtration of the drilling fluid into the formation is the most critical parameter that causes well control problem and formation damage, especially in drilling deep wells [18]. Srivatsa et al. [18] found that sized silica nanoparticles is better than sized calcium carbonate for surface plugging and the polymer-surfactant solution is better than using a bio-polymer or surfactant based for rheology and filtration control. Srivatsa et al. concluded that fluid loss can be reduced by using nanoparticles and the nanoparticles polymer-surfactant mixture is the excellent fluid to drill horizontal shale reservoirs. Srivatsa et al. [18] studied different concentrations (10,20, 30 wt %) nanosilica with water based drilling fluid to control rheological properties and filtration. They mentioned that nanoparticles can penetrate the shale pores and work as a bridging material, which cause wellbore strengthen. Wellbore instability is the common problem in drilling shale formation. This is because of the interaction of the conventional drilling fluids with the clay minerals in shale formation that lead to a change in the mechanical properties of the rock and cause clay swelling [19]. Sensoy et al. [20] used different concentrations of nanosilica with water based drilling fluid to minimize fluid invasion. To prevent this interaction, nanoparticles should be added to the water-based drilling fluid, which significantly reduce the invasion of water into the shale formation. Nanoparticles can plug different types of shale formation (Atoka and Gulf of Mexico shale) [20] and [21]. Cai et al. [21] used 10 wt % nanosilica with water based

drilling fluid to decrease water invasion. Jung et al. [19] concluded that nanoparticles water-based drilling fluid had a durable physical plugging of shale formation and caused a large reduction in shale permeability than based mud, which does not contain nanoparticles. Zhang et al. [22] stated that shale wellbore instability can be avoided by preventing drilling fluid filtrate and forming an ideal filter cake and sealing the micro-cracks and the pores near the wellbore. Particle sizes in the conventional drilling fluid are larger than the shale pore throat size, so the filter cake may not be conducted on the shale surface. This issue could be solved by using nanoparticles. Zhang et al. [22] concluded that the sized calcium carbonate is not effective for shale plugging because of the small pore throat of shale. In addition, the strength coefficient of the filter cake become larger after adding nanoparticles.

Shale formations with pores in the range of 10 nm to 0.1 μm can cause fluid loss and this issue could not be stopped by using lost circulation materials (0.1-100 μm). Nanoparticle such as loss circulation materials with different size domain could solve this problem [23] and [18]. Mud invasion in shale can be decreased by adding nanoparticles to the water-based drilling fluid [20]. Berret et al. [24] observed the formation of the super micellar aggregates because of the interaction of nanoparticles with co-polymer.

Zakaria et al. [25] concluded that the use of nanoparticles as a loss circulation material with oil-based drilling fluid had more than 70% reduction in fluid loss compared to 9% reduction when using typical loss circulation materials. They stated that oil-based drilling fluid with nanoparticles had stable properties for more than 6 weeks.

Nanographite with drilling mud was enhanced the rheological properties such as (viscosity, gel strength, etc.) under HPHT conditions. In future, nanoparticles can be synthesized to develop drilling fluids with using less expensive nanoparticles [26]. Nanoparticles (palygorskite Pal, clay) can make the drilling mud rheology stable under high-pressure and high-temperature conditions. Nanoparticles (Pal) can be used to optimize wellbore stability, lubricity, penetration rates [27]. Abdo and Haneef [27] studied different concentrations (0, 2, 4, 6, 8 wt %) of nanoclay with water based drilling fluid to enhance the rheological properties. The rheological properties (yield point YP, plastic viscosity PV, apparent viscosity AV, gel strength) of drilling mud increased by increasing bentonite with nanoclay. The quantity of increasing based on the amount of bentonite, nanoclay and temperature. Increasing the amounts of bentonite, nanoclay and temperature decreased electrical resistivity of the drilling fluids [28]. Vipulanandan and Mohammed used different concentrations of nanoclay with water based drilling fluid to improve the rheological properties.

Nanoparticles were used to control a sag in invert-emulsion fluid (IEF) system and to make a water-in-oil emulsion of an IEF is stable. Drilling fluid with nanoparticles showed excellent sag resistance in diverse base oils with smallest oil separation. Nanoparticles had a positive effect on the emulsion stability of the invert-emulsion fluid, the loss of the fluid can be under control [29]. Nanoparticles calcium-based (0.5 wt. %) decreased fluid loss of the drilling mud (20-30%) in high-pressure high temperature [30]. Mud drilling that contains bentonite ($H_2Al_2O_6Si$) with nanoparticles (aluminosilicate clay hybrid ASCH and iron-oxide clay hybrid ICH) can decrease fluid loss 37% and 47% comparing to without nanoparticles in low temperature low pressure (25 °C , 6.9 bar) and high temperature high

pressure (200 °C ,70 bar) conditions [31]. Nanoparticles such as nanosilica were applied in hydraulic fracturing to remain fractures open under stress. Nanosilica keeps the fractures longer and more conductive if it is with linear gels or water before larger proppants is injected. Some nanoparticles (nanosilica) have been developed as a successful technology to decrease fluid loss in tight reservoirs. Nanosilica is light; it had not precipitated during injection processing. Nanosilica can decrease the damage that is caused by fine migration [32].

2.2 Nanoparticles stability

Nanomaterials in the drilling fluid should be dispersed and stable when mixed with the other components of drilling fluids. The stability and dispersion of the materials in the solutions can be identified by using zeta potential. Zeta potential measurements are determined by using a phase analysis light scattering (PALS). The reading of zeta potential is between -220 and 220 mV [33]. The particle surface charge can be the function of the zeta potential. Zeta potential is the function of changing pH, salinity, and particular additives concentration such as polymer [34]. The surface charges can be affected by zeta potential. It shows significant information of surface potential, the point of zero charge, double layer structure, and colloid characteristic. The value of zeta potential can be decreased by increasing nano-particles concentration [35]. The point between two separate particles can be obtained by the zeta potential and the strength of electrostatic attraction and repulsion between them. The zeta potential indicates the stability or non-stability of a solution. The zeta potential can measure the stability of suspensions. The electrophoretic mobility is used to get the zeta potential [36]. The difference in the zeta potential is due to the variation in the supporting electrolyte concentrations and chemical compositions and

mineralogical. The zeta potential is sensitive to the temperature [37]. The value of zeta potential can be increased by adding Ca^{2+} ions or Mg^{2+} ions to the solution such as CaCl_2 and MgCl_2 . The zeta potential value can be decreased by adding CO_3^{2-} ions to the solution such as Na_2CO_3 . The zeta potential value is less than zero whereas CaCO_3 of biogenic origin and it is more than zero when the CaCO_3 is mineral or synthetic origin. The zeta potential can be used to obtain the solid surface charges of the suspended particles [38]. The variation of zeta potential values is due to the different positions of the plane of shear stress [39]. The zeta potential measures the relative motion between the mineral surface and the electrolyte. The zeta potential is the function of salinity. The presence of ions in the fluid can modify the values of zeta potential [40]. When the total number of electrons does not have the total number of protons, it is called an ion. The ion can effect on electrical charges and this will effect on zeta potential. The zero of zeta potential measurement is called Zero Point of Charge (ZPC) [41]. Zero Point of Charge neutralize positive charge effect to negative charge effect that means the double layer thickness decreased and the attraction force of electrostatic increased. It flocculates the particles and it does not disperse the particles [42]. It can be shown by particle in the suspension. It is the variations of medium and the layer of the fluid. Most clay minerals show negative charges in the water. The zeta potential of Ca^{2+} depends on pH due to the divalent ion of Ca [42]. The zeta potential indicates the stability of the colloidal system. The colloidal system is stable when the value of zeta potential is more than +30 mV or less than -30 mV. When the solution is acidic, the zeta potential can be positive because addition of acid will make a positive charge. When the solution is basic, the zeta potential can be negative because addition of alkali will make a negative charge. The zero point of zeta potential is called isoelectric

point where the system is the least stable [43]. The value of zeta potential can be decreased by increasing the concentration of the salt because it compresses electrical double layer. Divalent anions such as SO_4^{2-} and CO_3^{2-} reduce the zeta potential measurements comparing the monovalent anions such as (Cl^- and NO_3^-) at the higher value of pH and the lower value of pH [44]. The zeta potential can be determined by following equations:

$$\zeta = 113000 \text{ EM } V_t / D_t \quad (1)$$

Where:

ζ : zeta potential (mV).

EM: electrophoretic mobility.

V_t : viscosity of the suspending liquid in poises.

D_t : dielectric constant of the suspending liquid.

$$\sigma = \epsilon. \epsilon_o \zeta / \lambda d \quad (2)$$

Where :

σ : the total amount of charge q per unit area a ($\sigma = q/a$).

$\epsilon. \epsilon_o$: the dielectric constants of two phases.

λd : debye distance up to which the ions get adsorbed on the surface to meet the bulk liquid called slipping plane.

2.3 Electronegativity

Electronegativity is a measure of the tendency of an atom to attract a bonding pair of electrons. Electronegativity can be used as indicator of the zeta potential. When the electronegativity is high, the zeta potential value will be close to the zero point and the material in the solution will not be stable. When the electronegativity is low, the zeta potential value will be far away from the zero point and the material in the solution will be stable,[45] **Figure 1.**

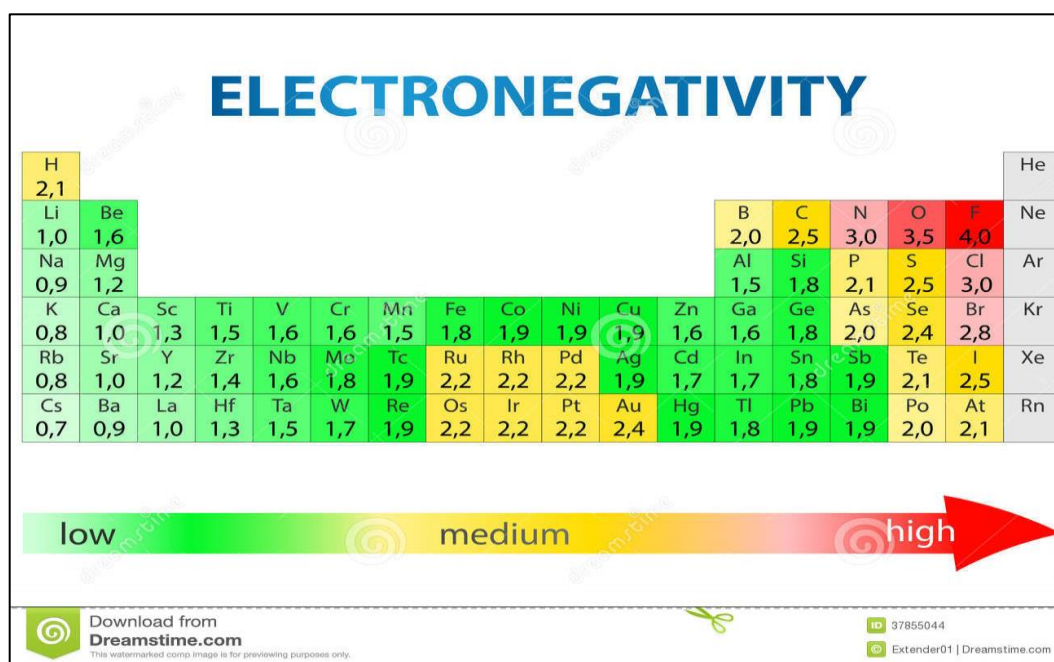


Figure 1: Electronegativity of elements, [45]

CHAPTER 3

Materials and Experiments

3.1 Materials

The weighting materials such as barite, calcium carbonate and ilmenite can be used to increase the density of the drilling fluid. There are many viscosifier materials such as bentonite and xc-polymer. Viscosifier can be used to suspend the cuttings and the weighting materials during noncirculation. Sodium sulfide can be used as oxygen scavenger in drilling fluid. Adding salts (NaCl and KCl) to drilling fluid to decrease shall swelling. The following materials were used as drilling fluid additives in this study.

- Barite.
- Calcium Carbonate.
- Ilmenite.
- Bentonite.
- Xc-polymer.
- Starch
- Sodium sulfide
- Nanomaterials (nanoclay, nanosilica)
- Salts (NaCl, KCl,)
- (NaOH) and hydrogen chloride (HCl).

3.2 Stability Test

3.2.1 Zeta Potential Measurements

Basically the stability test will be conducted for the additives (barite, calcium carbonate, and bentonite) drilling fluids with nanoparticles to study the conditions of stability in certain type, pH and concentrations of the nanoparticles. The subsequent steps will be followed to do the test:

- Change pH of water from 2 to 12 by NaOH/HCl
- Adding the samples with different concentrations of the drilling fluid additives to water.
- Adding nanoparticles with different concentrations to the additives.
- Mixing the samples for 24 hours by using shaker, **Figure 2**.
- Measure zeta potential for each sample by using Zeta Pals, **Figure 3**.

Zeta pals machine

The zeta pals machines can use a phase analysis light scattering technique to find the electrophoretic mobility of charged colloidal suspensions, and then find the zeta potential in mV.



Figure 2: Shaker

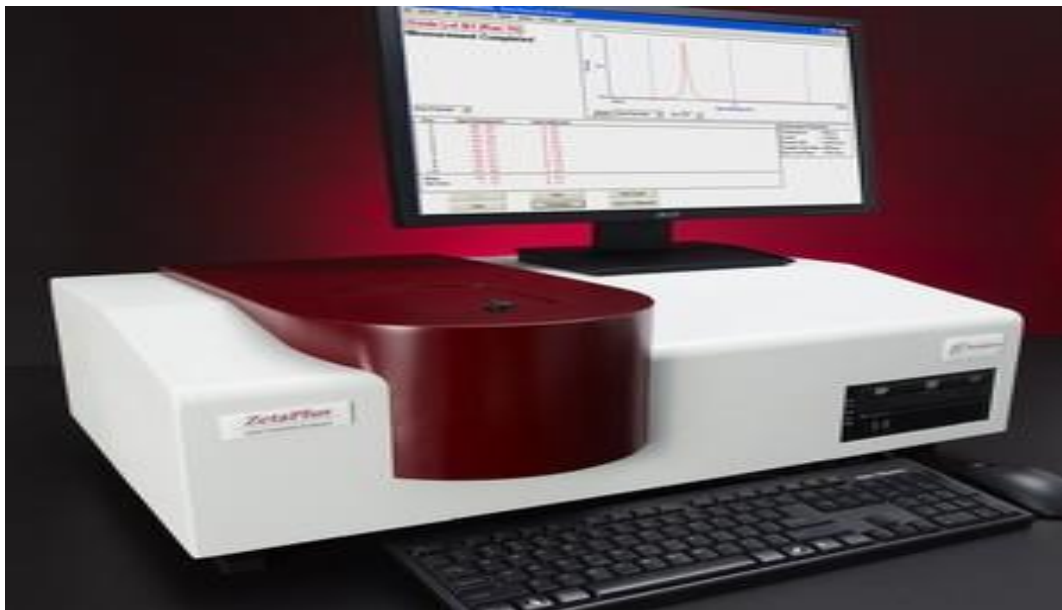


Figure 3: Zetal Pals machine

XRF (X-ray fluorescence) machine

It is a non-destructive analytical technique. XRF can be used to find the composition of materials. XRF machine can find the chemistry of samples by measuring the fluorescent XR emitted from samples when they are excited by a primary XR source. In this study, we used XRF **Figure 4** to determine the composition of drilling fluid additives such as barite and nanoclay.



Figure 4: XRF machine

FTIR (Fourier transform infrared spectroscopy) and NMR (Nuclear magnetic resonance spectroscopy) machines

FTIR is used to find an infrared spectrum of emission of liquids, solids or gases, **Figure 5**. The functional groups are specific groups of bonds within molecules that are responsible for the chemical reactions of those molecules. FTIR was used to determine the peaks of the functional groups of the materials. NMR was used to determine the organic molecules such as carbons and hydrogen in the material to give a clear functional groups, **Figure 6**.



Figure 5: FTIR machine



Figure 6: NMR machine

3.3 Rheology Test

3.3.1 Apparent Viscosity and Yield Point Test

The apparent viscosity μ_a , plastic viscosity (PV) and yield point (YP) can be measured by using HPHT rheometer, **Figure 7**.

HPHT rheometer machine

It is high pressure and high temperature, rotational and coaxial cylinder rheometer. It can work up to 1000 psi and 500°F. It can be used to measure different rheological properties of fluids. It can be used to test samples with high acid concentrations up to 30% HCL. HPHT rheometer is easy to set up, run and give the data into Microsoft Excel. HPHT rheometer takes 50 ml volume to test the sample.

The following steps will be followed to do the apparent viscosity and yield point test:

- Prepare the drilling mud samples with adding different concentrations of nanomaterials (0.5wt %, 1wt %, 3wt %, and 5wt %).
- Fill the container in HPHT rheometer with the sample to the volume specified by 50 mL.
- Set the HPHT rheometer at a sequence to measure the rheological properties of the samples at different conditions.

From Bingham plastic fluid model, we can find the following:

$$PV(cP) = \theta_{600} - \theta_{300} \quad (3)$$

$$YP (lb/100ft^2) = \theta_{300} - PV \quad (4)$$

$$\mu_a = \frac{300 \theta_N}{N} \quad (5)$$

$$\mu_a = \frac{\theta_{600}}{2} \quad (6)$$

Where θ is the dial reading of viscometer at the rpm.

- The Rheology test will measure at room temperature, 120°F, 150°F, and 200°F temperatures.

3.3.2 Gel Strength Test

The gel strength can also be obtained by using the HPHT rheometer . The following steps will be followed to do the gel strength test:

- Set the HPHT Rheometer at a sequence to measure the gel strength (10 second, 10 minutes, and 30 minutes) of the samples at different conditions.
- The gel strength test will measure at room temperature, 120 °F, 150 °F and 200 °F temperatures.



Figure 7: HPHT Rheometer

3.4 Filtration Test

Filtration properties of drilling fluids can be obtained by using HPHT Filter Press, **Figure 8**. Filtration behaviour can be affected by the temperature and the pressure and the type, quantity, and particle sizes. HPHT Filter Press is made for active and safe testing.

HPHT Filter press machine

HPHT filter press is designed to measure the filtration of drilling fluids under elevated pressure and temperature. HPHT filter press can work up to 1800 psig on the cell and 750 psig on the back pressure and up to 500 °F.



Figure 8: HPHT filter press

3.5 Removal efficiency measurement

Chelating agents GLDA (Glutamic-Di Acetic Acid) 20 wt % Ph=4 was used as removal fluid. The filter cake was soaking for 24 hours by the removal fluid. The following equations were used to determine the removal efficiency and retained permeability, [46]:

$$\text{Removal efficiency} = \frac{W_2 - W_3}{W_2 - W_1} \quad (7)$$

Where:

W_1 = the weight of the disk saturated with water, g.

W_2 = the weight of the disk saturated with filter cake, g.

W_3 = the weight of the disk saturated after removal process, g.

$$K = \frac{122.812 * q * \mu * h}{\Delta p * d^2} \quad (8)$$

Where:

d = diameter of the disk flow, in.

h = disk thickness, in.

K = permeability of the disk, md.

Q = flow rate, $\frac{cm^3}{min}$.

μ = fluid viscosity, cP.

Δp = differential pressure across the disk, psi.

$$k_r = \frac{k_f}{k_i} * 100 \quad (9)$$

k_f : final permeability, md.

k_i : initial permeability, md.

k_r : retained permeability.

CHAPTER 4

RESULTS AND DISCUSSION

4.1 Results of the Stability of the Drilling Fluid

4.1.1 Zeta potential of the drilling fluid

Clay minerals, such as chlorite that has iron has small value of positive zeta potential at pH 7 and negative zeta potential at pH 12. Illite and kaolinite (clay minerals) have negative zeta potential at low and high pH [47], [48]. On the top surface charges will never change with any pH but at the edge interlayer depend on pH. The chlorite charge is the function of pH, ions number and the charge distribution of both surfaces (face and edge). Fe^{3+} can be responsible to balance the negative charge of the hydroxyl group surfaces. When the pH increase, the ion shielding will be on the edge hydroxyl group surface such as Si-OH and Mg-OH, and as pH increase the negative value of zeta potential will increase[49], [50].

Two different particle sizes of barite were used. The first one has a particle size ranged from 75 to 95 micron. The second barite particle size was less than 75 micron with mean of 35 to 45 micron. Nanosilica and nanoclay were used in this study to evaluate the effect of adding these nanoparticles to the drilling fluid additives such as; barite, calcium carbonate, and ilmenite. The mixtures were prepared using deionised water and the pH of water was changed by using NaOH and HCl. Finally, the drilling fluid additives, nanoclay and nanosilica with different concentrations were added to the water.

4.1.2 Results and discussion of zeta optional

4.1.2.1 Effect of barite particular size on zeta potential values:

The pH of the deionized water was adjusted at values between 2 to 12 by using HCl and NaOH. Then, different sizes of barite (40-75 μm or 75 – 95 μm) were added to the adjusted water as shown in **Table 1**. The results showed that for pH higher than 10 there was no effect of changing the particle size of barite, **Figure 9**. Barite is $BaSO_4$ that means the value of zeta potential decrease at the high pH. For pH lower than 10, the effect of barite particle size on zeta was miner, **Figure 9**. The isoelectric point for barite (40-75 μm) is at pH=3 and for barite (75 – 95 μm) is at pH 3.5. The particular sizes of barite have minor effect on the zeta potential.

Table 1: Barite with different particle size

Mixtures no.	Weighting material	Nano material	pH
1	Barite 0.5 wt.% Particular Size (less 75)	---	2 to 12
2	Barite 0.5 wt.% Particular Size (75-95)	---	2 to 12

From XRF of barite, the barite have the same chemical minerals as the Illite and Kaolinite. The barite has negative zeta potential at high pH.

Zhong Hang et al. [51] mentioned that the value of zeta potential is positive at low pH and negative at high pH for nanoparticles of barite. The solid concentration of barite nanoparticles effect on the zeta potential values. The solid/liquid ratio effects on the zeta potential measurements, therefor the ratio keep constant at 0.5 gm wt% for zeta potential

measurements. Multivalent cations have a more effect on the zeta potential than monovalent ions of barite. Monovalent cations can decrease the zeta potential values by compress the electrical double layer, therefor the multivalent anions can change the zeta potential sign of barite, [51]. The zeta potential of barite with multivalent anions can be more decreased than barite with monovalent. Electronegativity is a measure of the tendency of an atom to attract a bonding pair of electrons. Electronegativity of elements affects the zeta potential. When the electronegativity increase, the zeta potential will decrease. The electronegativity of Sulfur in barite is 2.5 that means this make the barite has less zeta potential and it is not stable, **Table 2**.

Table 2: XRF and electronegativity for barite

Atomic number	Symbol	Element	Concentration	Electronegativity
13	Al	Aluminum	9.6	1.5
14	Si	Silicon	10.63	1.8
15	P	Phosphorus	9.1318	2.1
16	S	Sulfur	11.576	2.5
19	K	Potassium	8.9241	0.8
20	Ca	Calcium	9.0592	1.0
26	Fe	Iron	9.0983	4.0
38	Sr	Strontium	9.0025	1.0
56	Ba	Barium	22.98	0.9

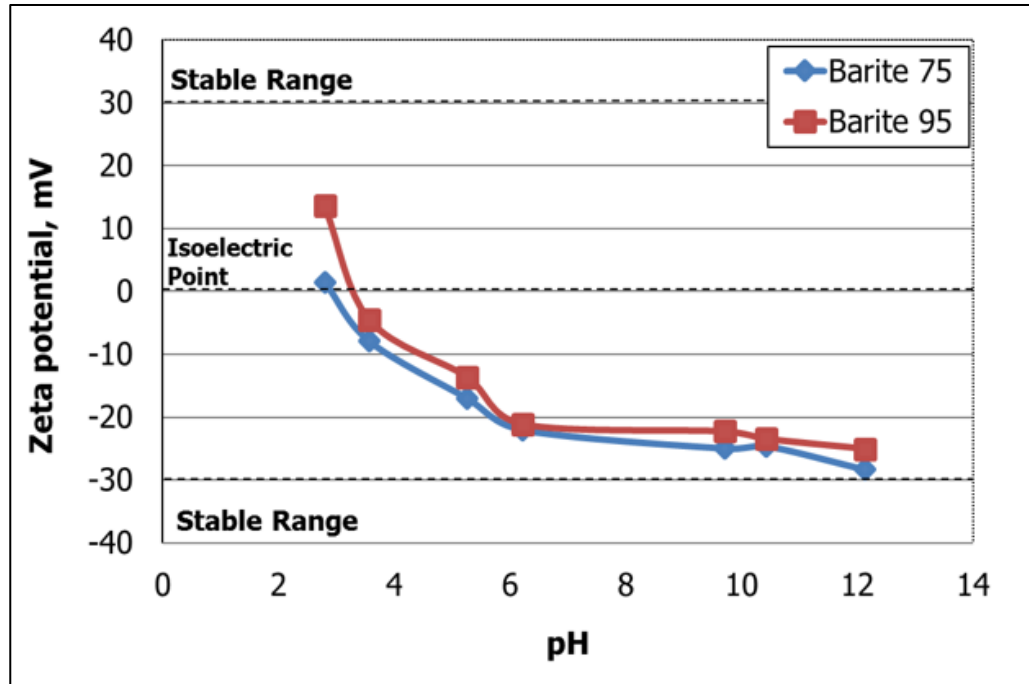


Figure 9: Zeta potential measurements for barite (less 75 micr. m and 75-95 micr. m)

4.1.2.2 Effect of adding nanosilica to barite on the zeta potential values:

A concentration of deionized water and barite with nanosilica was prepared that contains 0.5 wt% concentration of barite and nanosilica with water at diverse concentrations of barite with nanosilica at different pH as shown in **Table 3**. The value of zeta potential can be decreased by increasing nano-particles concentration [3]. The barite with nanosilica 1:1 concentration (0.25 wt% barite and 0.25 wt% nanosilica) is not stable at any pH value as exposed in **Figure 10**. The stability of barite with nanosilica can be decreased due to the reduction of the concentration of nanosilica in the solution. The different concentrations of barite with nanosilica have a dissimilar isoelectric point that means nanosilica effects on the stability of barite.

The zeta potential value of nanosilica in low pH is linear function with pH. Therefore, there is no complexation of charged sites with the Cl^- counter ions. The negative charge can be decreased by only increasing HCl concentration. For the pH values that are more than zero point, the contribution of $[SiO^-]$ and $[SiO^- \dots Na^+]$ are predominant [52]. In wide range of pH, silica has negative surface charge,[53]. Amorphous silica is more stable at pH more than 9 [52]. The dissolution of silica make silicate $HSiO_3^-$ ions which behave same an electrolyte. The surface charge can be increased at high pH because of silica dissolution and sodium hydroxide [52]. The coordination number of each surface atom may increase because silica structure is open enough. The isoelectric point for nanosilica is at pH=1.47 [52] . The electronegativity for nanosilica elements have low values, this makes the zeta potential of nanosilica more negative and closed to -30 mV, **Table 4**.

Table 3: Barite with nanosilica

Mixtures no.	Barite concentration	NanoSilca concentration	pH
1	0.5 wt.%	---	2-12
2	---	0.5 wt.%	2-12
3	0.25 wt.%	0.25 wt.%	2-12

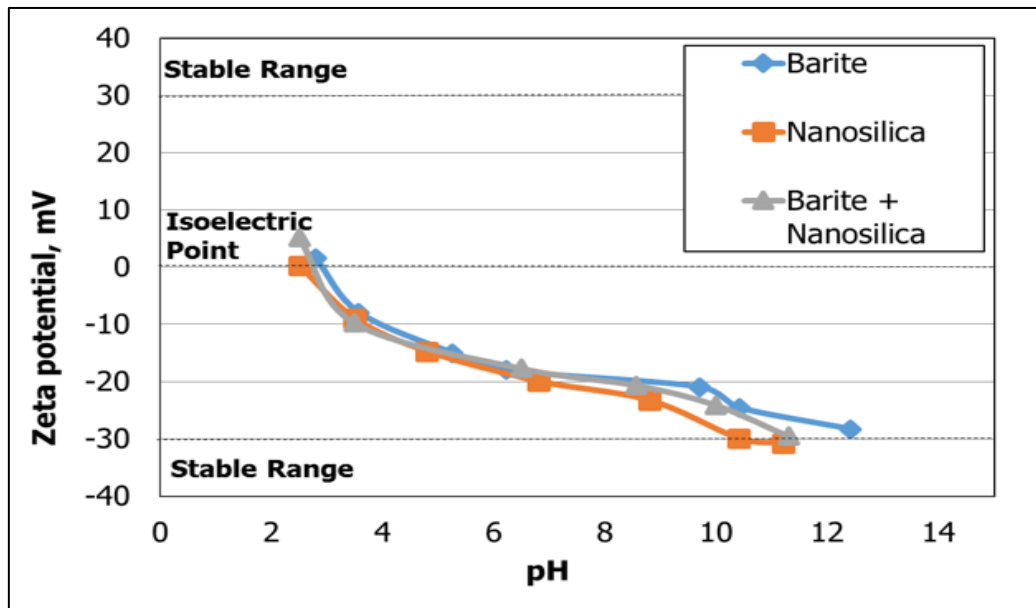


Figure 10: Zeta potential measurements for barite with nanosilica

Table 4: XRF and electronegativity for nanosilica

Atomic number	Symbol	Element	Concentration	Electronegativity
14	Si	Silicon	47.331	1.8
15	P	Phosphorus	8.9984	2.1
16	S	Sulfur	8.707	2.5
17	Cl	Chlorine	8.72	3.0
20	Ca	Calcium	8.786	1.0
22	Ti	Titanium	8.745	1.5
26	Fe	Iron	8.7278	4.0

The functional groups are specific groups of bonds with molecules that responsible for chemical reactions of this molecules. The function groups of nanosilica will help understand the value of the zeta potential of nanosilica. **Figure 11** shows the function groups of nanosilica. **Table 5** summarizes the function groups of nanosilica.

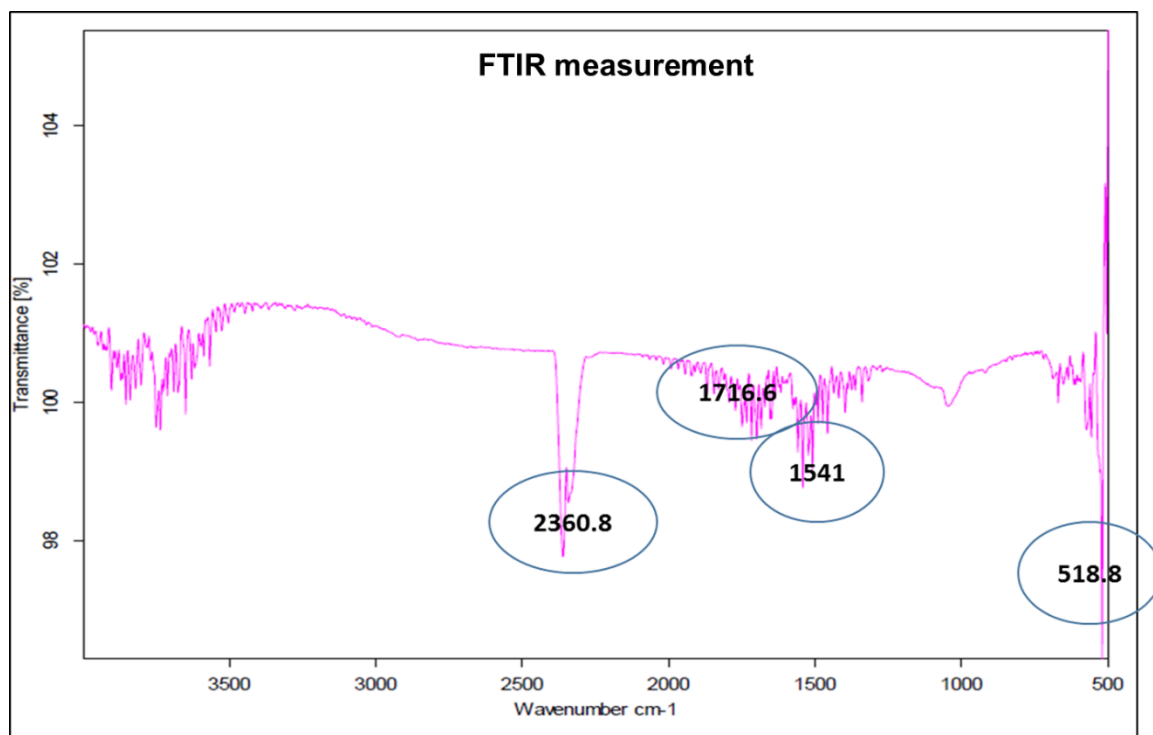


Figure 11: FTIR for nanosilica

Table 5: Functional groups of nanosilica

Peak	Functional group
518.8	Si–O–Si
1541	c-H
1716.6	C=O
2360.8	CO ₂

4.1.2.3 Effect of adding nanoclay to barite on the zeta potential values:

A mixture of deionized water and barite with nanoclay was prepared that contains 0.5 wt% concentration of barite and nanoclay with water at different concentrations of barite with nanoclay at dissimilar pH as shown in **Table 6**. The nanoclay alone is not stable at any pH value and the isoelectric point of nanoclay is at high pH value, **Figure 12**. The barite with nanoclay have the same concentration (0.25 wt% barite and 0.25 wt% nanosilica) that is not stable at any range of pH as shown in **Figure 12**. The stability of nanoclay with barite is changing with pH. Adding nanoclay to barite can be affected on the isoelectric point of the solution, **Figure 12**.

Zeolite zeta potential value depends on the ionic strength of the suspension, the pH, and Aluminum content of the framework. Zeolite has the crystal surfaces structure with silanol and aluminol groups [54]. The functional group Si-O^- can make the surface more negatively charged at a wide pH range [55]. Decreasing the ratio Si/Al in zeolite, this effect counteracts the effect of protonation of silanol groups in acidic solutions and this will change zero point to lower pH. Zeolite has Al-OH and Si-OH, so it is defined as a weak electrolyte [56]. Chlorine in nanoclay has high electronegativity, this means that nanoclay have less zeta potential because of increasing electronegativity of the nanoclay, **Table 7**.

Table 6: Barite with nanoclay

Mixtures no.	Barite concentration	Nanoclay concentration	pH
1	0.5 wt. %	---	2-12
2	---	0.5 wt. %	2-12
3	0.25 wt. %	0.25 wt. %	2-12

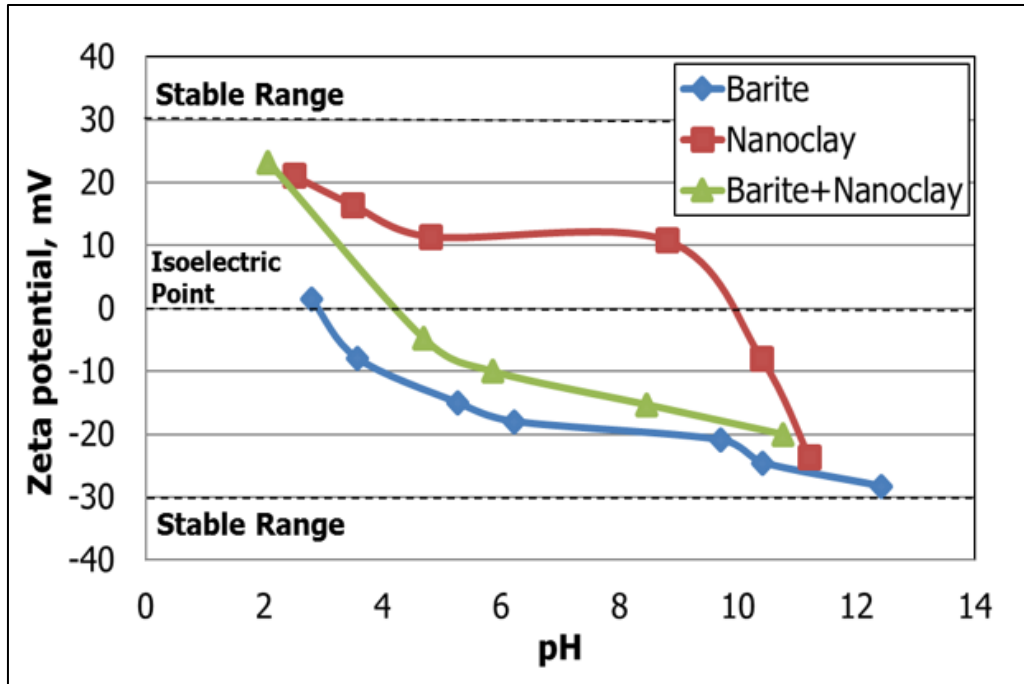


Figure 12: Zeta potential measurements for nanoclay with barite

Table 7: XRF and electronegativity for nanoclay

Atomic number	Symbol	Element	Concentration	Electronegativity
13	Al	Aluminum	16.479	1.5
14	Si	Silicon	41.359	1.8
15	P	Phosphorus	5.3072	2.1
16	S	Sulfur	4.7268	2.5
17	Cl	Chlorine	7.8804	3.0
19	K	Potassium	4.7143	0.8
20	Ca	Calcium	5.1791	1.0
22	Ti	Titanium	4.8153	1.5
26	Fe	Iron	9.559	1.8

The functional groups of nanoclay will help understand zeta potential of nanoclay. **Figure 13** shows the functional groups of nanoclay. **Table 8** summarizes the functional groups of nanoclay.

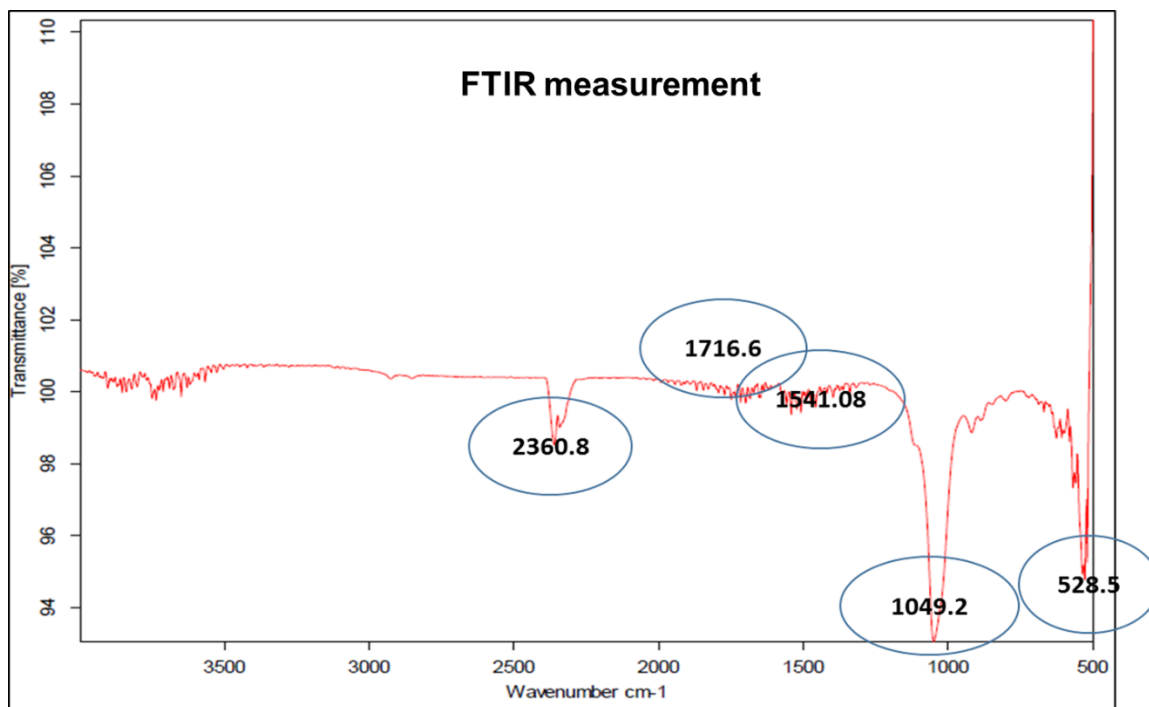


Figure 13: FTIR for nanoclay

Table 8: Functional groups of nanoclay

Peak	Functional group
528.5	CH ₂ F ₂
528.5	Al-O-Si
1049.2	Si-O stretching
1541.08	c-H
1716.6	C=O
2360.8	-NH stretching

4.1.2.4 Effect of adding nanoparticulars (nanosilica and nanoclay) to CaCO_3 on the zeta potential measurement:

A combination of deionized water and CaCO_3 with nanoparticulars (nanosilica and nanoclay) was arranged that involves 0.5 wt% concentration of CaCO_3 and nanoparticulars (1:1 concentration of CaCO_3 with nanoparticulars) at different pH as displayed in **Table 9** . **Figure 14** shows that CaCO_3 with nanosilica is stable at the range of pH (11.5-12). The isoelectric point of CaCO_3 is at pH=9.5 and the isoelectric point of CaCO_3 with nanoclay is at pH=10.5. When the nanosilica is added to the CaCO_3 , the solution is stable at pH(11.5-12). The adding nanoclay to CaCO_3 does not effect on the stability of CaCO_3 on the solution. The electronegativity of elements of CaCO_3 have large values so the CaCO_3 has less zeta potential, **Table 12**.

Table 9: CaCO_3 with nanoparticles

Mixtures no.	CaCO_3	Nanoclay	Nansilica	pH
1	0.5 wt. %	---	---	2-12
2	0.25 wt. %	0.25 wt. %	---	2-12
3	0.25 wt. %	---	0.25 wt. %	2-12

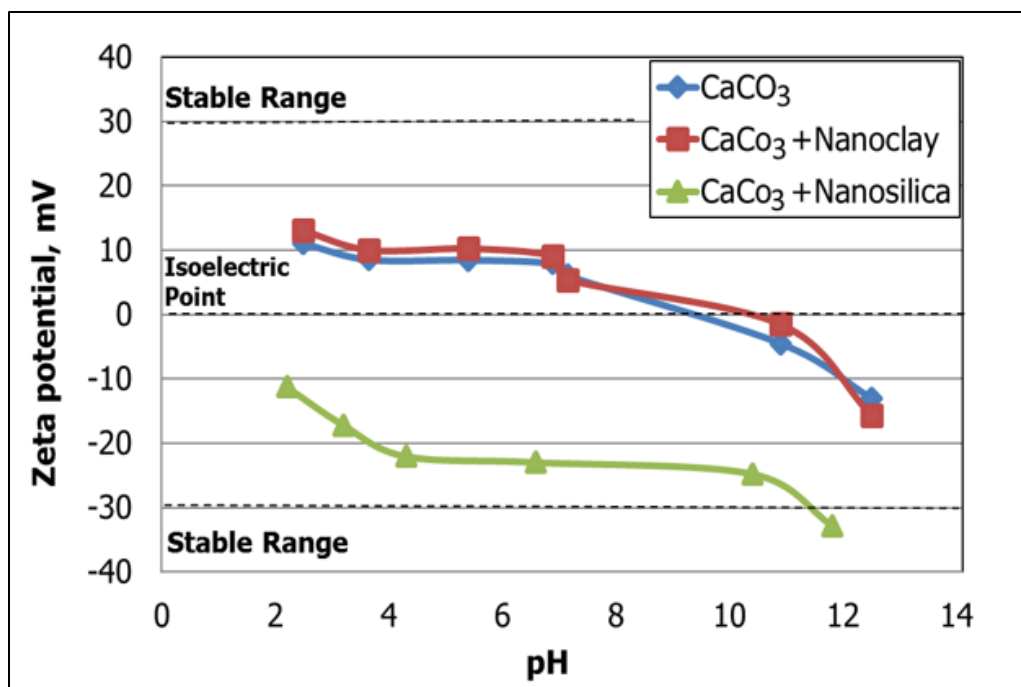


Figure 14: Zeta potential measurements for CaCO_3 and nanoparticles

4.1.2.5 Effect of adding nanoparticulars (nanosilica and nanoclay) to ilmenite on the zeta potential values:

A blend of deionized water and ilmenite with nanoparticles (nanosilica or nanoclay) was destined that includes 0.5 wt% concentration of ilmenite with nanoparticles (1:1 concentration of ilmente with nanoparticles) at unlike pH as exhibited in **Table 10**. **Figure 15** presents that the ilmenite with (nanoclay or nanosilica) 1:1 concentration (0.25 wt% ilmenite and 0.25 wt% nanosilica or nanoclay) is stable at the range of pH (10.2-11.8). When the nanosilica or nanoclay is added to ilmenite, both of them have the same effect on the stability of ilmenite. The isoelectric point of ilmenite is at pH=3.5 and the isoelectric point of ilmenite with nanoclay is at pH=3, **Figure 15**. The elements of ilmenite have less electronegativity. The less electronegativity will increase the zeta potential, **Table 11**.

Table 10: Ilmenite with nanoparticles

Mixtures no.	Ilmenite	Nanoclay	Nanosilica	pH
1	0.5 wt. %	---	---	2-12
2	0.25 wt. %	0.25 wt. %	---	2-12
3	0.25 wt. %	---	0.25 wt. %	2-12

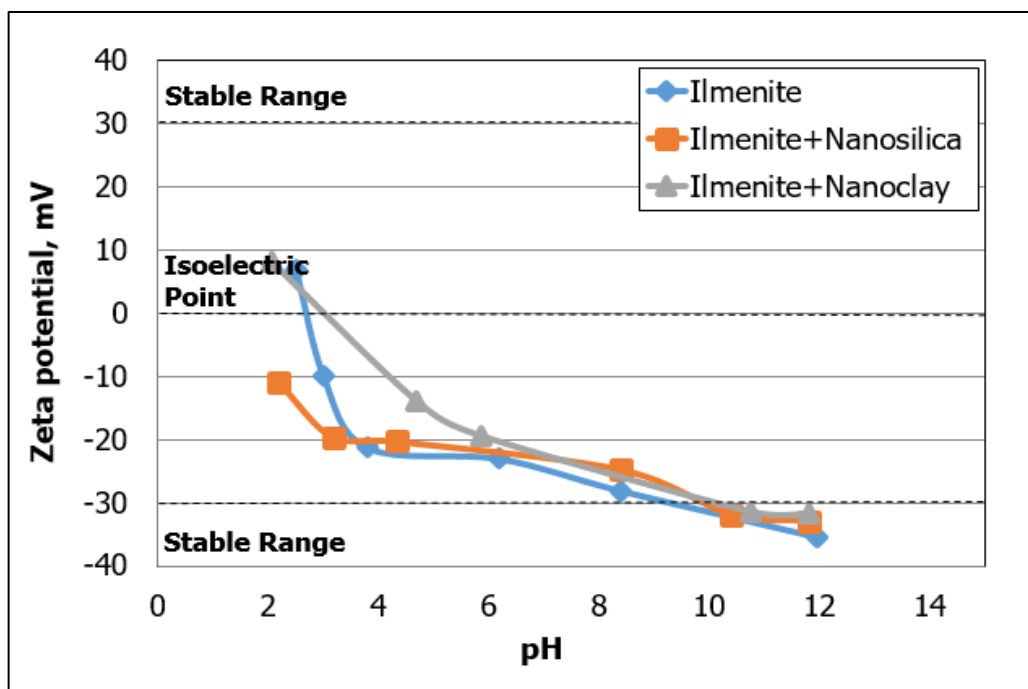


Figure 15: Zeta potential measurements for ilmenite with nanoclay and nanosilica

Table 11: XRF and electronegativity for ilmenite

atomic number	Symbol	Element	Concentration	Electronegativity
13	Al	Aluminum	6.16875	1.5
14	Si	Silicon	5.79375	1.8
15	P	Phosphorus	4.74735	2.1
16	S	Sulfur	4.8115	2.5
19	K	Potassium	4.77085	0.8
20	Ca	Calcium	4.99605	1.0
22	Ti	Titanium	26.60615	1.5
24	Cr	Chromium	4.79465	1.6
25	Mn	Manganese	5.89815	1.5
26	Fe	Iron	31.4361	1.8

4.1.2.6 Effect of adding salts (KCl and NaCl) with nanosilica on the zeta potential values:

A mixing of deionized water with KCl (0.3 wt%) and with NaCl (0.3 wt%) and nanosilica was prepared 0.5 wt% concentration of nanosilica at different Ph values. **Figure 16** shows that the stability of nanosilica can be reduced by adding KCl and NaCl to the solution. Nanosilica is stable at pH 11.5 but the nanosilica with KCl and NaCl are not stable at any value of pH. The isoelectric point of nanosilica is at pH 2.5. The elements of salts such as Cl have large value of electronegativity, the salts have less zeta potential, **Table 12**.

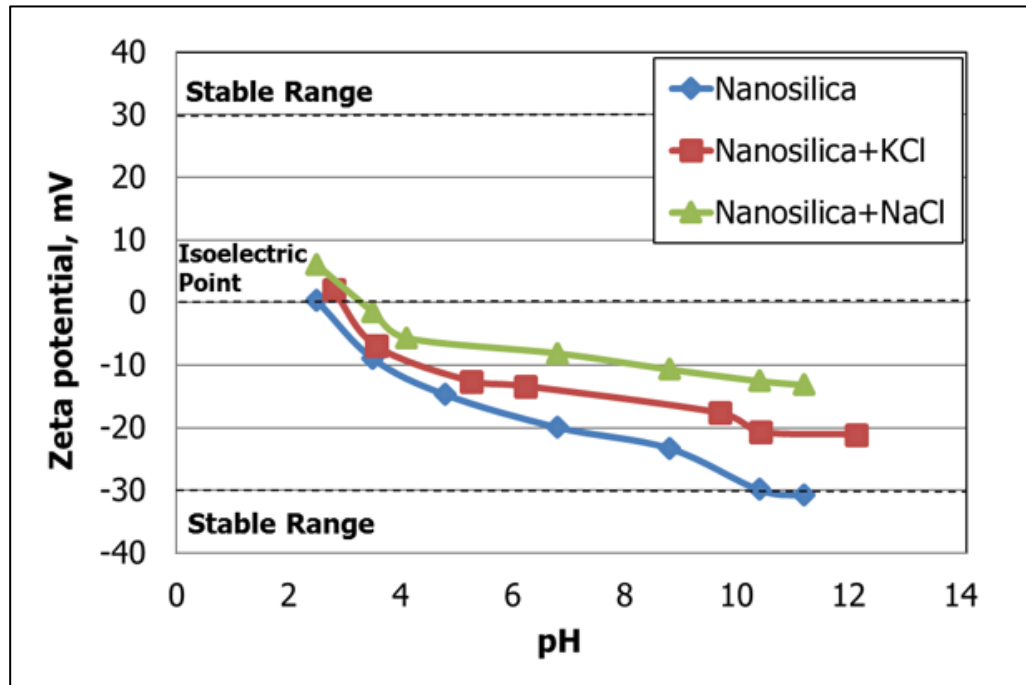


Figure 16: Zeta potential measurements for nanosilica with KCl and NaCl

4.1.2.7 Effect of adding salts (KCl and NaCl) with nanoclay on the zeta potential values:

A mixture of deionized water with KCl (0.3 wt%) and NaCl (0.3 wt%) and nanoclay was prepared that contains 0.5 wt% concentration of nanoclay at different pH. **Figure 17** exhibits that the stability of nanoclay can be reduced by adding KCl and NaCl to the solution. The nanoclay is not stable at any pH value. The isoelectric point of nanoclay is at pH 11 and the isoelectric point of nanoclay with KCl is at pH 11.5. The chlorine in the salts has high electronegativity to take the zeta potential of the salts to zero point.

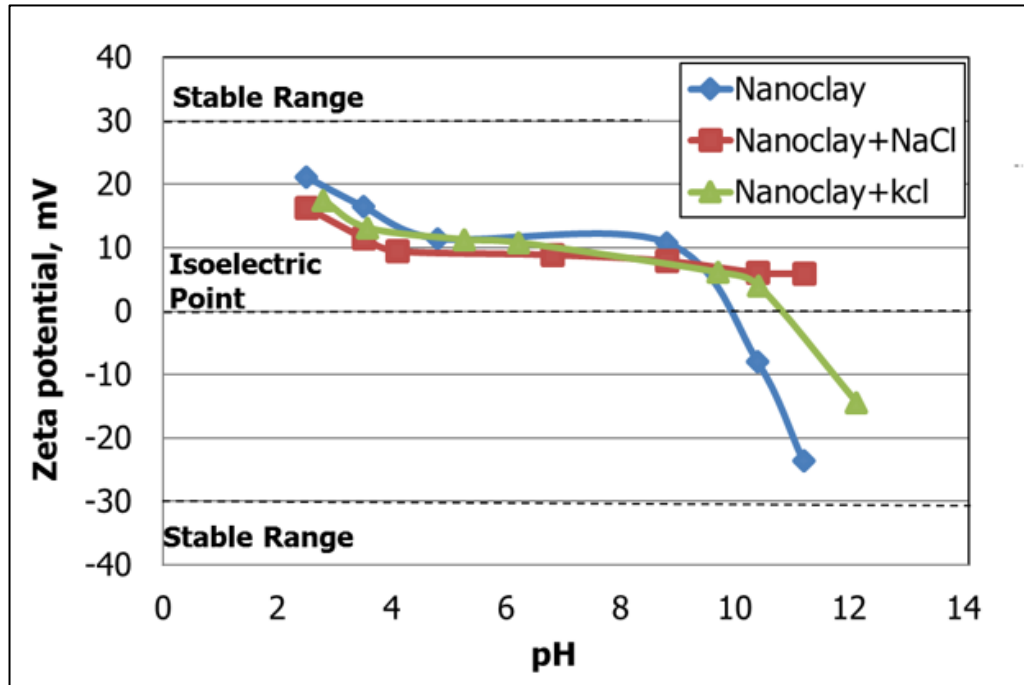


Figure 17: Zeta potential measurements for nanoclay with KCl and NaCl

Table 12: XRF and electronegativity for KCl and NaCl and CaCO₃

atomic number	Symbol	Element	Electronegativity
20	Ca	Calcium	1.0
6	C	Carbone	2.5
8	O	Oxygen	3.5
19	K	Potassium	0.8
11	Na	Sodium	0.9
17	Cl	Chlorine	3.0

4.1.2.8 Zeta potential measurements for bentonite:

Montmorillonite the Aluminum and silicon have different valences between the ions of them make a many negative charge in the alumina-silicate crystal structure,[59].The bentonite is stable from 5-12 pH value, **Figure 18**. The values of electronegativity of elements of bentonite are small, the bentonite have large negative zeta potential, **Table 13**.

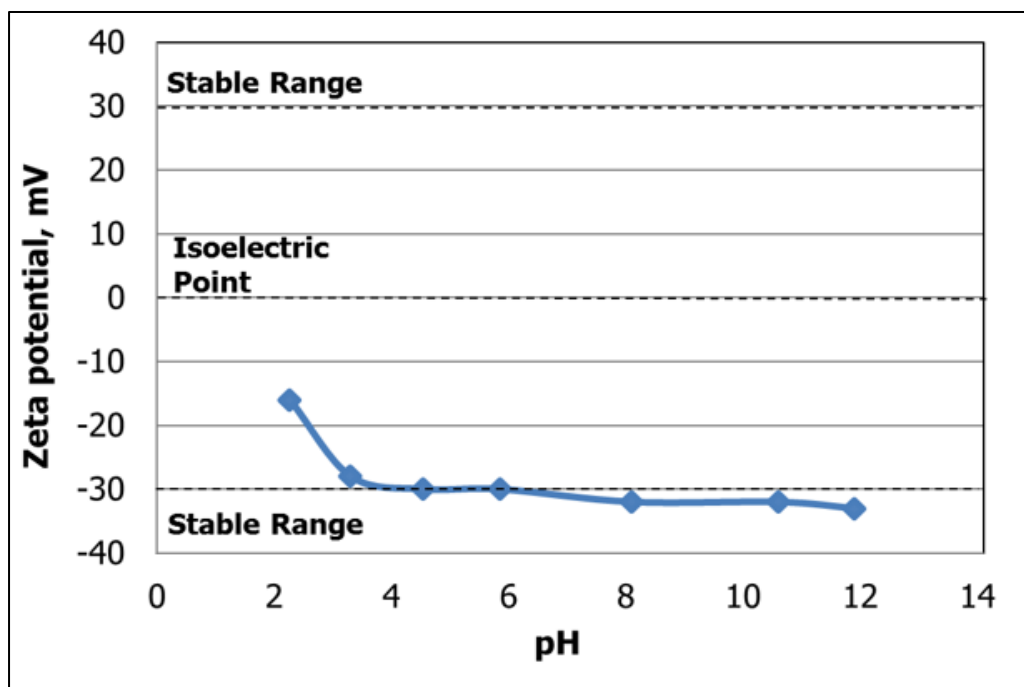


Figure 18: Zeta potential measurements of bentonite

Table 13: XRF and electronegativity for bentonite

Atomic number	Symbol	Element	Concentration	Electronegativity
13	Al	Aluminum	13.38	1.5
14	Si	Silicon	29.895	1.8
15	P	Phosphorus	5.7714	2.1
16	S	Sulfur	5.2671	2.5
17	Cl	Chlorine	5.5621	3.0
19	K	Potassium	5.9177	0.8
20	Ca	Calcium	5.9051	1.0
22	Ti	Titanium	6.886	1.5
25	Mn	Manganese	16.125	1.5
26	Fe	Iron	7.659	1.8

4.2 Results of the rheological properties and gel strength of the drilling fluid

The rheological properties (apparent viscosity, plastic viscosity, and yield point) and gel strength are important properties of drilling fluid to carry and suspend the cuttings in the time of circulation and when the pump is off. The apparent viscosity is defined as the viscosity that measures the fixed shear rate at estimate the given conditions (pressure and temperature). Bingham model is used to find the plastic viscosity and yield point. The plastic viscosity and yield point is the slope and intercept by plotting the shear rate versus shear stress, respectively.

The yield point depends on the electro chemical charges in the drilling fluid under the same conditions. When the electro chemical charges attract each other, the yield point increase. The yield point is the attractive force between the particles in the drilling fluid. The yield point should increase to clean the wellbore hole and to increase the equivalent circulating density. The plastic viscosity depends on the concentrations, sizes and shape of the solid in the drilling fluid. Increasing plastic viscosity will increase differential sticking and decrease the rate of penetration [57]. Yield point is the measure of the thixotropic properties of the drilling mud at flow conditions and the gel strength is the thixotropic properties of drilling fluid at static conditions, [57].

The gel strength is the attractive force between the particles in the drilling fluid at the static conditions. When the yield point increases, the gel strength will increase because both of them depend on the thixotropic properties of the drilling fluid. There are two types of gel strength, a weak gel strength and strong gel strength. The weak gel strength is the gel strength of a thin drilling fluid and the strong gel strength is the gel strength of a thicker

drilling fluid. The weak gel strength becomes initially high and easy to break and increase only slightly with the increase of the stagnation time. The strong gel strength is not easily to break in the initial rotation of the drilling fluid. The strong gel strength will increase with the increasing of stagnation time, [58].

To increase yield point and gel strength, the chemicals should be added to the drilling fluids. The addition of solids to the drilling fluid will increase, the plastic viscosity. Both chemicals and solids will increase the yield point and gel strength and plastic viscosity [59]. The formula of the drilling fluid that is used is listed in, **Table 14**.

Table 14: Drilling fluid formula for lab scale

Material	Quantity	Units	Mixing Time, minutes
Distilled Water	308	g	---
Defoamer	0.33	cm ³	0.5
Bentonite	Different concentrations	g	20
Xc-polymer	1.5	g	20
Starch	6	g	20
KCL	80	g	20
KOH	0.3	g	1
Sodium sulfide	0.25	g	1
Nanoparticles	Different concentrations	g	20
CaCO ₃	30	g	10

The main objectives of this study were to investigate:

- The effect of pressure on the rheological properties (apparent viscosity, plastic viscosity and yield point) and gel strength (10 second, 10 minutes and 30 minutes).
- The effect of temperature on the rheological properties (apparent viscosity, plastic viscosity and yield point) and gel strength (10 second, 10 minutes and 30 minutes).
- Measure the rheological properties and gel strength of water based drilling fluid with different concentrations of bentonite at different temperatures (85°F, 120°F, 150°F, 200°F).
- Compare the rheological properties and gel strength of water based drilling fluid with different concentrations (1,3,5,7.5,10% wt) of nanoparticles (nanoclay and nanosilica) with 10% wt and without bentonite at different temperatures (85 °F, 120 °F, 150 °F, 200 °F).
- Study the gel strength (10 second, 10 minutes and 30 minutes) of water based drilling fluid with different concentrations of bentonite and nanoparticles (nanoclay and nanosilica) at different temperatures (85 °F, 120 °F, 150 °F, 200 °F).

4.2.1 Rheological properties of base drilling fluid

The rheometer was used to measure the rheological properties at 85 °F at different pressures (14.7 psi to 500 psi). **Figure 19** shows that there was no effect of the pressure on the rheometer reading; the behavior of the drilling fluid was almost the same at different shear rate and different pressure. The drilling fluid has a plastic viscosity of 16.75 cP and a yield point of 13.85 lb/100 ft². The gel strength was measured at different time (10 s, 10 min and 30 min) , at 85 °F and at 300 psi and it was found to be 3.8 lb/100 ft² **Figure 20** .

By increasing the temperature to 120°F, the drilling fluid behavior was measured at different pressure as shown in **Figure 21**. The plastic viscosity was 16.75 cP and the yield point was 13.85 lb/100 ft². By calculating the gel strength at different time periods, it was found that the gel strength increased from 2.9 lb/100 ft² at 10 s to 3.2 lb/100 ft² at 10 min and decreased to 1.9 lb/100 ft² at 30 min, **Figure 20**. This behavior is very important as if the drilling fluid lost the gel strength, the cutting will precipitate and accumulate and stuck will happen.

By increasing the temperature to 150°F, the behavior of the drilling fluid was measured at different applied pressure, **Figure 22**. The plastic viscosity reduced from 16.75 cP to 12.83 cP by increasing the temperature from 120°F to 150°F. The yield point decreased also from 13.85 lb/100 ft² to 10.16 lb/100 ft² by increasing the temperature from 120°F to 150°F. Increasing the temperature from 120°F to 150° increased the gel strength from 2.3 lb/100 ft² at 10 s to 3.0 lb/100 ft² at 10 min and decreased to 1.7 lb/100 ft² at 30 min, **Figure 20**.

For further investigation about the effect of temperature on the rheological properties of the base formulation, the temperature increased to 200°F and the rheological properties

were measured. **Figure 23** shows the behavior of the drilling fluid at different pressure and 200°F. The plastic viscosity decreased to 11.77 cP and the yield point decreased to 7.20 lb/100 ft². At 200°F, the gel strength was found to be zero lb/100 ft² after 30 min(**Figure 20**) which is very dangerous in the drilling operation. Sticking problem will occur as a result of cuttings accumulation in time of no circulation as the drilling fluid has no gel strength at 200°F. The plastic viscosity and yield point of the based drilling fluid are constant at different pressure and at the same temperature **Figure 24, Figure 25**.

Table 15: Drilling fluid formulation for the based case

Material	Quantity	Units	Mixing Time, minutes
Distilled Water	308	g	---
Defoamer	0.33	cm ³	0.5
Xc-polymer	1.5	g	20
Starch	6	g	20
KCL	80	g	20
KOH	0.3	g	1
Sodium sulfide	0.25	g	1
CaCO ₃	30	g	10

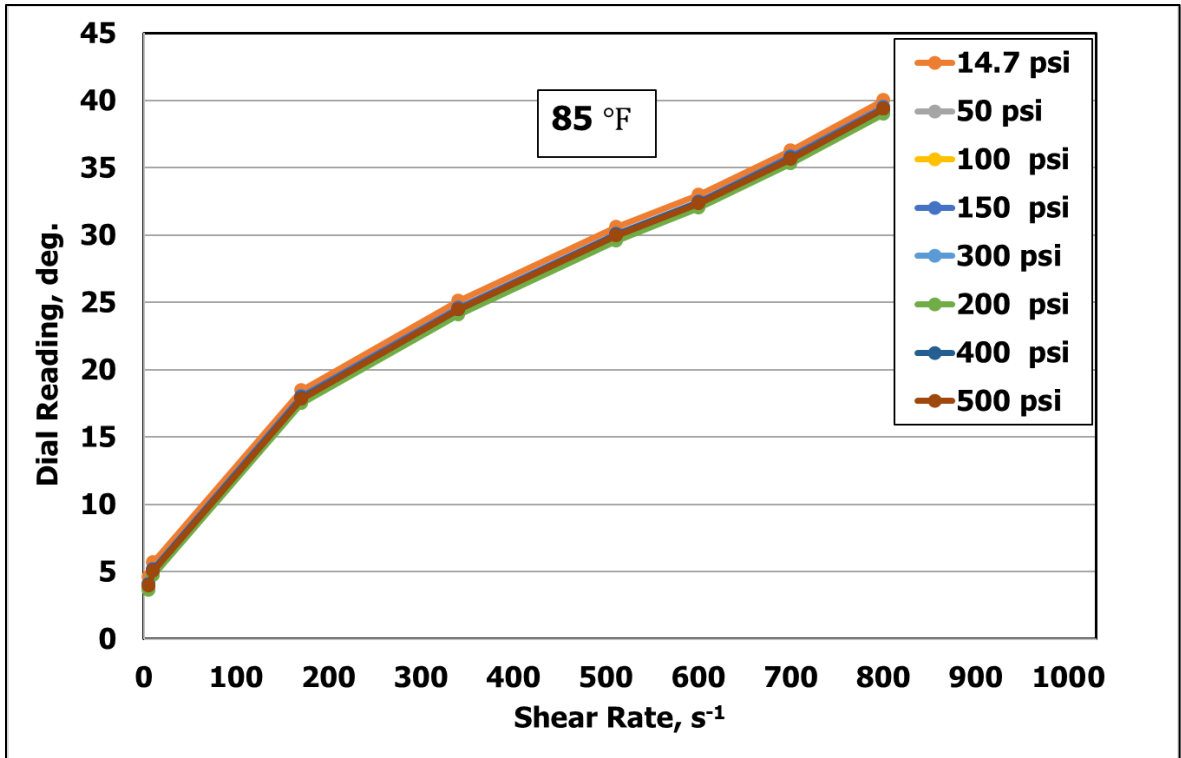


Figure 19: Based fluid behavior at 85 °F with different applied pressure

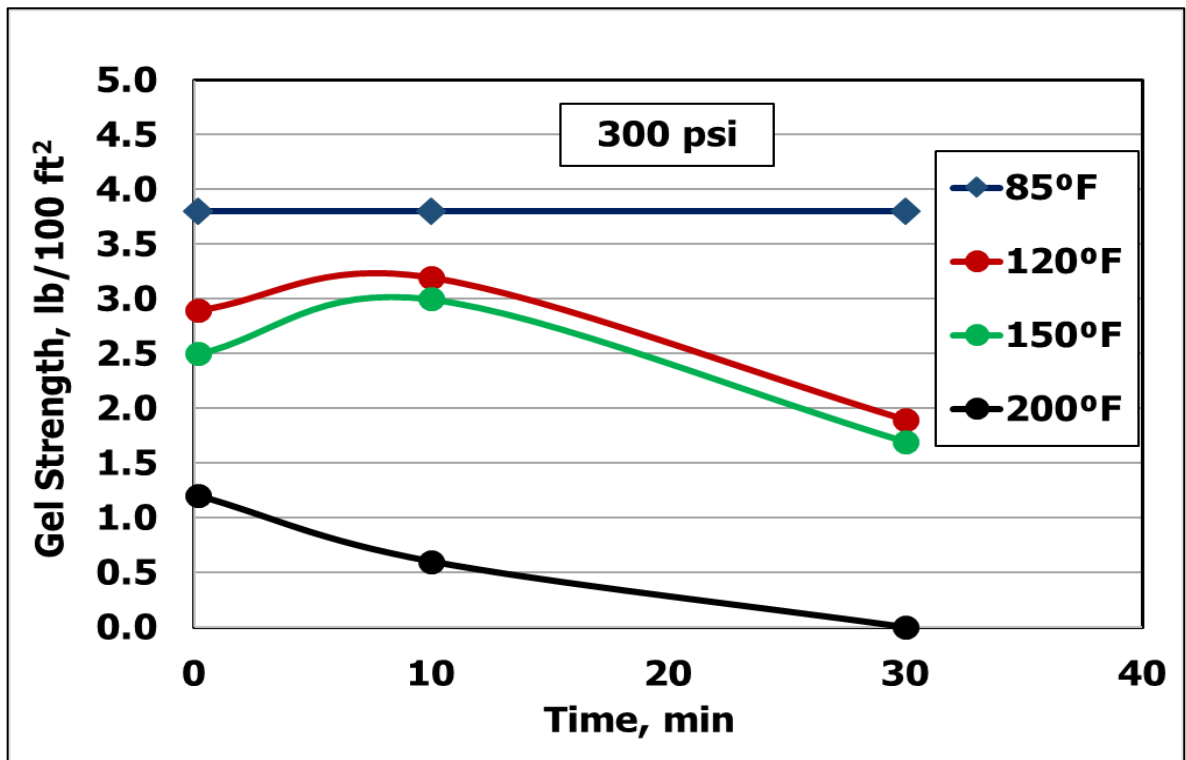


Figure 20: The gel strength of based drilling fluid

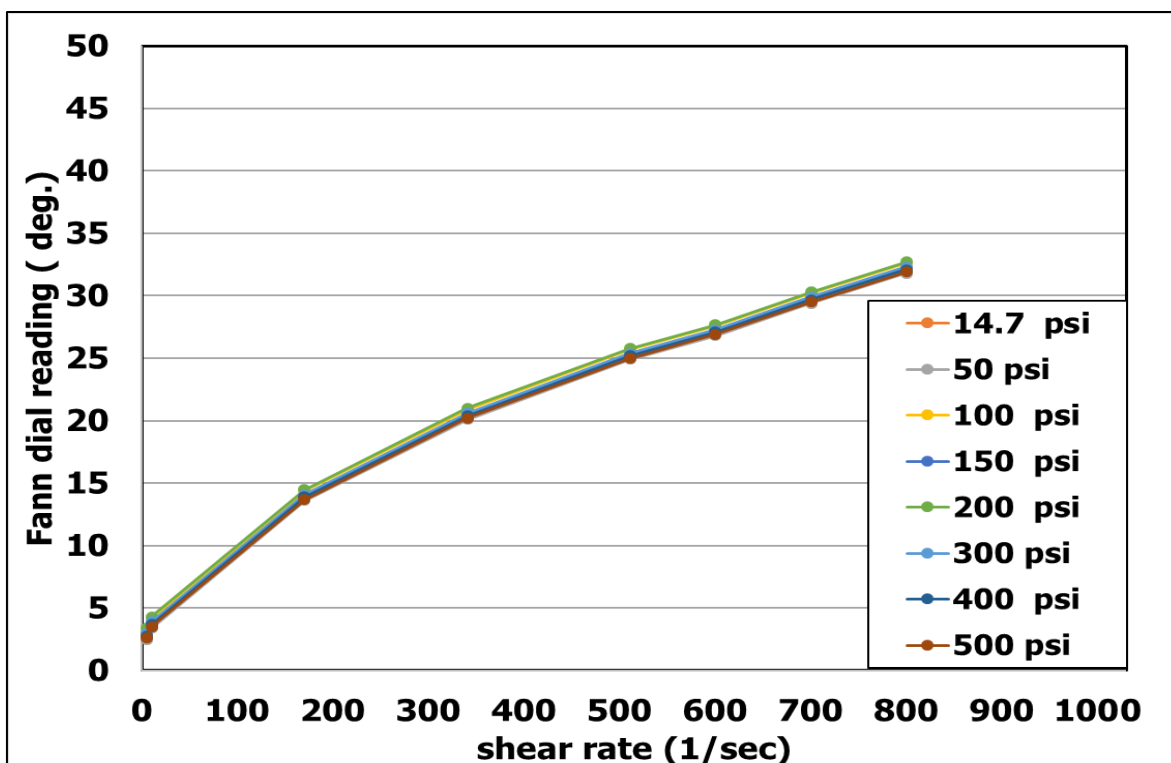


Figure 21: Based fluid behavior at 120 °F with different applied pressure

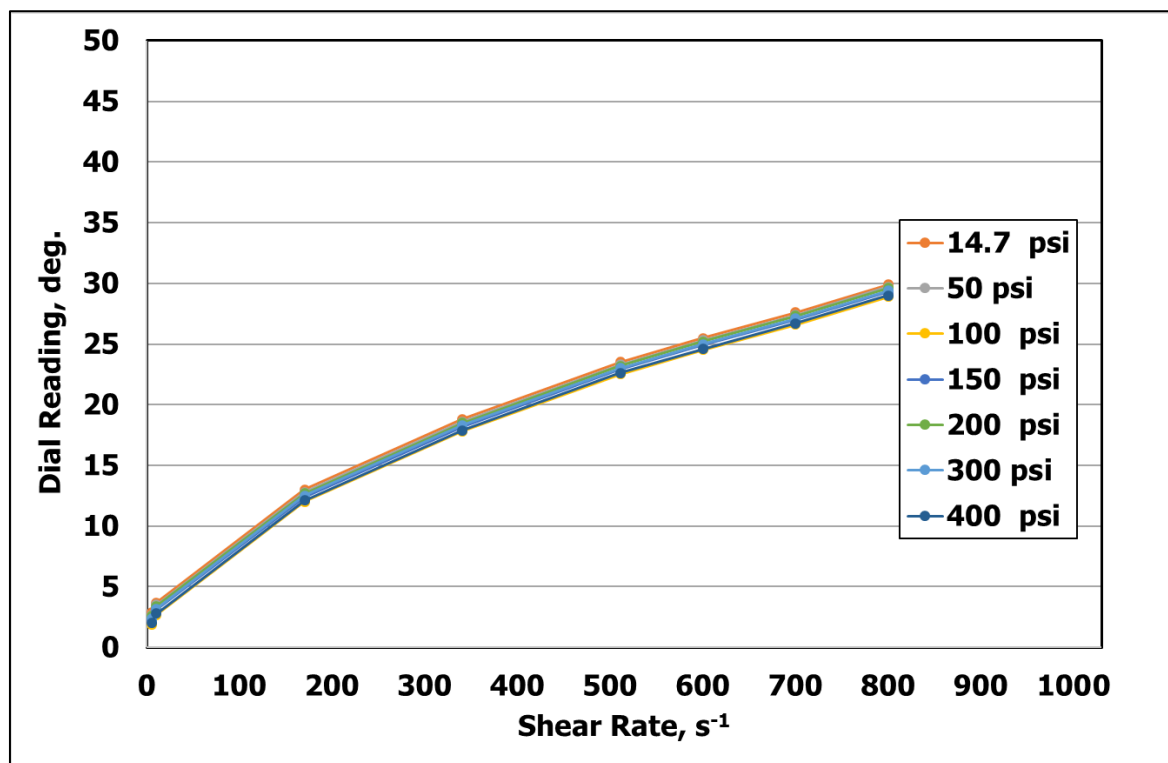


Figure 22: Based fluid behavior at 150 °F with different applied pressure

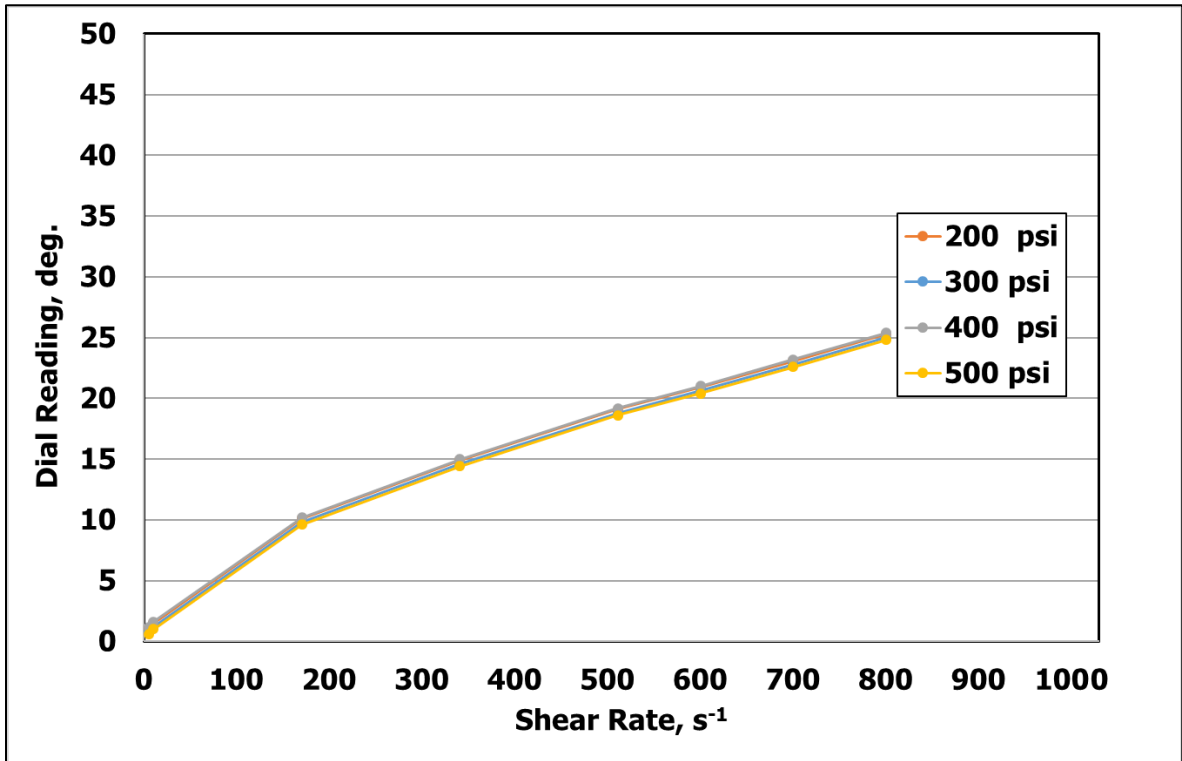


Figure 23: Based fluid behavior at 200 °F with different applied pressure

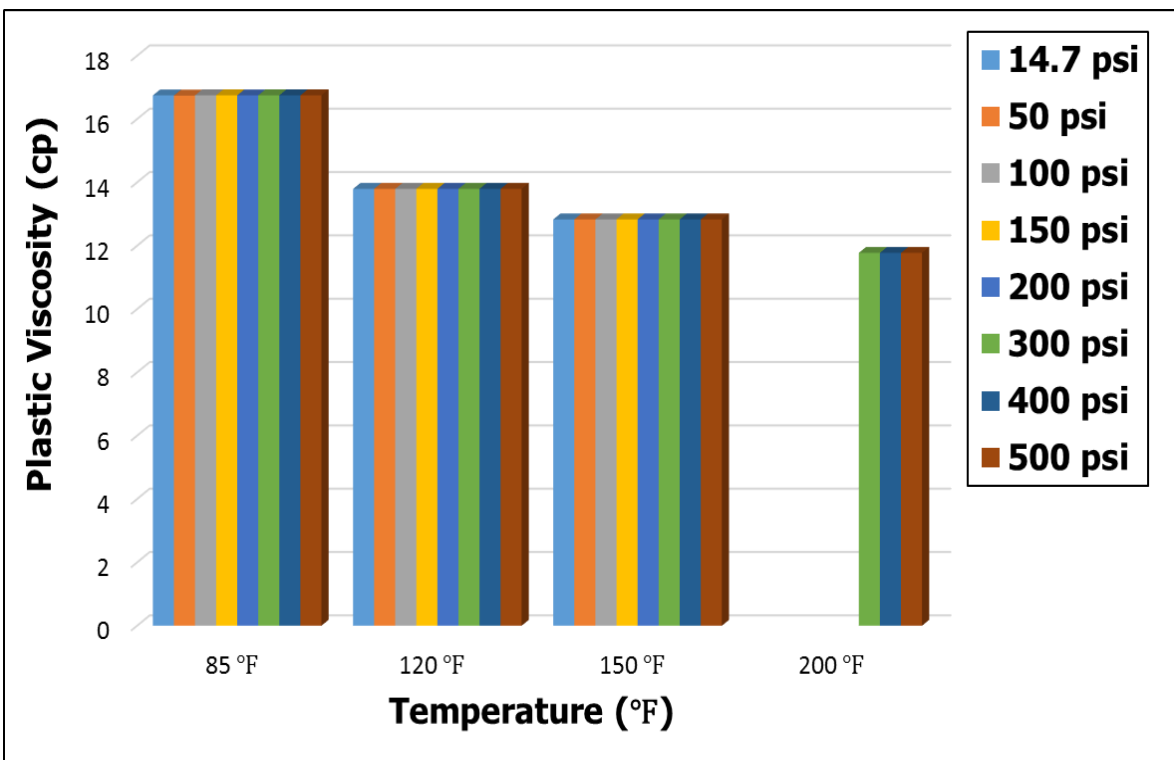


Figure 24: The plastic viscosity of based drilling fluid

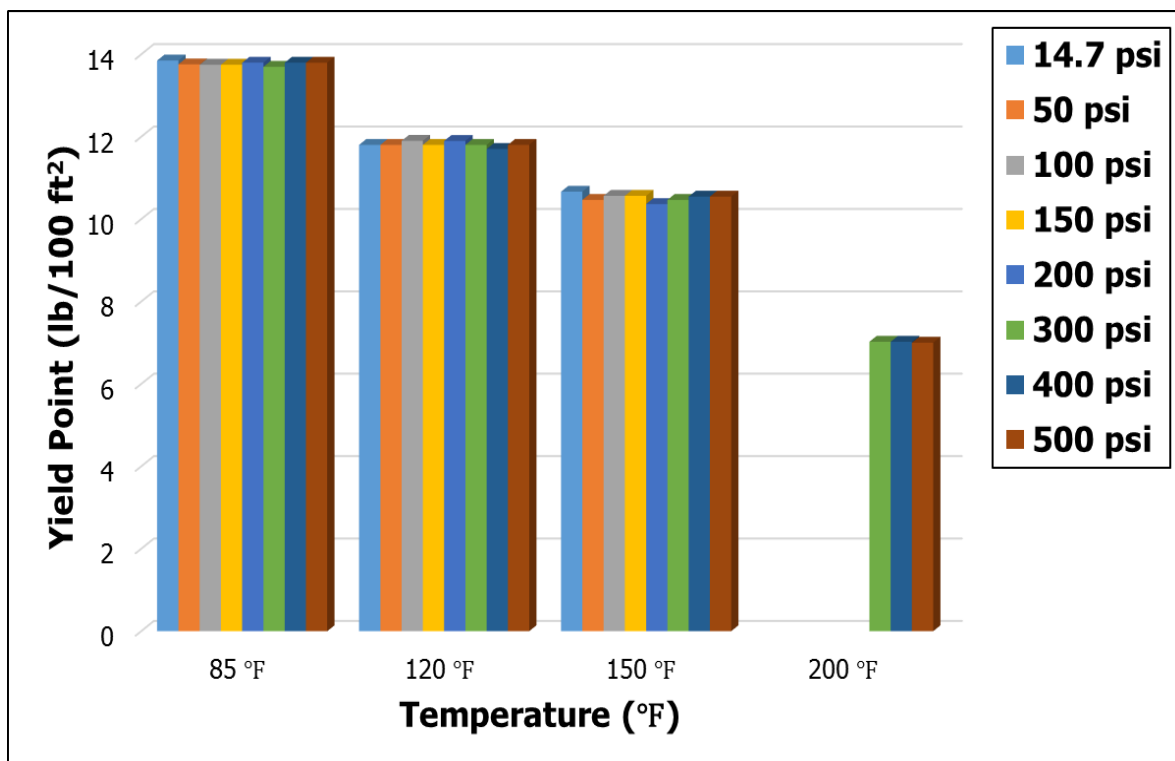


Figure 25: The yield point of based drilling fluid

4.2.2 Effect of bentonite concentrations in the rheological properties of drilling fluid

Sticking problem will occur as a result of fluid cuttings accumulation in time of no circulation as the drilling fluid has no gel strength at the based drilling fluid at 120 °F and more than 120 °F. To overcome this problem, different concentrations of bentonite were added to the drilling fluid. Rheological properties were measured at 300 psi and different temperature, **Table 16**. Adding different concentrations of bentonite to the drilling fluid increased the rheological properties at 85 °F, **Figure 26**. **Figure 27** shows that the gel strength increased from 4.5 lb/100 ft² at 10 s to 5.5 lb/100 ft² at 10 min and 5.5 lb/100 ft² at 30 min using 3.33 wt % bentonite. The gel strength at 6.6 wt % bentonite increased from 4.6 lb/100 ft² at 10 s, 6.4 lb/100 ft² at 10 min to 7.3 lb/100 ft² at 30 min. And the gel strength at 10 wt % bentonite increased from 7.5 lb/100 ft² at 10 s, 9.7 lb/100 ft² at 10 min. and then increased to 14.7 lb/100 ft² at 30 min, **Figure 27**.

For further investigation about the effect of temperature on the rheological properties of the different concentrations of bentonite with the drilling fluid, the temperature increased to 120 °F and the rheological properties were measured. By increasing the temperature, the behavior of the drilling fluid decreased. At the same temperature 120 °F, the behavior increased by increasing the concentrations of the bentonite, **Figure 28** . Increasing the temperature from 85 °F to 120 °F, the gel strength started to increase from 3 lb/100 ft² at 10 s to 3.5 lb/100 ft² at 10 min and started to decrease to 2.1 lb/100 ft² at 30 min, **Figure 29** The gel strength at 6.6 wt % bentonite increased from 4 lb/100 ft² at 10 s to 4.5 lb/100 ft² at 10 min and increased to 5 lb/100 ft² at 30 min, **Figure 29**. And the gel strength at 10

wt % bentonite was increased from 6.9 lb/100 ft² to 8 lb/100 ft² (10 s to 10 min) and then was increased to 13.7 lb/100 ft² at 30 min.

By increasing the temperature to 150 °F, the drilling fluid properties were measured at different concentrations of bentonite and at 300 psi as shown in **Figure 30**. The gel strength at 150 °F and at 3.33 wt % bentonite increased from 2.5 lb/100 ft² at 10 s to 3.1 lb/100 ft² at 10 min and then decreased to 1.9 at 30 min, **Figure 31**. At 6.6 wt % bentonite, the gel strength increased from 2.9 lb/100 ft² at 10 s to 4 lb/100 ft² at 10 min and increase to 4.1 lb/100 ft² at 30 min, **Figure 31**. At 10 wt % bentonite, the gel strength increased from to 3.1 lb/100 ft² at 10 s to 5.1 lb/100 ft² at 10 min and increased to 7.1 lb/100 ft² at 30 min, **Figure 31**.

To deep understand the effect of temperature on the rheological properties of the different concentrations of bentonite, the temperature was increased to 200 °F and the rheological properties were measured. **Figure 32** shows the behavior of the drilling fluid at 300 psi and 200 °F. The gel strength at 200 °F and at 3.33 wt % bentonite increased from 2.5 lb/100 ft² at 10 s to 3 lb/100 ft² at 10 min and was decreased to 1.8 lb/100 ft² at 30 min, **Figure 33**. The gel strength at 200 °F and at 6.6 wt % bentonite increased from 2.5 lb/100 ft² at 10 s to 3.4 lb/100 ft² at 10 min and 3.5 lb/100 ft² at 30 min, **Figure 33**. The gel strength at 10 wt % bentonite was increased from 2.5 lb/100 ft² at 10 s to 4 lb/100 ft² at 10 min and then increased to 4.8 lb/100 ft² at 30 min, **Figure 33**.

The optimum concentration of bentonite was 6.6 wt % bentonite since increasing the concentration of bentonite in the reservoir section will cause damage. The rheological properties of the drilling fluid with bentonite were increased by increasing the

concentration of bentonite. The rheological properties were increased because bentonite platelets dispersed in starch polymer networks and swollen granules [60].

Table 16: Drilling fluid formulation for different concentrations of bentonite

Material	Quantity	Units	Mixing Time, minutes
Distilled Water	308	g	---
Defoamer	0.33	cm ³	0.5
Xc-polymer	1.5	g	20
Bentonite	1,2,3	g	20
Starch	6	g	20
KCL	80	g	20
KOH	0.3	g	1
Sodium sulfide	0.25	g	1
CaCO ₃	30	g	10

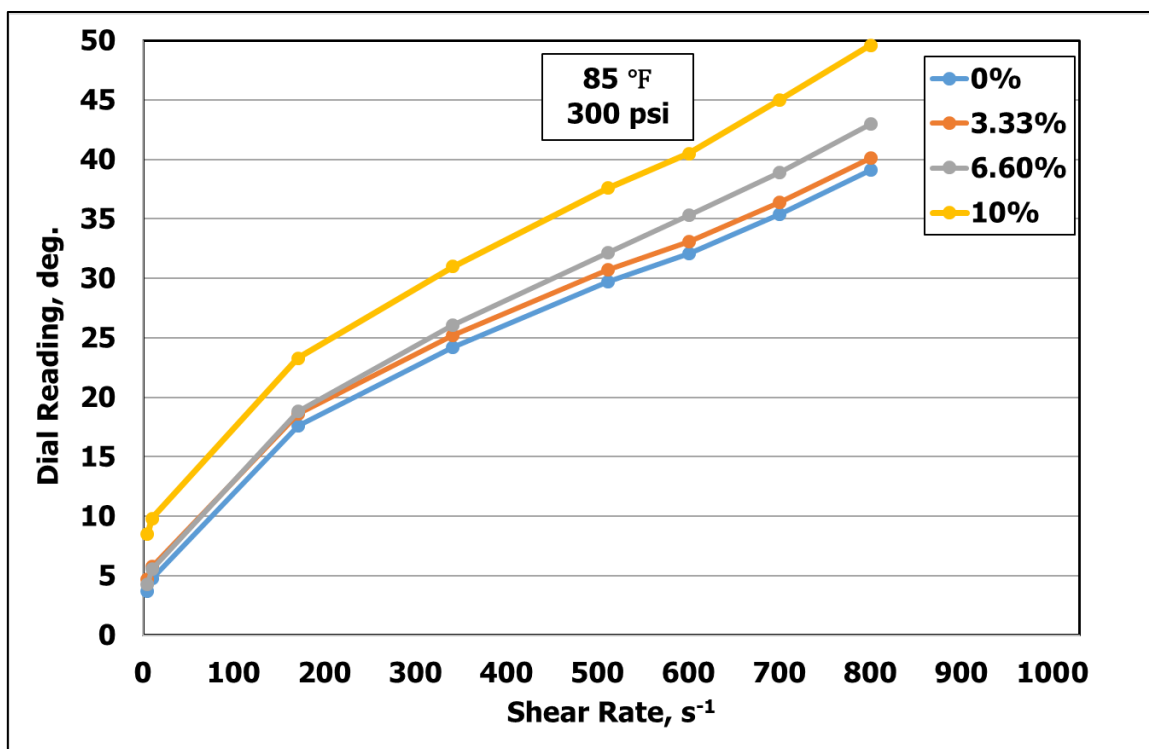


Figure 26: Different concentrations of bentonite with drilling fluid behavior at 85 °F

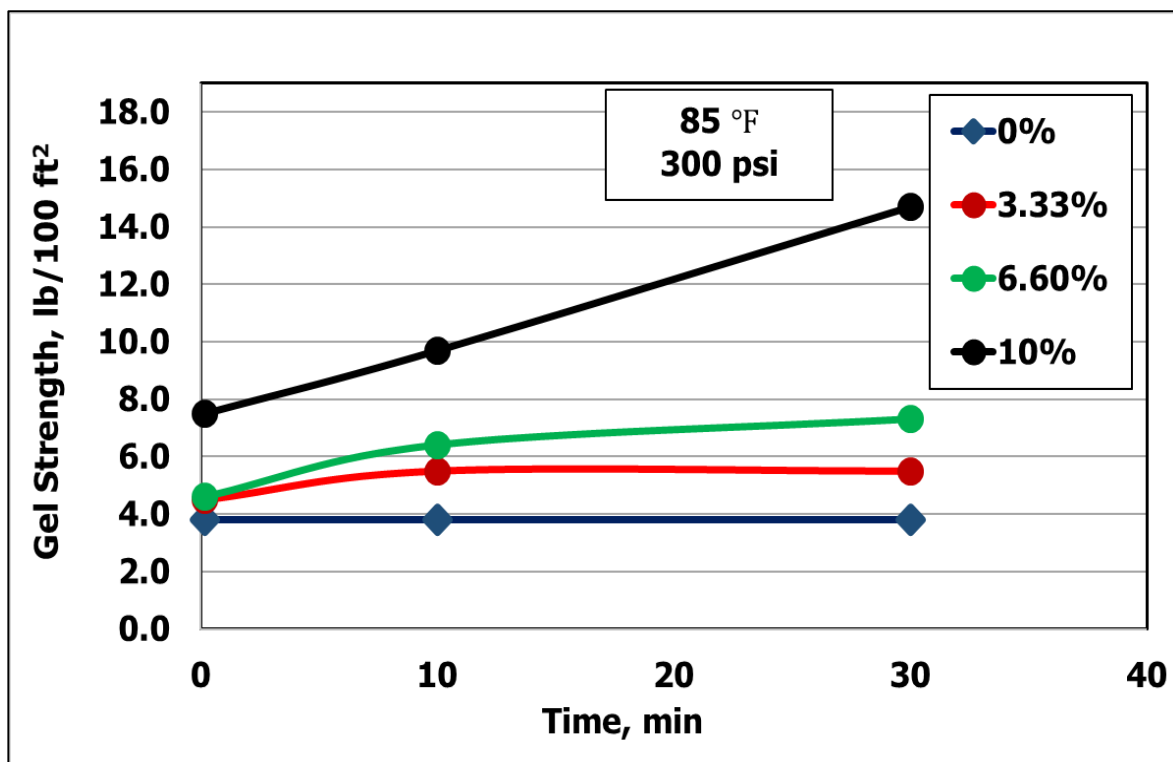


Figure 27: The gel strength of different concentrations of bentonite with drilling fluid at 85 °F

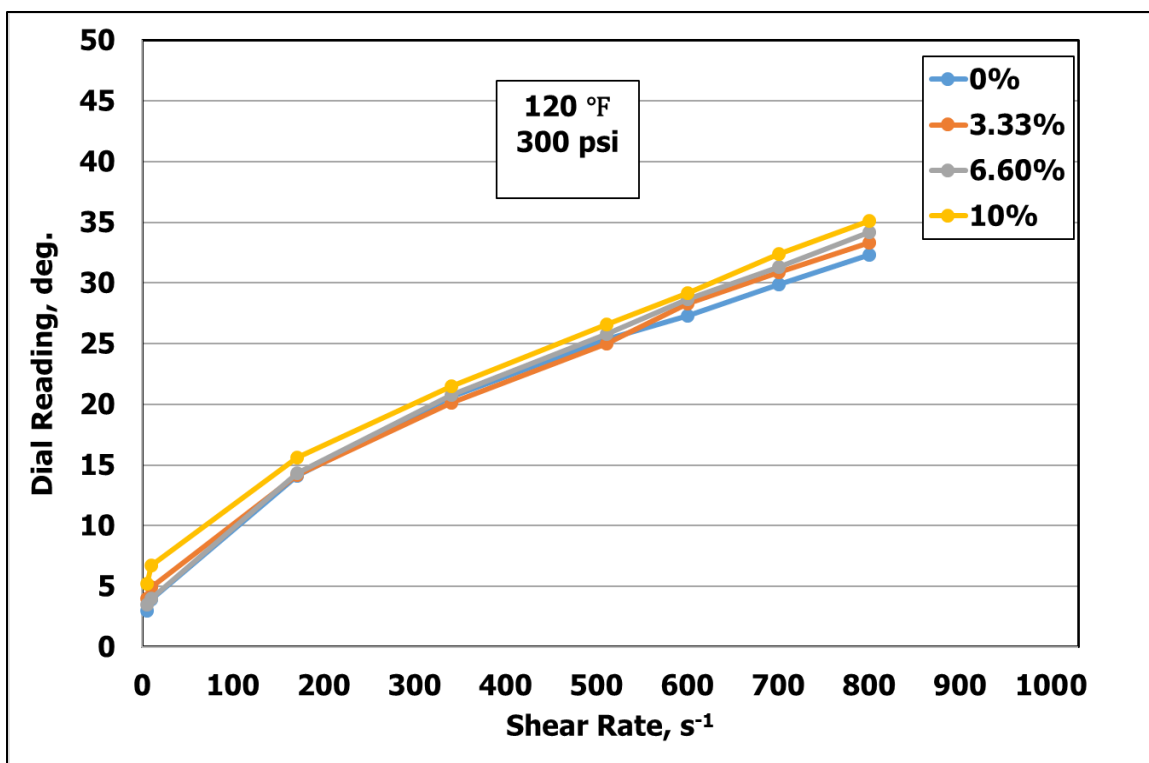


Figure 28: Different concentrations of bentonite with drilling fluid behavior at 120 °F

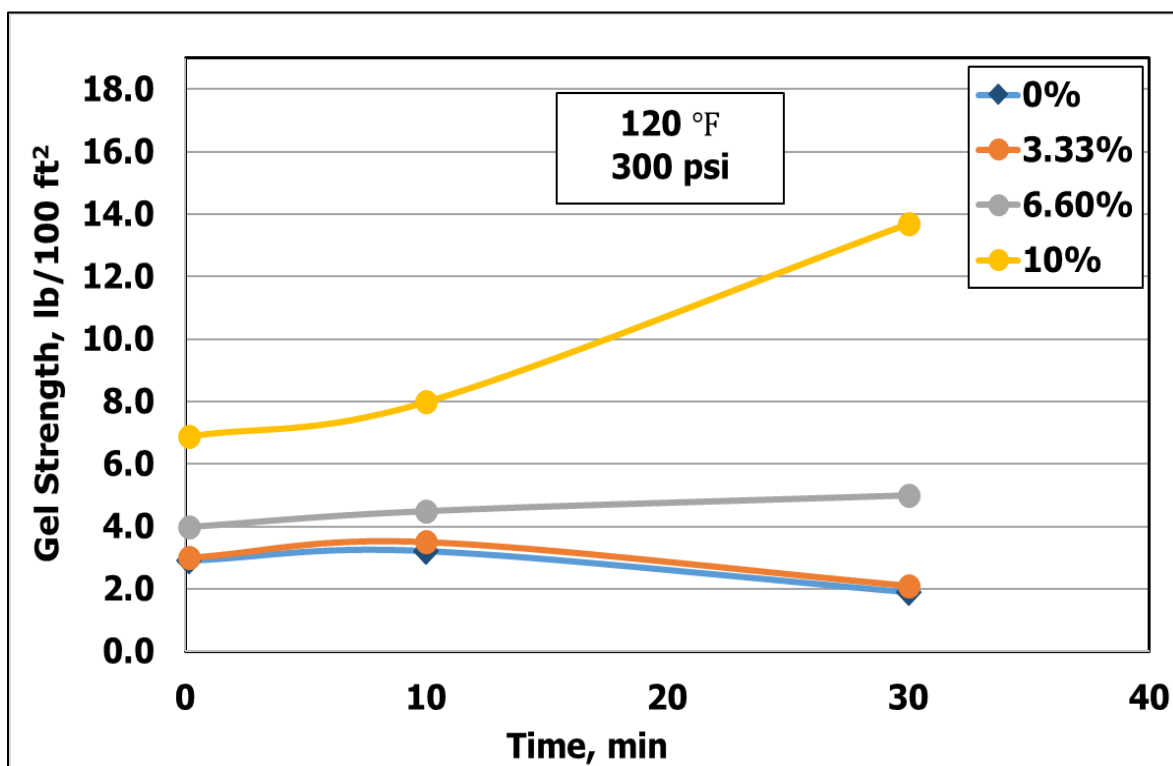


Figure 29: The gel strength of different concentrations of bentonite with drilling fluid at 120 °F

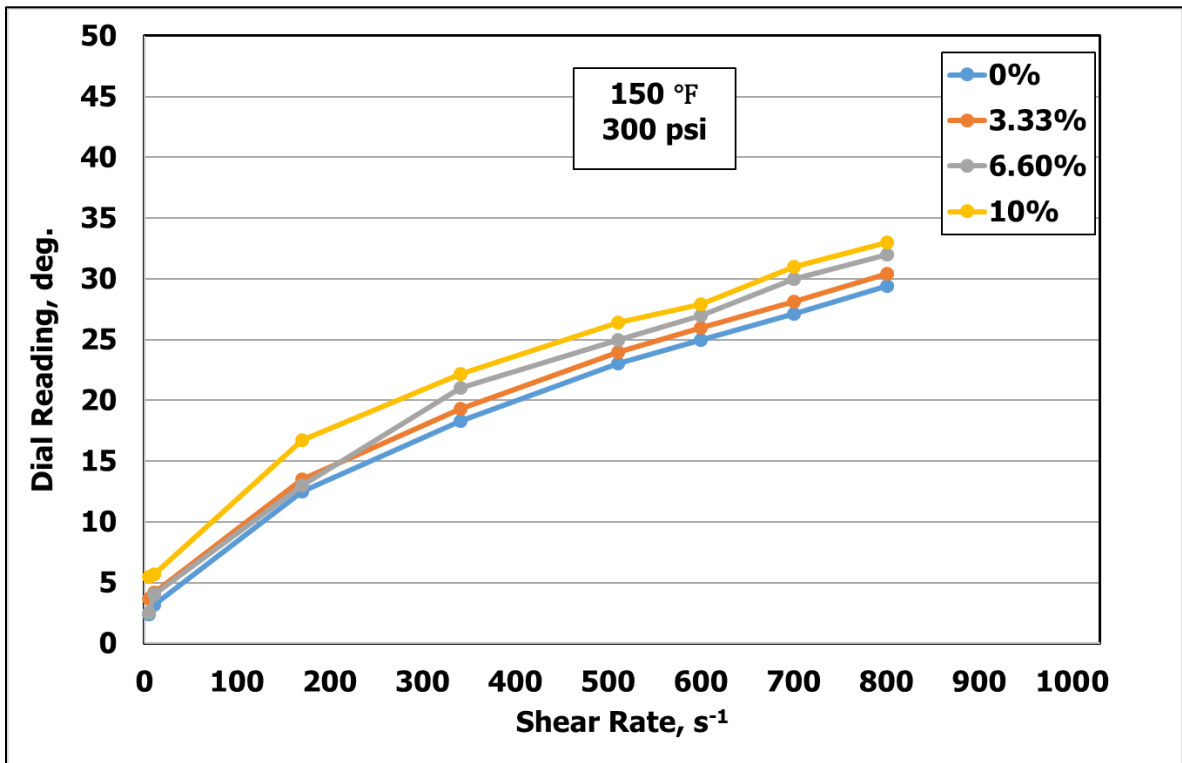


Figure 30: Different concentrations of bentonite with drilling fluid behavior at 150 °F

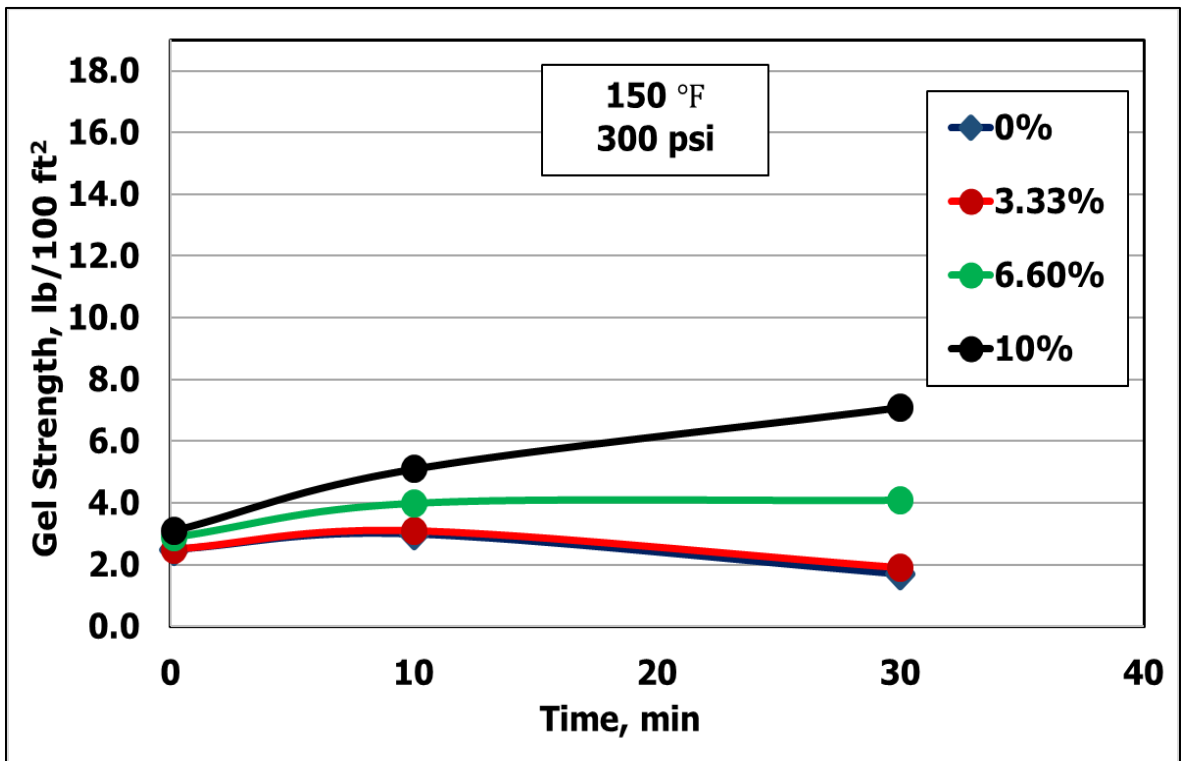


Figure 31: The gel strength of different concentrations of bentonite with drilling fluid at 150 °F

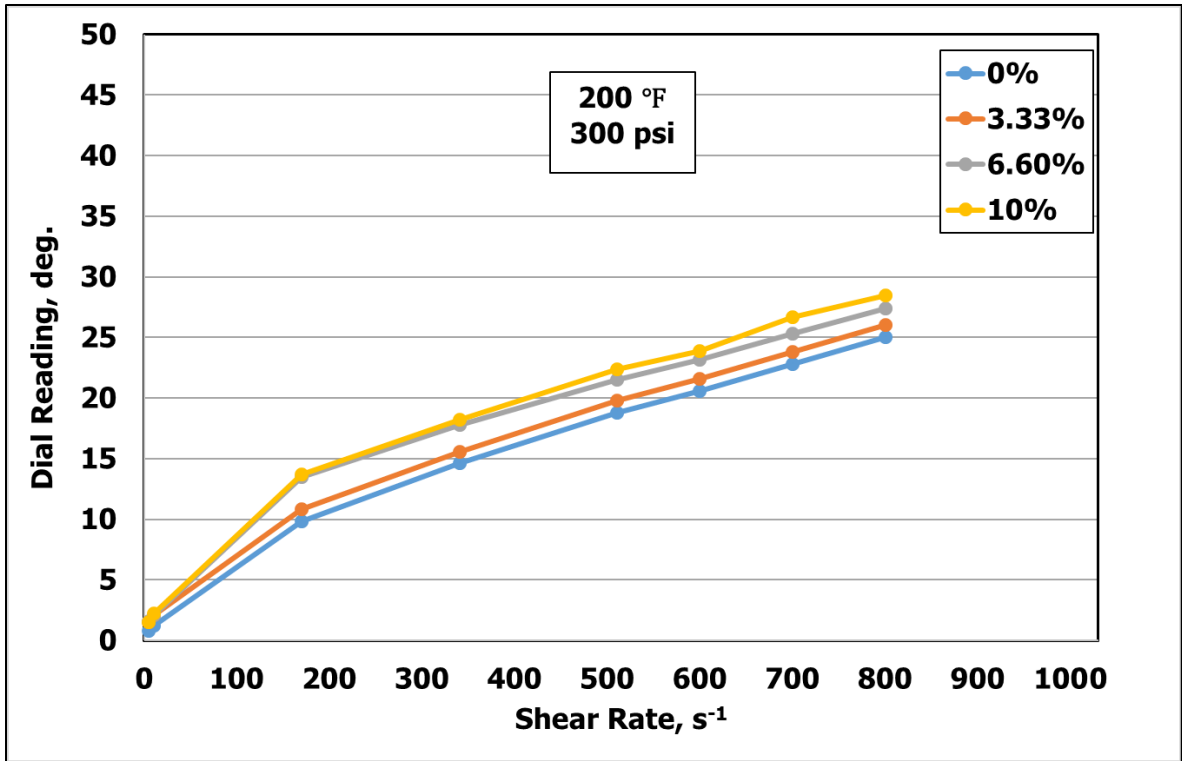


Figure 32: Different concentrations of bentonite with drilling fluid behavior at 200 °F

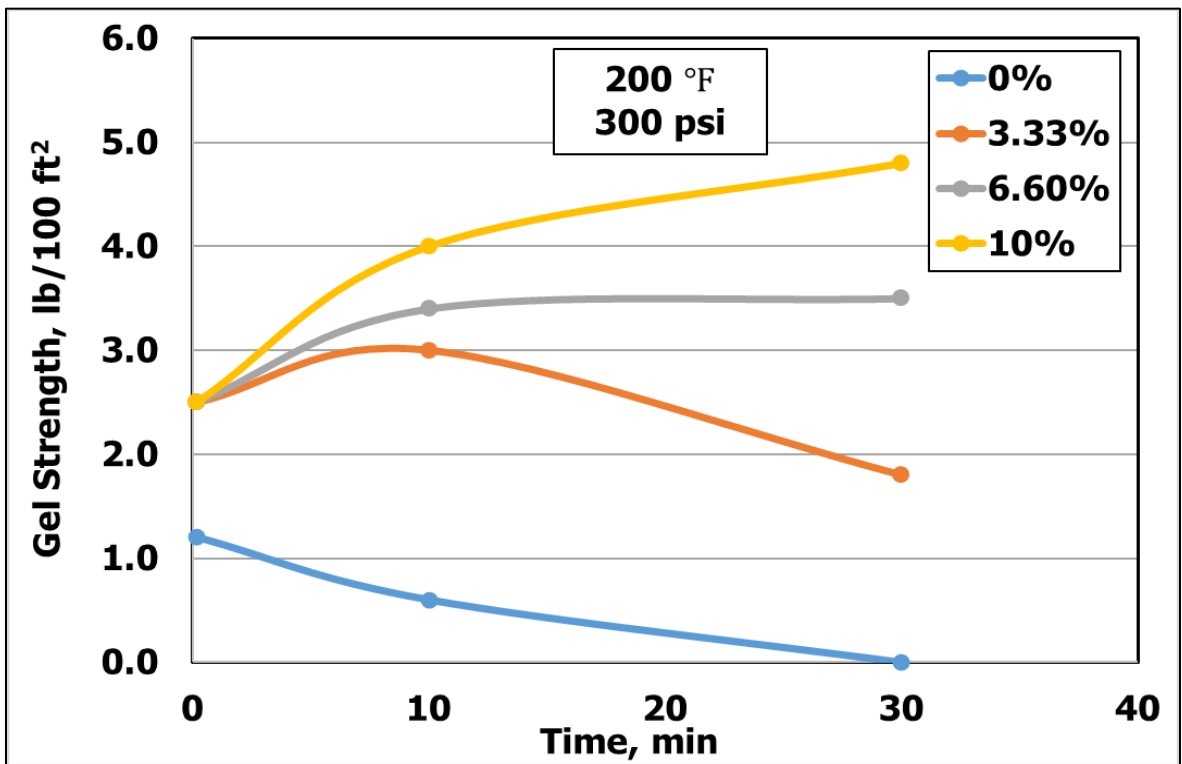


Figure 33: The gel strength of different concentrations of bentonite with drilling fluid at 200 °F

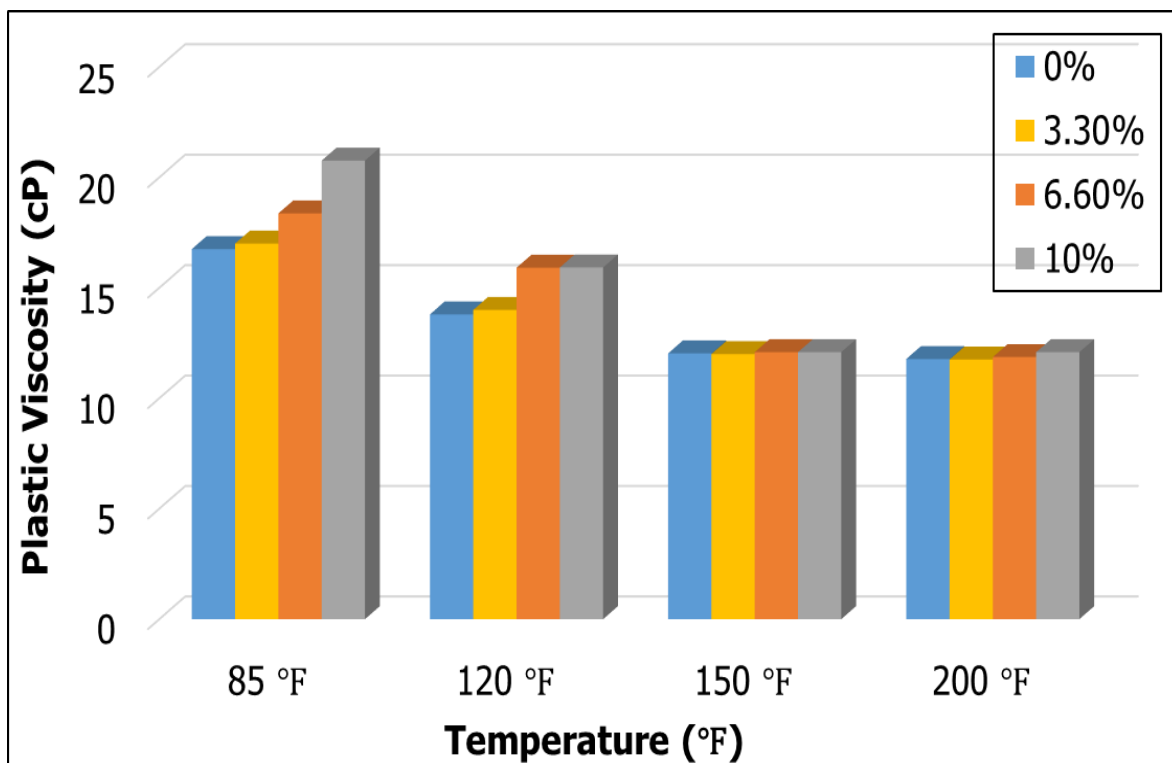


Figure 34: The plastic viscosity of different concentrations of bentonite with drilling fluid

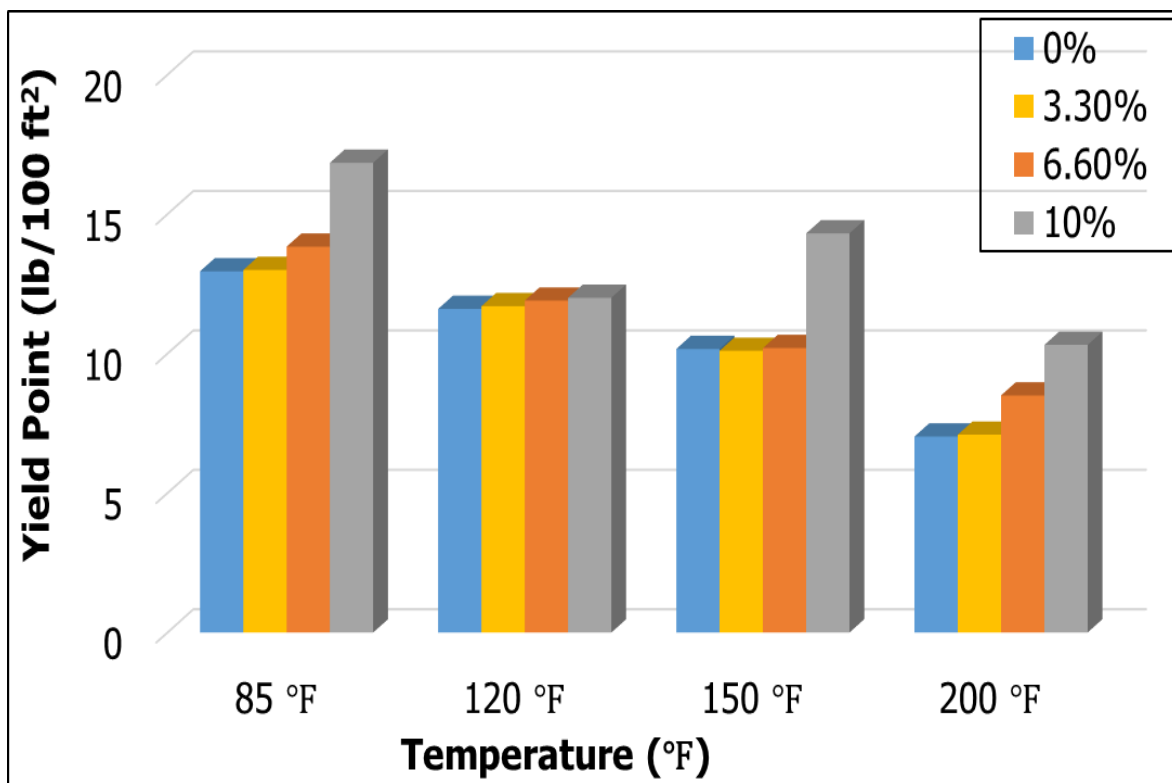


Figure 35: The yield point of different concentrations of bentonite with drilling fluid

4.2.3 Rheological properties of different concentrations of nanoclay with drilling fluid

Sticking problem will happen as a result of cuttings accumulation in time of no circulation as the drilling fluid has no gel strength at the base drilling fluid at 120 °F and more than 120 °F. To overcome this problem, different concentrations of nanoclay were added to the drilling fluid. The properties of the drilling fluid with different concentrations of nanosilica were measured, **Table 17**. The behavior of the drilling fluid was measured at different shear rates, different concentrations of nanoclay, different temperatures (85 °F, 120 °F, 150 °F, 200 °F) and at 300 psi. Adding the nanoclay to the drilling fluid decreased the rheological properties of drilling fluid at 85 °F, **Figure 36**. **Figure 37** shows that the gel strength started to increase from 4.1 lb/100 ft² at 10 s to 4.2 lb/100 ft² at 10 min and 4.2 lb/100 ft² at 30 min at 1 wt % nanoclay. The gel strength at 3 wt % nanoclay was constant at 4.9 lb/100 ft² from 10 s to 10 min and then increased to 5.5 lb/100 ft² at 30 min. And the gel strength at 5 wt % nanoclay was constant at 4.5 lb/100 ft² from 10 s to 10 min and then increased to 4.7 lb/100 ft² at 30 min, **Figure 37**.

By increasing the temperature to 120 °F, the drilling fluid rheological properties was measured at different concentrations of nanoclay and at 300 psi as shown in **Figure 38**. The gel strength at 120 °F and at 1 wt % nanoclay was constant at 3.3 lb/100 ft² from 10 s to 10 min and then decreased to 2.2 3 lb/100 ft² at 30 min, **Figure 39**. Increasing the concentration of nanoclay to 3 wt %, the gel strength was constant at 4.8 lb/100 ft² from 10 s to 10 min and increased to 5.3 lb/100 ft² at 30 min, **Figure 39**. The gel strength at 5 wt % nanoclay was decreased from 3.6 lb/100 ft² 10 s to 3.1 lb/100 ft² at 10 min and 30 min, **Figure 39**.

The drilling fluid rheological properties was measured at different concentrations of nanoclay and at 150 °F and 300 psi as shown in **Figure 40**. The gel strength at 150 °F and at 1 wt % nanoclay increased from 2.8 lb/100 ft² at 10 s to 3 lb/100 ft² at 10 min and then decreased to 1.9 lb/100 ft² at 30 min, **Figure 41**. The gel strength at 3 wt % was constant at 3.5 lb/100 ft² from 10 s to 10 min and was decreased to 3.2 lb/100 ft² at 30 min, **Figure 41**. Increasing the concentration of nanoclay to 5 wt %, the gel strength was constant 2.9 lb/100 ft² from 10 s to 10 min and then decreased to 1.2 lb/100 ft² at 30 min, **Figure 41**.

For more understanding the effect of the temperature on the rheological properties of the different concentrations of nanoclay, the temperature increased to 200 °F and the rheological properties were measured. **Figure 42** shows the behavior of the drilling fluid at 300 psi and 200 °F. The gel strength at 200 °F and at 1 wt % nanoclay decreased from 1.5 lb/100 ft² at 10 s to 0.6 lb/100 ft² at 10 min and decreased to 0.3 lb/100 ft² at 30 min, **Figure 43**. The gel strength at 200 °F and at 3 wt % nanoclay decreased from 1.6 lb/100 ft² at 10 s to 0.6 lb/100 ft² at 10 min and decreased to 0 lb/100 ft² at 30 min, **Figure 43**. And the gel strength at 200 °F and at 5 wt % nanoclay decreased from 1.4 lb/100 ft² at 10 s to 0.5 lb/100 ft² at 10 min and was decreased to 0.1 lb/100 ft² at 30 min, **Figure 43**. Adding different concentrations of nanoclay to the drilling fluid did not enhance the rheological properties of the drilling fluid. Adding nanoclay to drilling fluid decrease the plastic viscosity because of selective adsorption of the high molecular mass (Mw) of polymer chains [61].

Table 17: Drilling fluid formulation for different concentrations of nanoclay

Material	Quantity	Units	Mixing Time, minutes
Distilled Water	308	g	---
Defoamer	0.33	cm ³	0.5
Xc-polymer	1.5	g	20
Starch	6	g	20
KCL	80	g	20
KOH	0.3	g	1
Sodium sulfide	0.25	g	1
Nanoclay	0.3, 0.9, 1.5	g	20
CaCO ₃	30	g	10

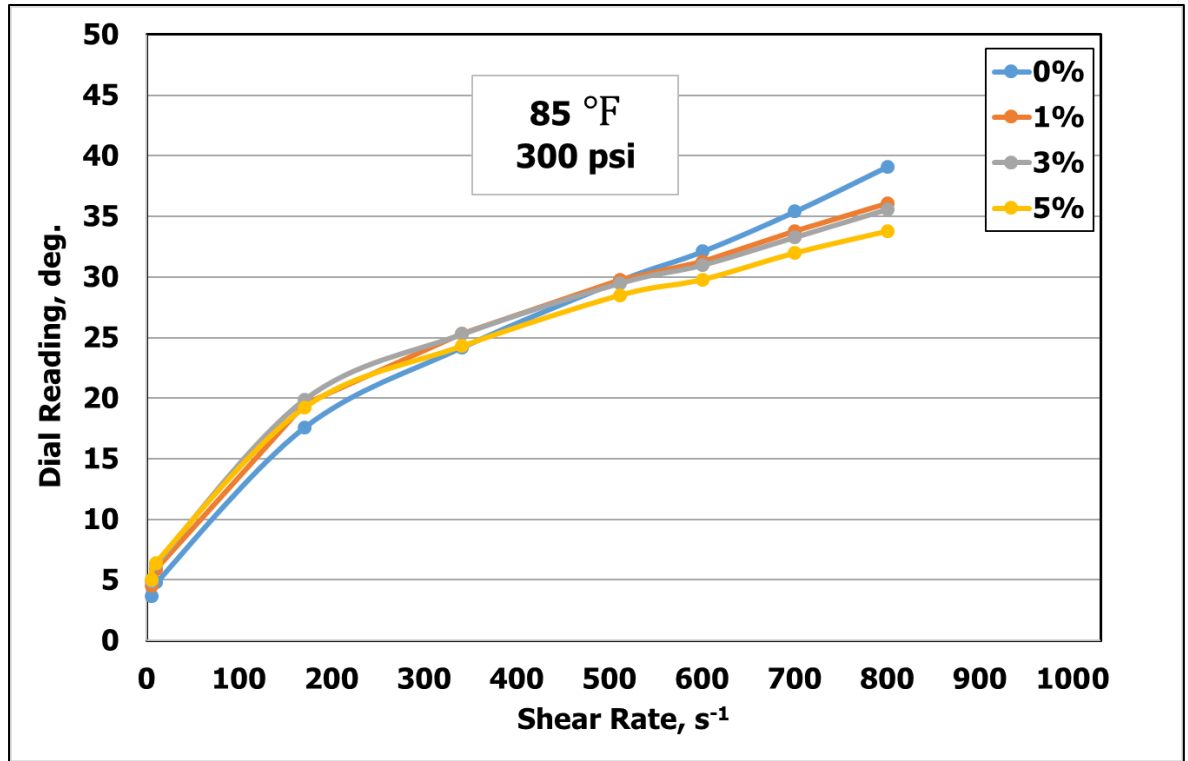


Figure 36: Different concentrations of nanoclay with drilling fluid behavior at 85 °F

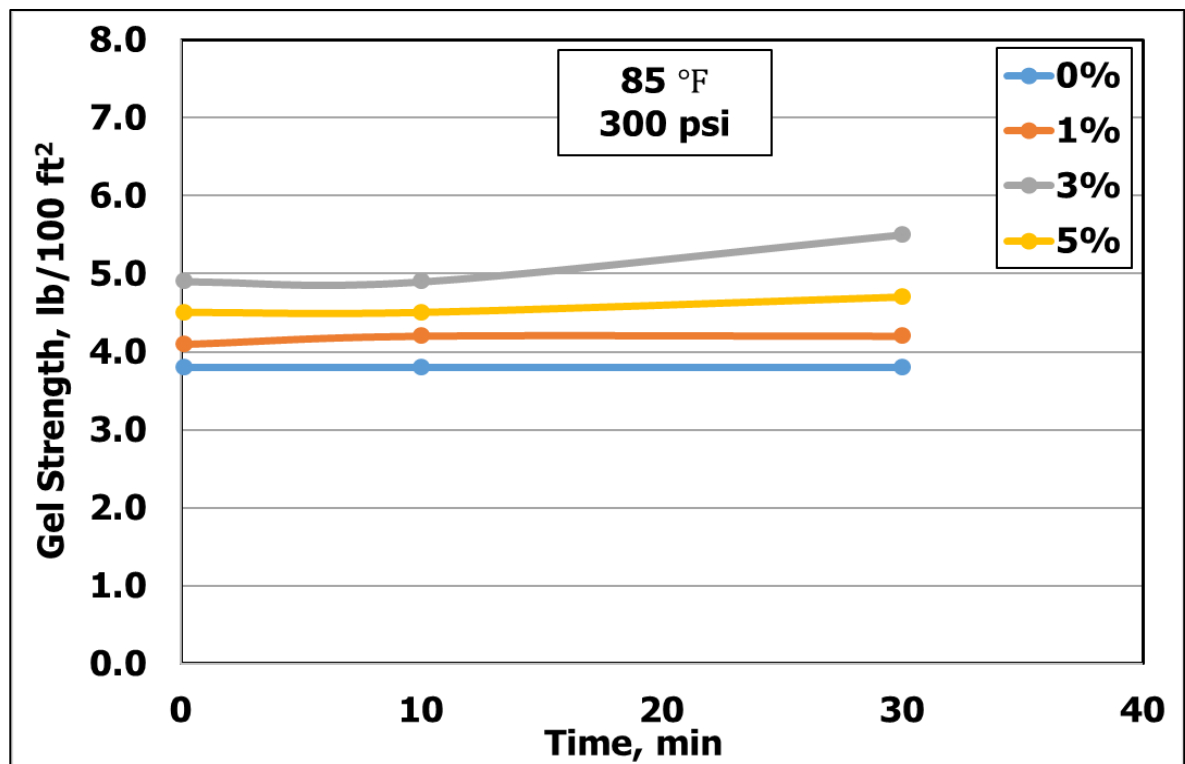


Figure 37: The gel strength of different concentrations of nanoclay with drilling fluid at 85 °F

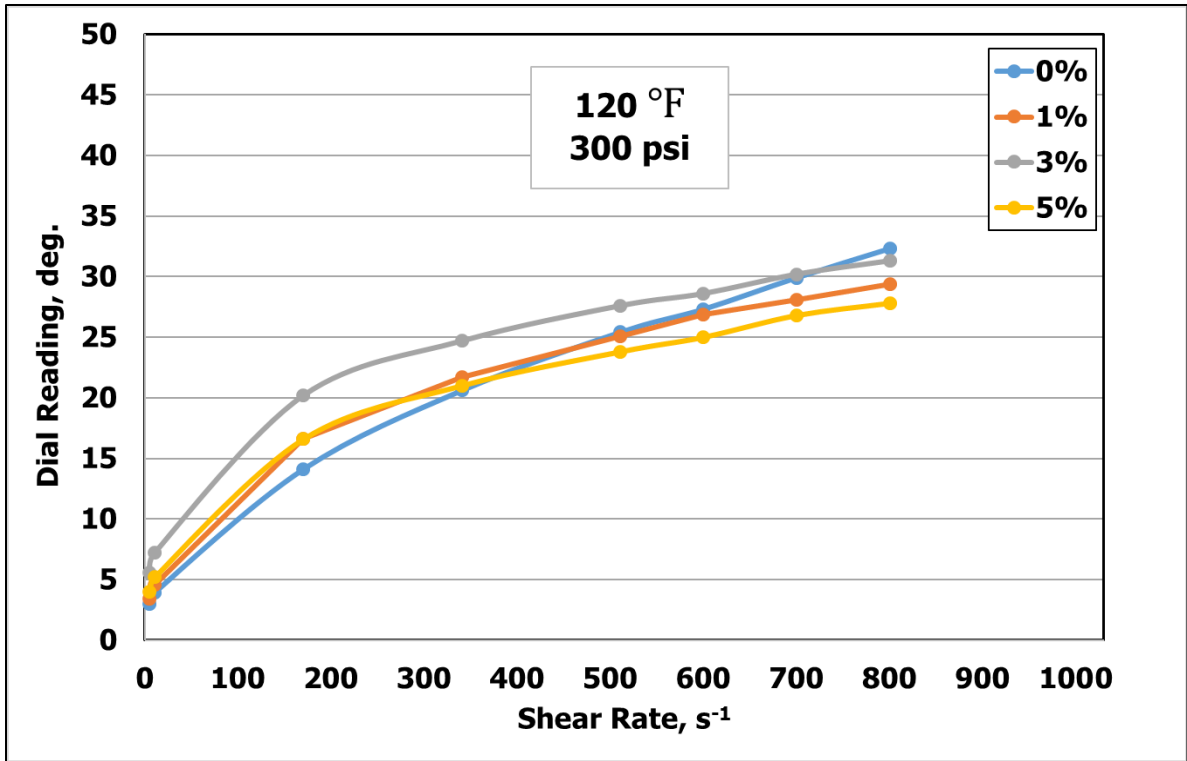


Figure 38: Different concentrations of nanoclay with drilling fluid behavior at 120 °F

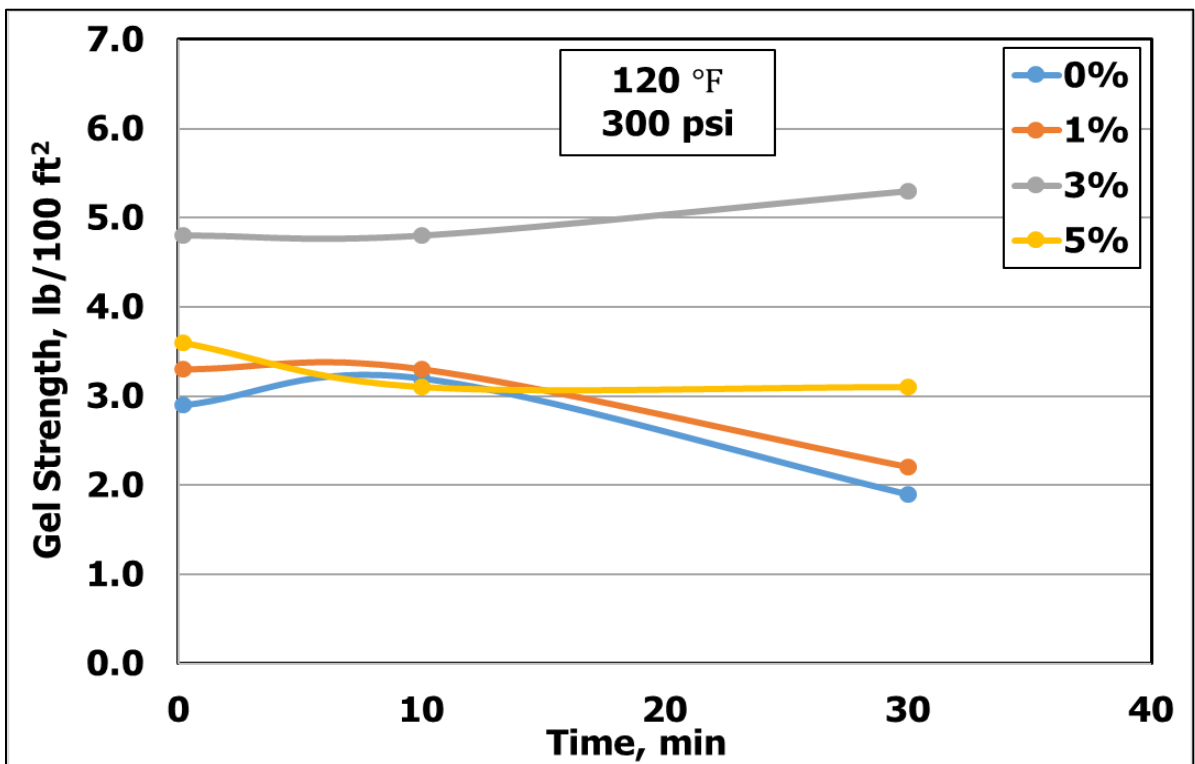


Figure 39: The gel strength of different concentrations of nanoclay with drilling fluid at 120 °F

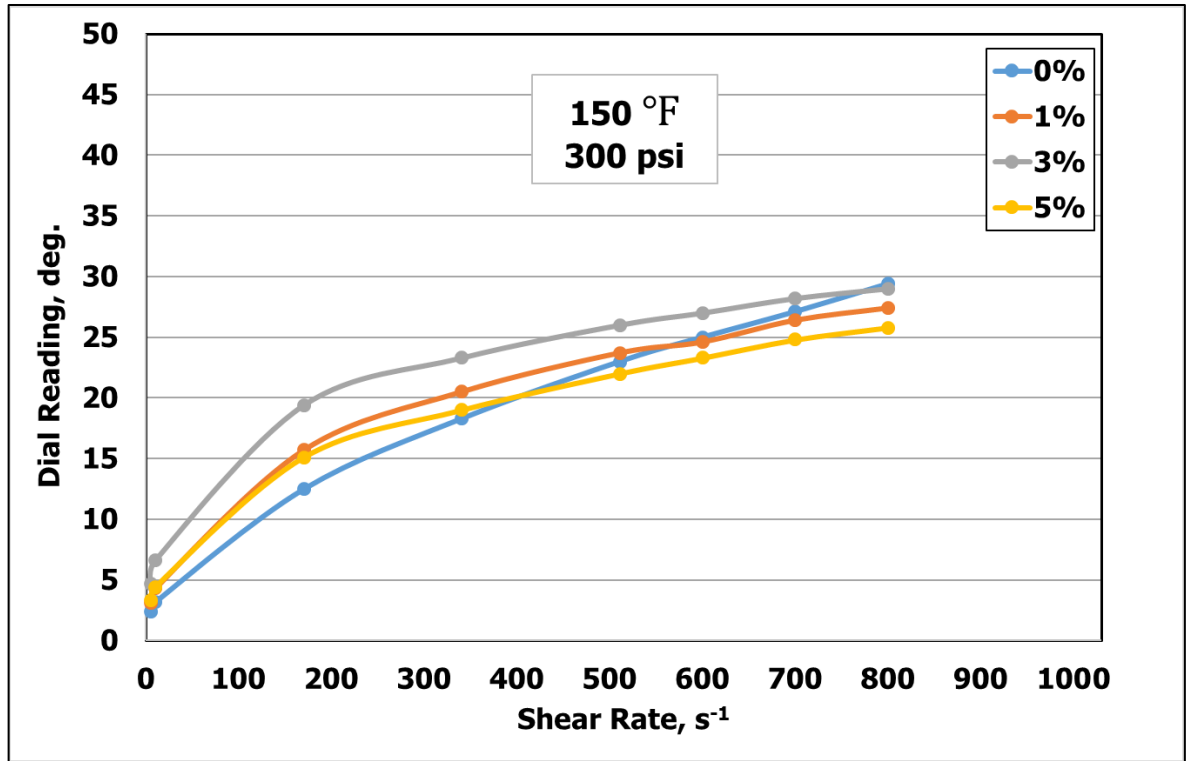


Figure 40: Different concentrations of nanoclay with drilling fluid behavior at 150 °F

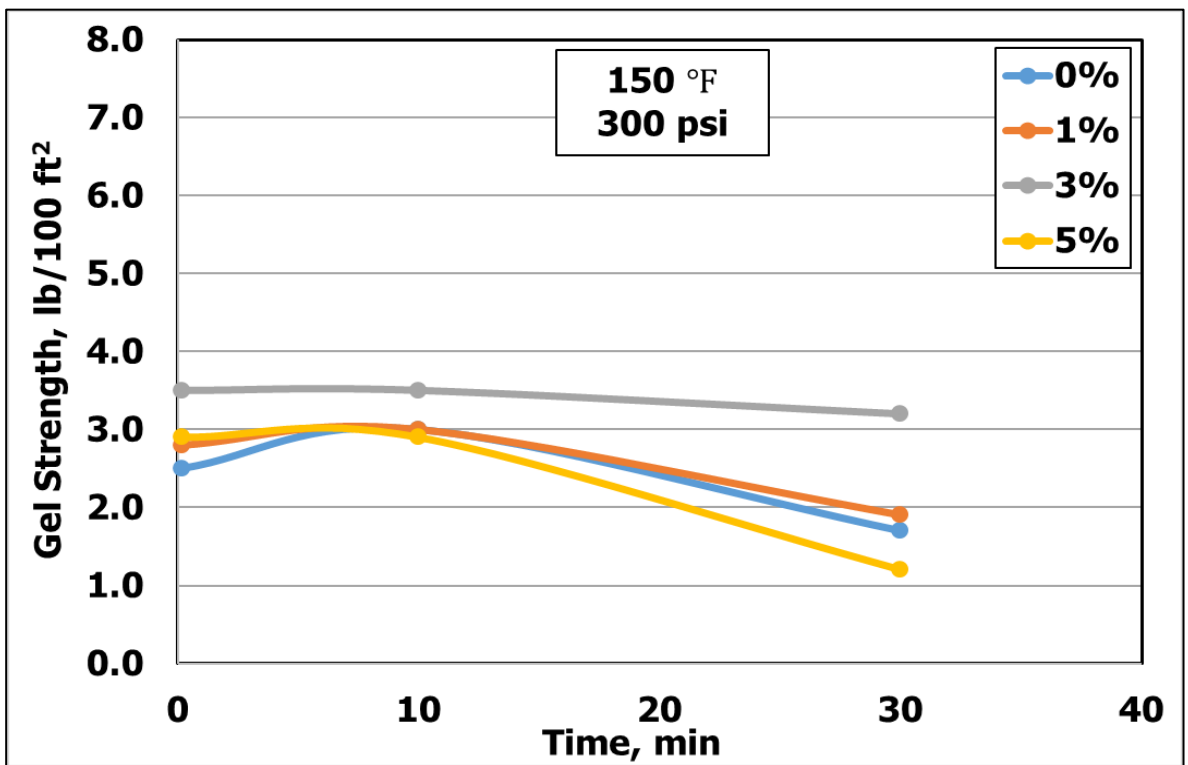


Figure 41: The gel strength of different concentrations of nanoclay with drilling fluid at 150 °F

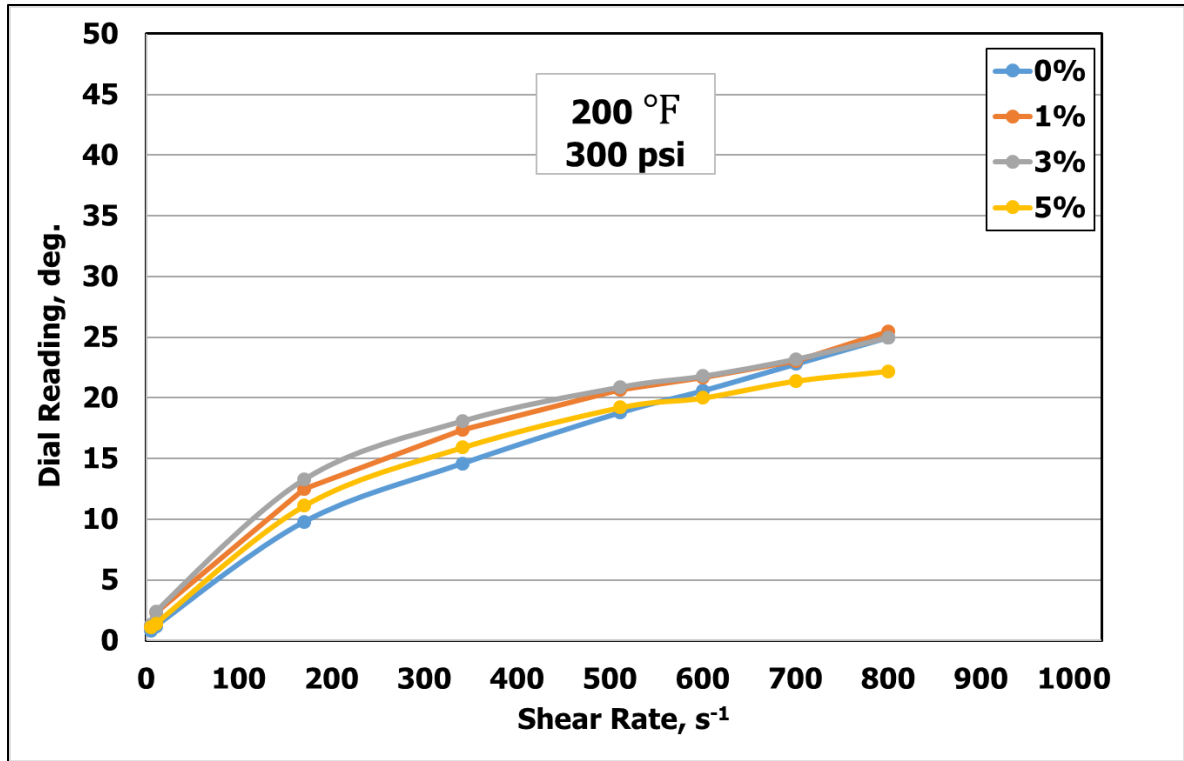


Figure 42: Different concentrations of nanoclay with drilling fluid behavior at 200 °F

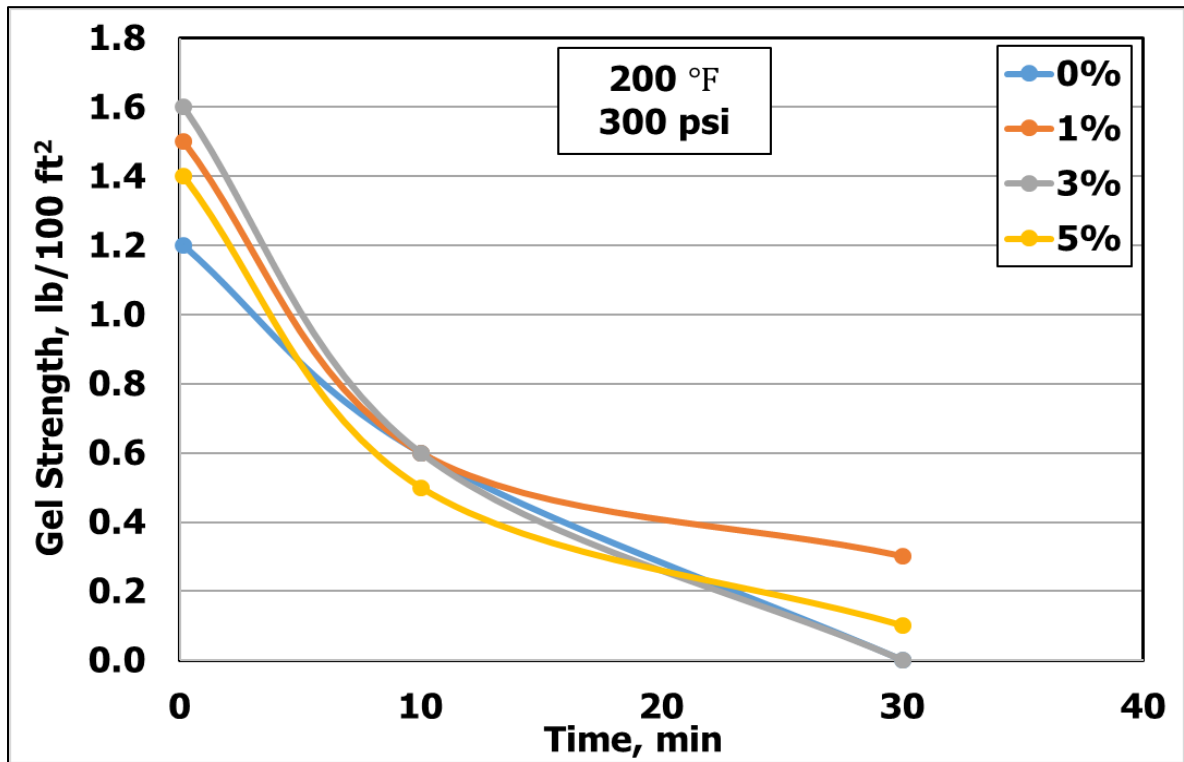


Figure 43: The gel strength of different concentrations of nanoclay with drilling fluid at 200 °F

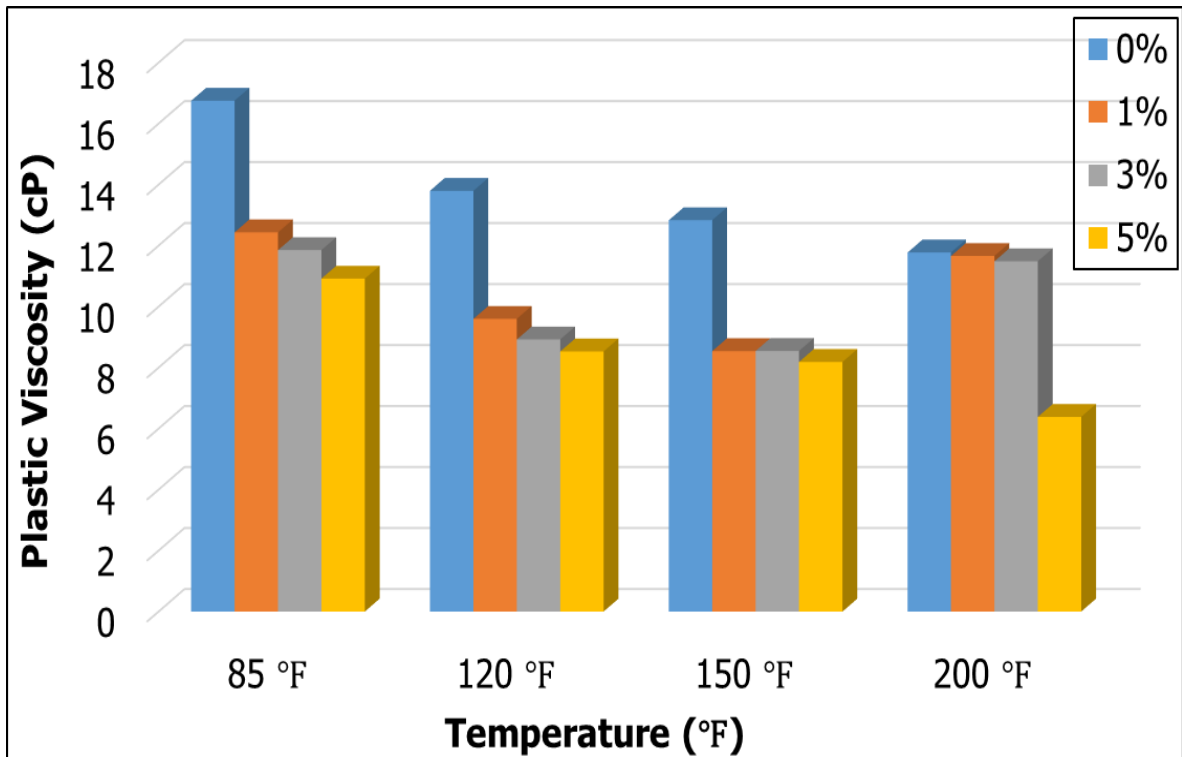


Figure 44: The plastic viscosity of different concentrations of nanoclay with drilling fluid

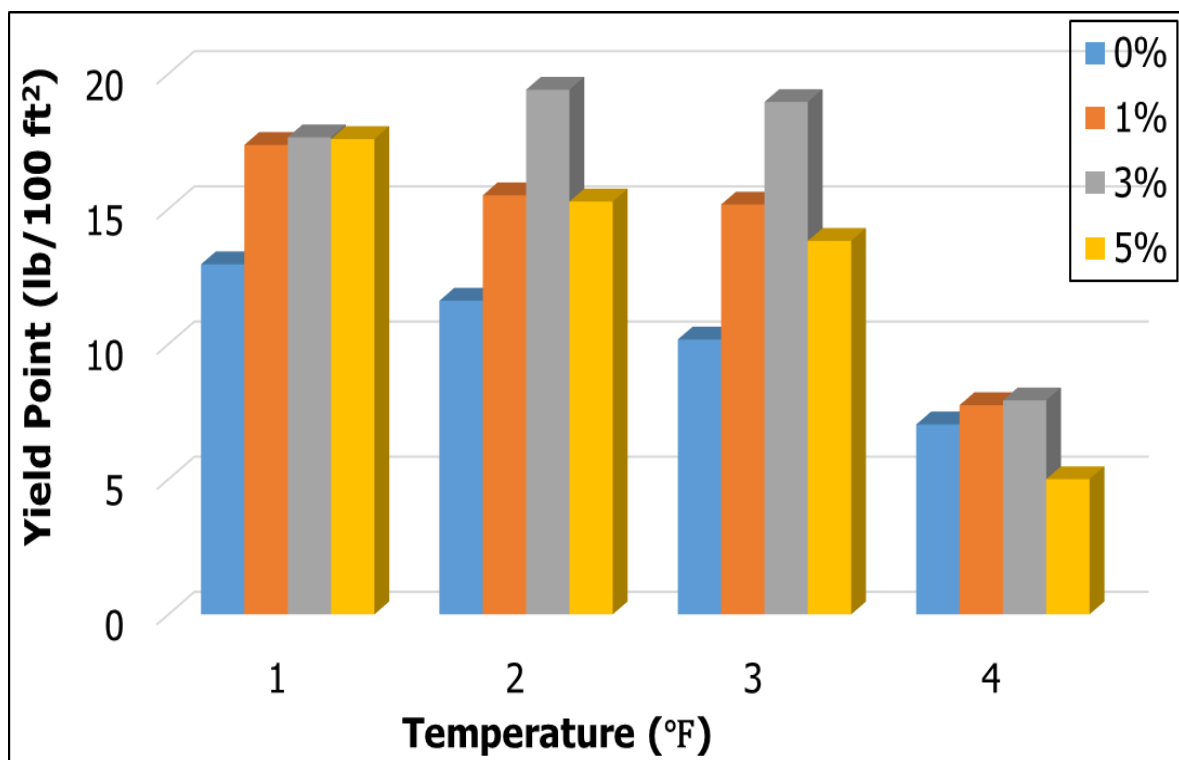


Figure 45: The yield point of different concentrations of nanoclay with drilling fluid

4.2.4 Effect of nanosilica on the rheological properties of the drilling fluid

Different concentrations of nanosilica were added to the drilling fluid to overcome the sticking problem at 120 °F and more than 120 °F. The properties of the drilling fluid with different concentrations of nanosilica were measured, **Table 18**. The behavior of the drilling fluid was measured at different shear rates, different concentrations of nanosilica, different temperatures (85 °F, 120 °F, 150 °F, 200 °F) and at 300 psi pressure. Increasing the concentrations of nanosilica, the drilling fluid rheological properties increased at 85 °F, **Figure 46**. The gel strength at 85 °F and at 1 wt % nanosilica was constant at 3.8 lb/100 ft² from 10 s to 30 min, **Figure 47**. Increasing the concentration of nanosilica to 3 wt %, the gel strength constant at 3.8 lb/100 ft² from 10 s to 10 min and was increased to 3.9 lb/100 ft² at 30 min, **Figure 47**. The gel strength at 5 wt % nanosilic was constant at 4.3 lb/100 ft² 10 s to 10 min and then increased to 5 lb/100 ft² at 30 min, **Figure 47**. By increasing the concentration of nanosilica to 7.5 wt %, the gel strength increased from 4.6 lb/100 ft² to 5.4 lb/100 ft² (10 s to 10 min) and then to 5.7 lb/100 ft² at 30 min, **Figure 47**. Increasing the concentration of nanosilica to 10 wt %, the gel strength was increased from 4.6 lb/100 ft² at 10 s to 5.4 lb/100 ft² at 10 min and then increased to 5.7 at 30 min, **Figure 47**.

To deep understand the effect of temperature on the rheological properties of the different concentrations of nanosilica with the drilling fluid, the temperature was increased to 120 °F and the rheological properties were measured. At the temperature 120 °F, the behavior increased by increasing the concentrations of the nanosilica, **Figure 48** . Increasing the temperature from 85 °F to 120 °F, the gel strength at 1 wt % nanosilica increased from 3.1

lb/100 ft² at 10 s to 3.2 lb/100 ft² at 10 min and decrease to 2.4 lb/100 ft² at 30 min, **Figure 49**. The gel strength at 3 wt % nanosilica was constant 3.2 lb/100 ft² from 10 s to 10 min and then decreased to 2.8 lb/100 ft² at 30 min, **Figure 49**. Increasing the concentration of nanosilica to 5 wt %, the gel strength increased from 3.9 lb/100 ft² at 10 s to 4.1 lb/100 ft² at 10 min and increased to 4.2 lb/100 ft² at 30 min, **Figure 49**. By increasing the concentration of nanosilica to 7.5 wt %, the gel strength increased from 4.4 lb/100 ft² at 10 s to 5.1 lb/100 ft² at 10 min and increased to 5.2 lb/100 ft² at 30 min, **Figure 49**. The gel strength at 10 wt % nanosilica was increased from 5.6 lb/100 ft² at 10 s to 6.4 at 10 min and then increased to 6.9 lb/100 ft² at 30 min, **Figure 49**.

By increasing the temperature to 150°F, the drilling fluid rheological properties was increased by increasing the concentrations of the nanosilica, **Figure 50**. The gel strength at 150 °F and at 1 wt % nanosilica increased from 2.6 9 lb/100 ft² to 3 9 lb/100 ft² (10 s to 10 min) and then decreased to 1.7 9 lb/100 ft² at 30 min, **Figure 51**. Adding 3 wt % nanosilica to the drilling fluid, the gel strength increased from 2.6 lb/100 ft² at 10 s to 3 lb/100 ft² at 10 min and then decreased to 1.9 lb/100 ft² at 30 min, **Figure 51**. By adding 5 wt % nanosilica to the drilling fluid, the gel strength decreased from 3.4 lb/100 ft² to 3.2 lb/100 ft² and then to 3.1 lb/100 ft² at 30 min, **Figure 51**. The gel strength at 7.5 wt % nanosilica and at 150 °F was constant 4 lb/100 ft² from 10 s to 30 min, **Figure 51**. By increasing the concentration of nanosilica to 10 wt %, the gel strength was constant 5.4 lb/100 ft² from 10 s to 30 min, **Figure 51**.

To deep understand the effect of temperature on the rheological properties of the different concentrations of nanosilica, the temperature was increased to 200 °F and the rheological

properties were measured. **Figure 52** shows the behavior of the drilling fluid at 300 psi and 200 °F and adding nanosilica to the drilling fluid increased the rheological properties of the drilling fluid. The gel strength at 200 °F and at 1 wt % nanosilica was decreased from 1.5 lb/100 ft² to 0.6 lb/100 ft² to 0 lb/100 ft² at (10 s to 10 min to 30 min), **Figure 53**. By adding 3 wt % nanosilica to the drilling fluid, the gel strength decreased from 1.6 lb/100 ft² to 0.7 lb/100 ft² to 0.4 lb/100 ft² at (10 s to 10 min to 30 min), **Figure 53**. The 5 wt % nanosilica was added to the drilling fluid to decrease the gel strength from 2.2 lb/100 ft² at 10 to 2 lb/100 ft² at 10 min and then decreased to 1.6 lb/100 ft² at 30 min, **Figure 53**. Adding 7.5 % wt nanosilica to the drilling fluid, the gel strength was constant at 3 lb/100 ft² from 10 s to 30 min, **Figure 53**. By adding 10 % wt nanosilica to the drilling fluid, the gel strength was constant at 3.4 lb/100 ft² from 10 s to 30 min, **Figure 53**. Increasing the concentration of nanosilica was decreasing the plastic viscosity of the drilling fluid, **Figure 54**. Yield point of the drilling fluid increased by adding different concentrations of nanosilica, **Figure 55**.

Table 18: Drilling fluid formulation for different concentrations of nanosilica

Material	Quantity	Units	Mixing Time, minutes
Distilled Water	308	g	---
Defoamer	0.33	cm ³	0.5
Xc-polymer	1.5	g	20
Starch	6	g	20
KCL	80	g	20
KOH	0.3	g	1
Sodium sulfide	0.25	g	1
Nanoclay	0.3, 0.9, 1.5	g	20
CaCO ₃	30	g	10

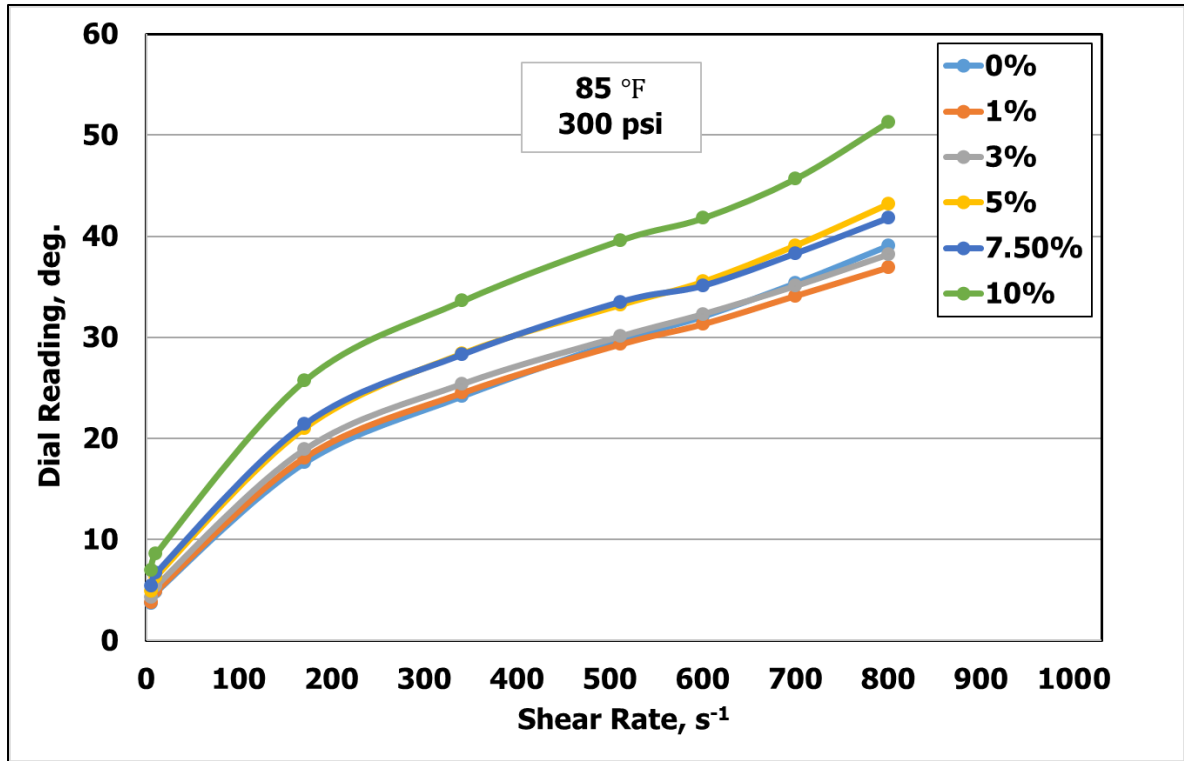


Figure 46: Different concentrations of nanosilica with drilling fluid behavior at 85 °F

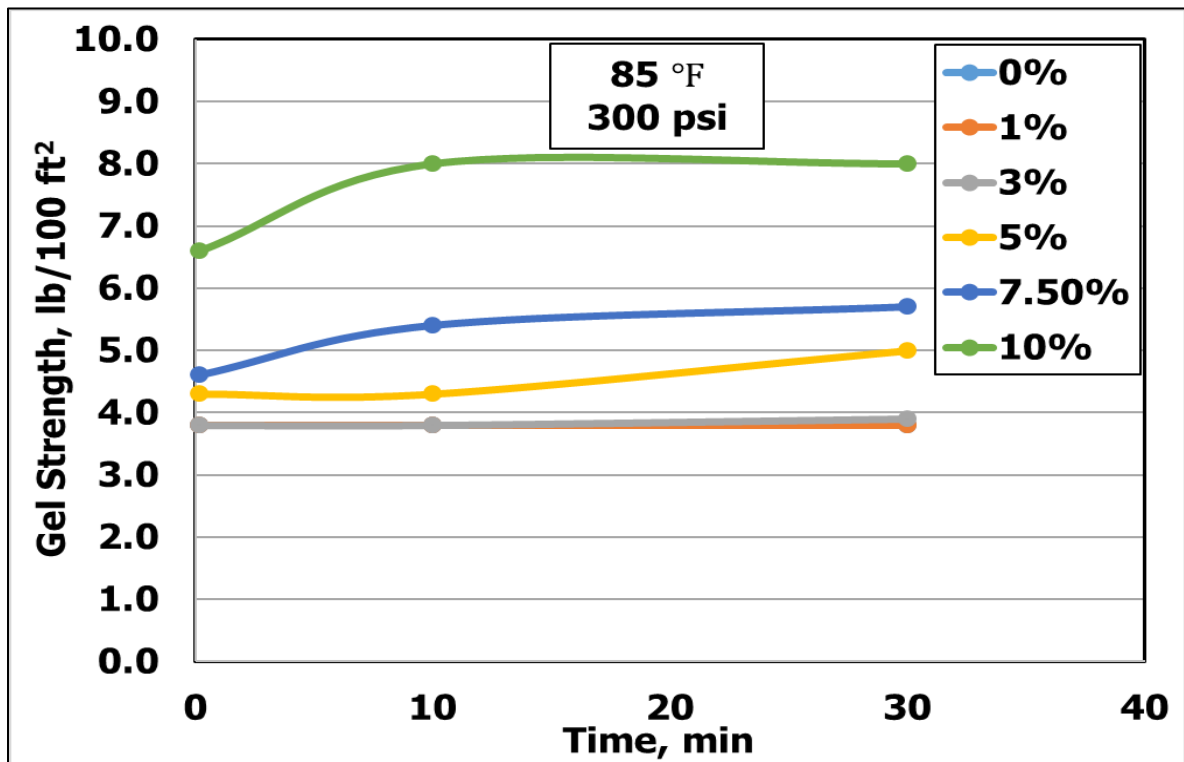


Figure 47: The gel strength of different concentrations of nanosilica with drilling fluid at 85 °F

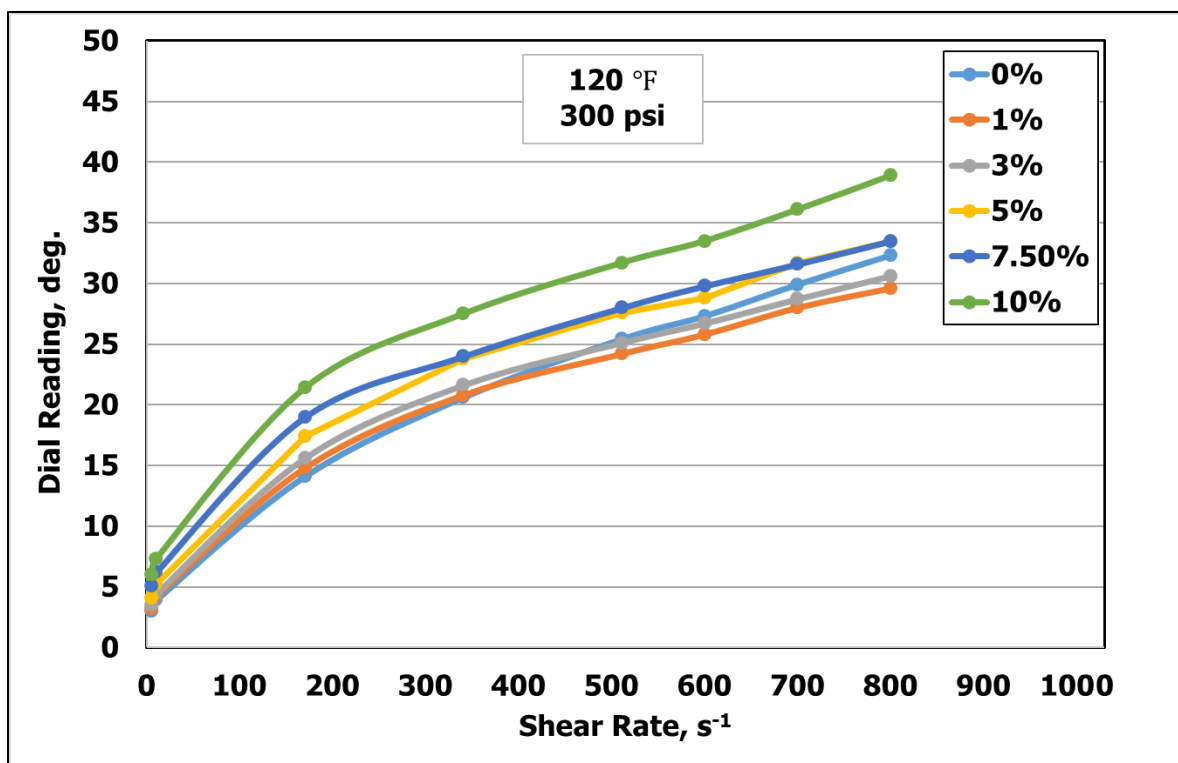


Figure 48: Different concentrations of nanosilica with drilling fluid behavior at 120 °F

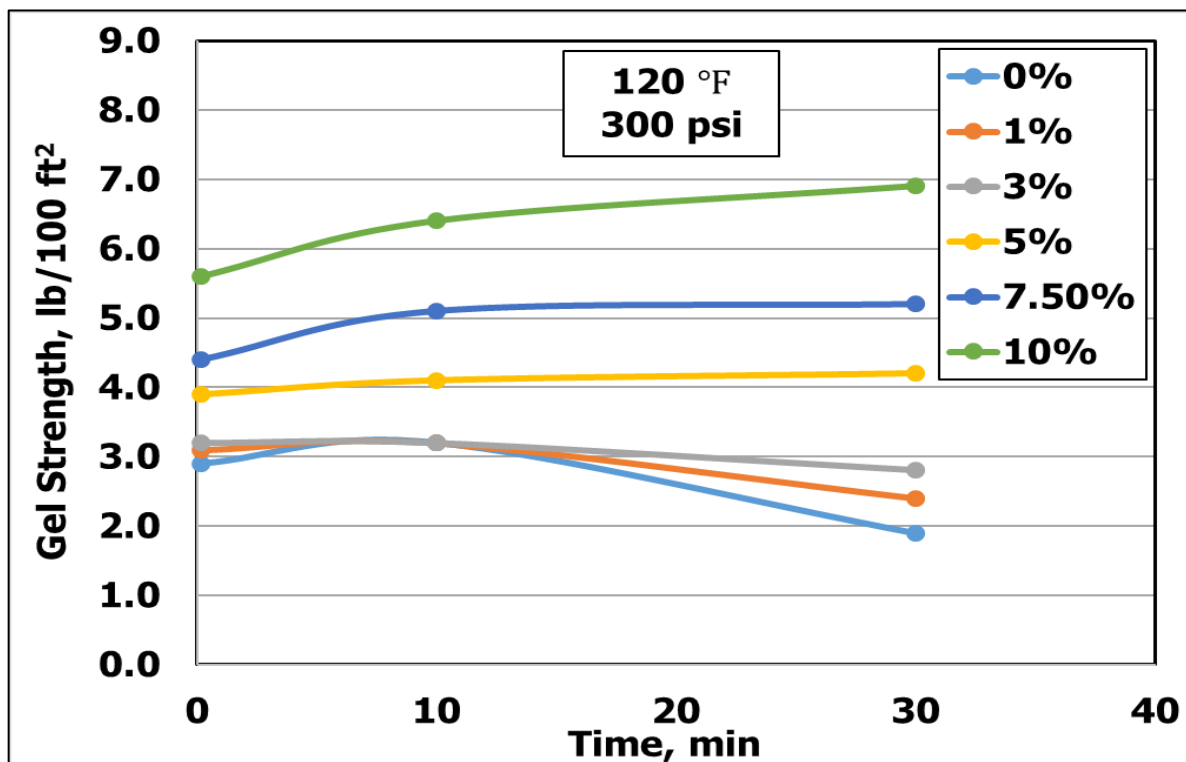


Figure 49: The gel strength of different concentrations of nanosilica with drilling fluid at 120 °F

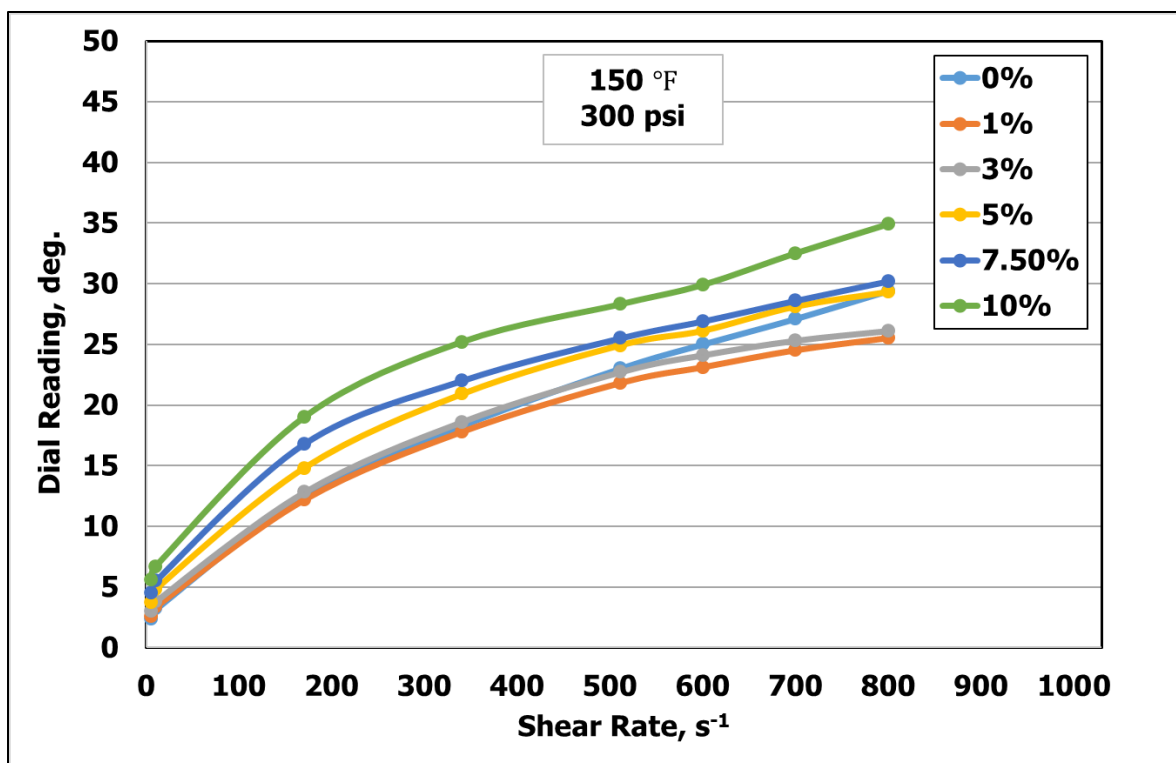


Figure 50: Different concentrations of nanosilica with drilling fluid behavior at 150 °F

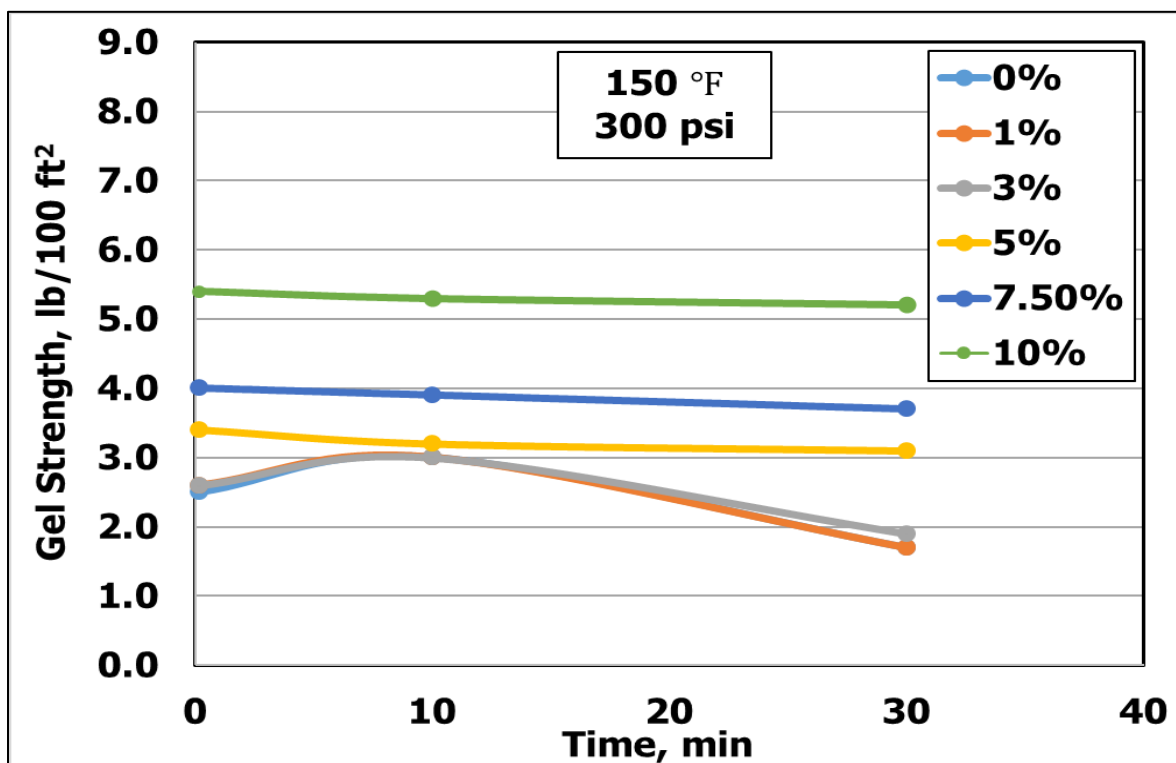


Figure 51: The gel strength of different concentrations of nanosilica with drilling fluid at 150 °F

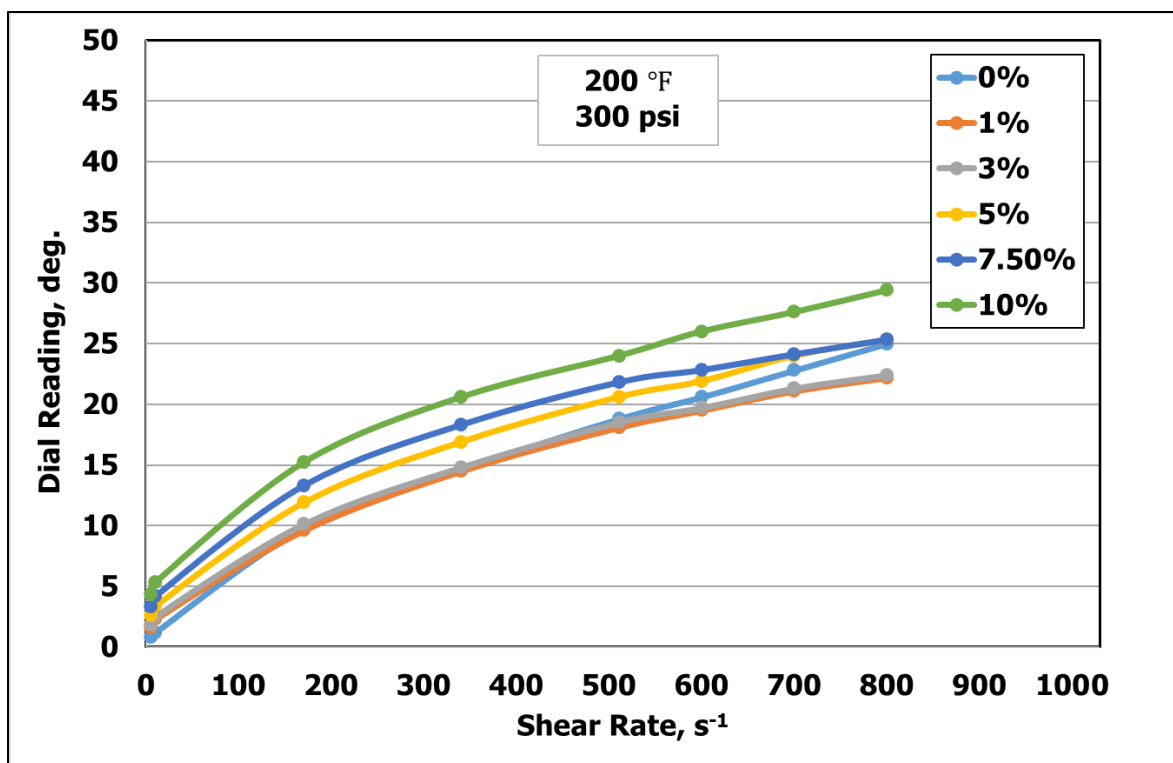


Figure 52: Different concentrations of nanosilica with drilling fluid behavior at 200 °F

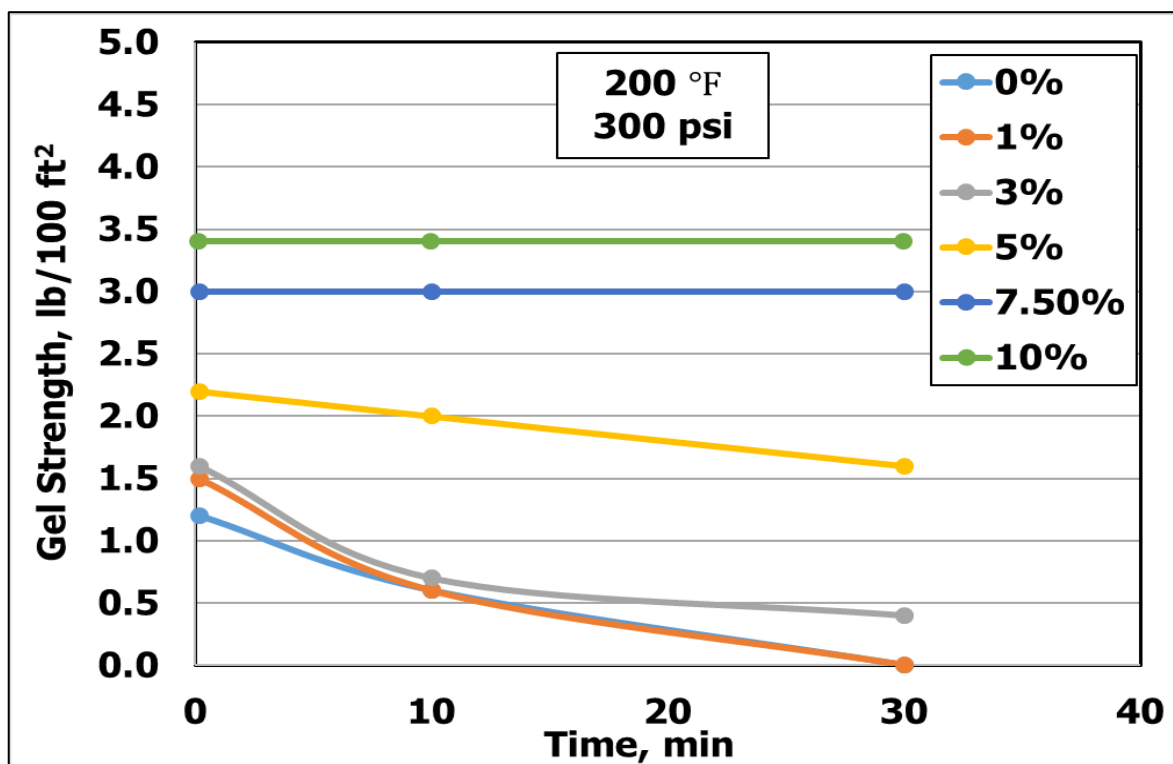


Figure 53: The gel strength of different concentrations of nanosilica with drilling fluid at 200 °F

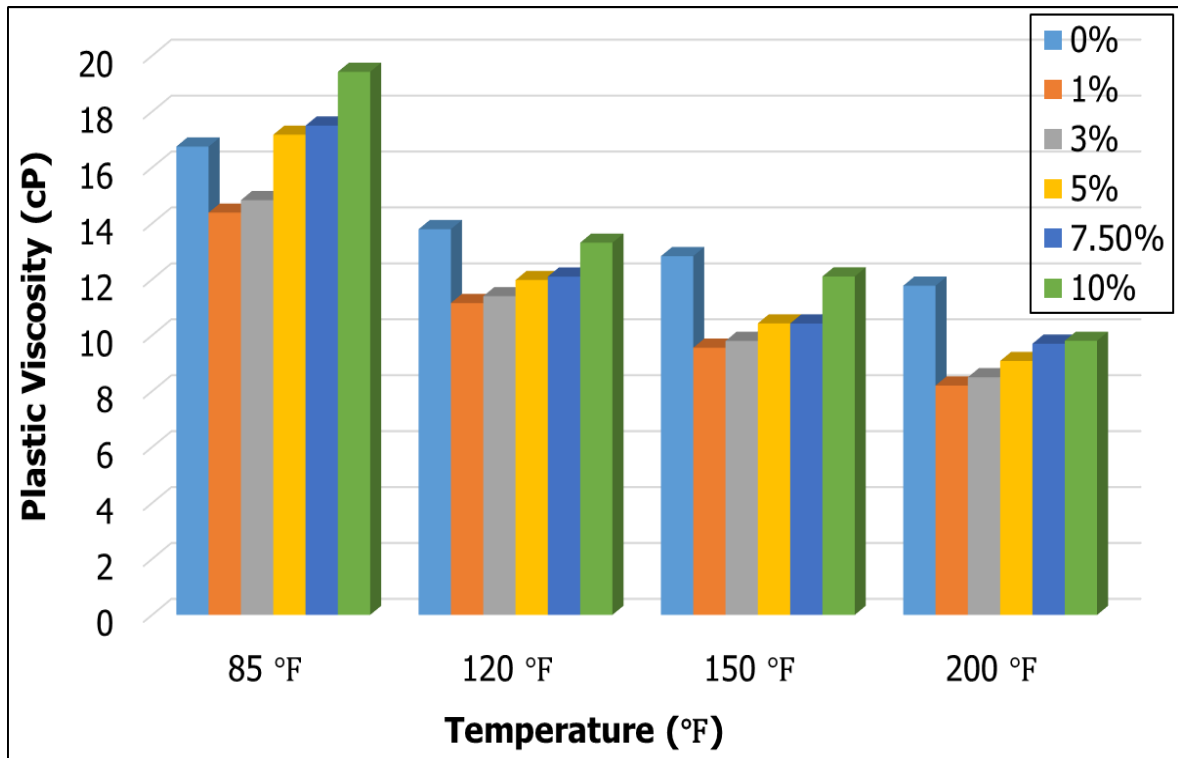


Figure 54: The plastic viscosity of different concentrations of nanosilica with drilling fluid

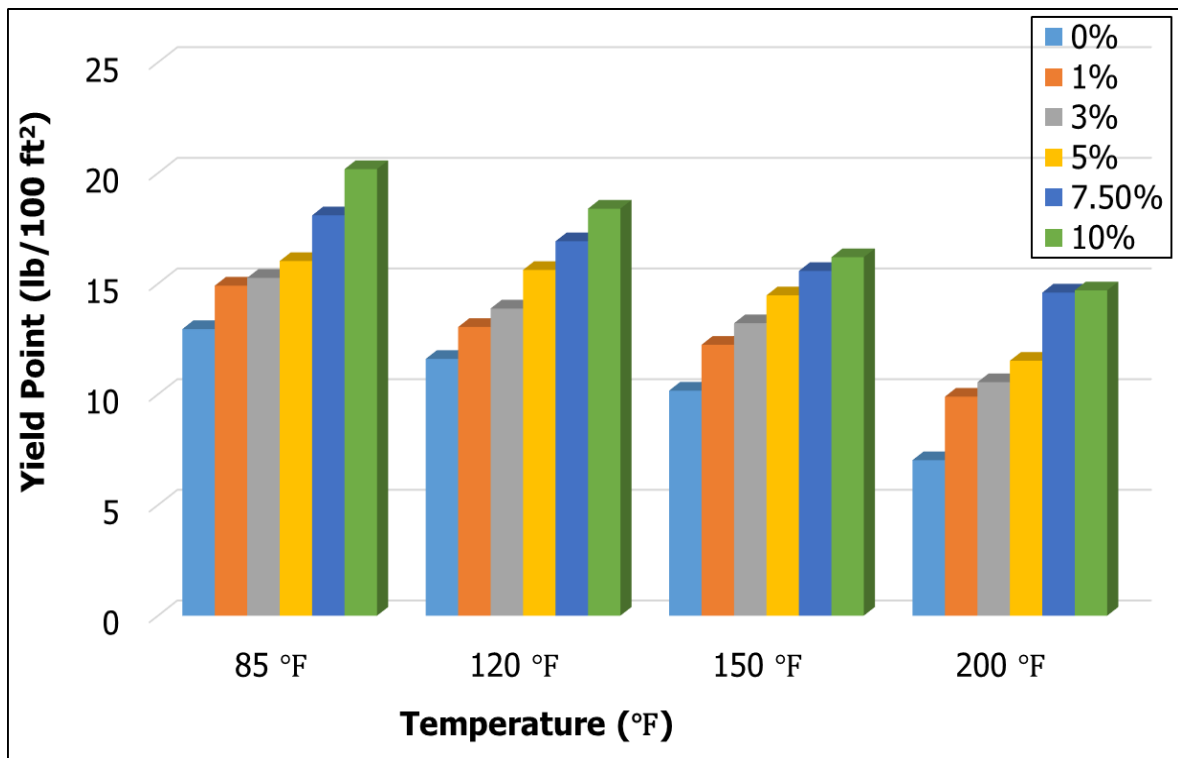


Figure 55: The yield point of different concentrations of nanosilica with drilling fluid

4.3 Filtration measurements of drilling fluid

From the rheological properties measurements, the optimum concentration of bentonite (6.6 wt %) and nanosilica (7.5 wt %) was selected. The filtration of the base drilling 6.6 wt % bentonite and drilling fluid with 7.5 wt % nanosilica was measured at 200 °F and 300 psi. The filtration volume of the drilling with 6.6 wt % bentonite and drilling fluid with 7.5 wt % nanosilica were decreased, **Figure 56**. The filter cake thickness of the base drilling fluid was 0.176 in, the filter cake thickness of the drilling fluid with 7.5 wt % nanosilica was 0.075 in and the filter cake thickness of the drilling fluid with 6.6 wt % bentonite was 0.072 in, **Figure 57**.

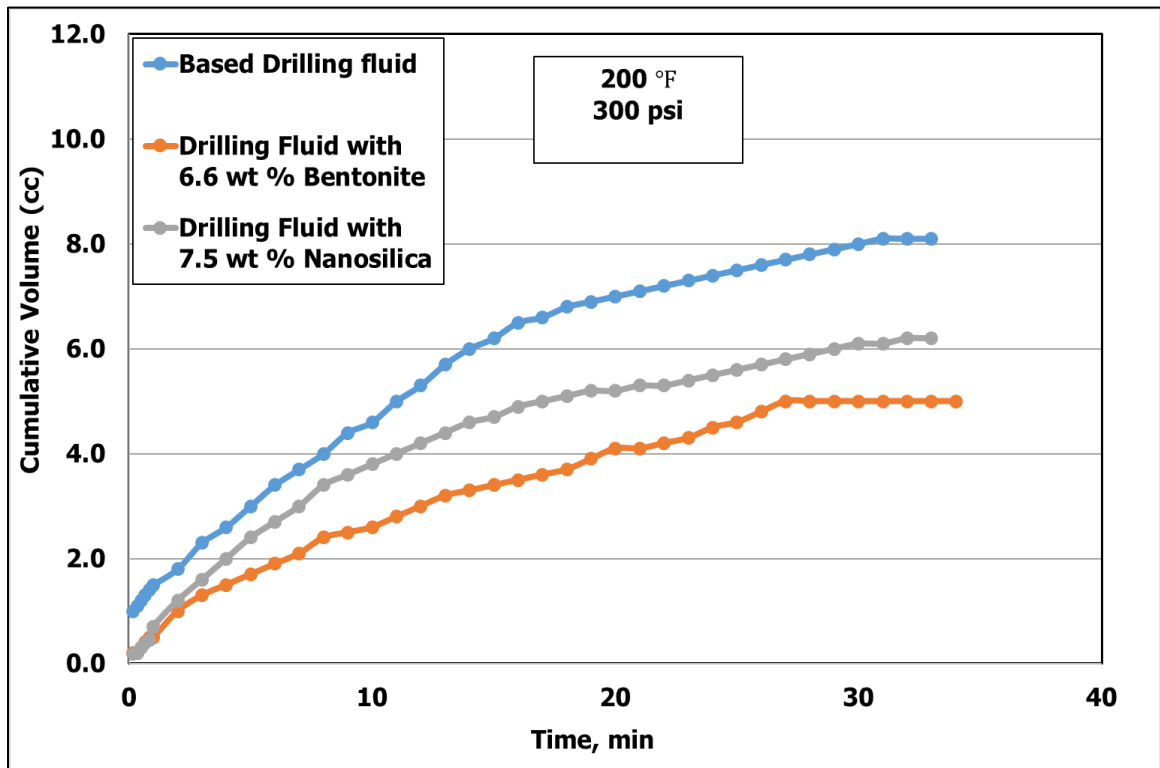


Figure 56: Filtration measurements of drilling fluid

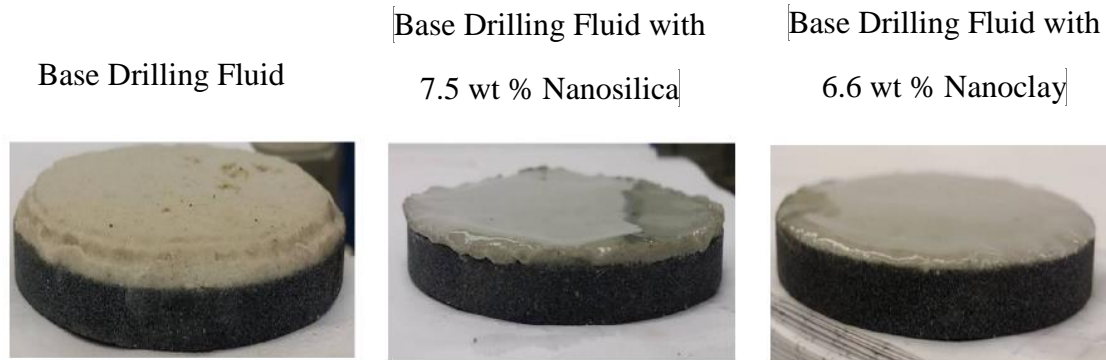


Figure 57: Filter cake thickness of the drilling fluid

4.4 Removal efficiency measurements of the drilling fluid

The mud cake was soaked for 24 hours with the removal fluid (20 wt %) GLDA at pH 4. After 24 hours, removal efficiency and retained permeability were estimated by using equations (1,2,3). The base drilling fluid has 100 % removal efficiency and 86 % retained permeability. The drilling fluid with 6.6 wt % bentonite has 96 % removal efficiency and 85 % retained permeability. The drilling fluid with 7.5 wt % bentonite has 100 % removal efficiency and 85.5 % retained permeability. Adding the different concentrations of bentonite to the drilling fluid has a minor effect on the removal efficiency of the drilling fluid. By adding the different concentrations of nanosilica to the drilling fluid did not affect the removal efficiency of the drilling fluid.

CHAPTER 5

Conclusions and Recommendation

5.1 Conclusions

This thesis studied the stability of drilling fluid additives such as barite and bentonite by using zeta potential measurements, rheological properties of drilling fluid and filtration of drilling fluid at different concentrations and different conditions. The conclusions divided in three phases as following :

Phase I: Zeta potential

- Barite, calcium carbonate, and nanoclay are not stable over a wide range of pH.
- Nanosilica is stable at high pH(>10).
- Adding nanosilica to calcium carbonate enhanced the stability especially at higher pH (>11).
- Bentonite is stable over a wide range of pH.
- Salts (KCl and NaCl) decrease the zeta potential values of the solids.

Phase II: Rheological Properties

- Gel strength of based drilling fluid is decreasing after 30 mins at 120 °F. It became zero at 200 °F.
- Adding bentonite (6.6 wt%) solved the issue of gel strength (30 mins) at 200 °F.

- Adding nanoclay with different concentrations did not overcome the gel strength problem over a wide range of temperature.
- Drilling fluid with 7.5 wt % nanosilica has a stable gel strength at 30 minutes at different temperature and even at 200 °F

Phase III: Filtration test

- Drilling fluid with 6.6 wt % bentonite decrease the filtration volume at 200 °F and at 300 psi.
- Drilling fluid with 7.5 wt % nanosilica decrease the filtration volume at 200 °F and at 300 psi.

5.2 Recommendation

The following recommendation can be done for future study

- Investigating the stability by using zeta potential and rheological properties measurements of both nanosilica and nanoclay with drilling fluid additives.
- Investigating the rheological properties and filtration measurements of the drilling fluid by using drilling fluid formula without starch .
- Investigating the rheological properties and filtration measurements of the drilling fluid by using drilling fluid formula with different particle sizes of calcium carbonate.
- Investigating the stability by using zeta potential and rheological properties measurements of different nanoparticles with drilling fluid additives.

References

- [1] V. Chilingarian, G. and P. Vorabutr, *Drilling and Drilling Fluid*. Elsevier, 1983.
- [2] T. M. Madkour, S. Fadl, M. M. Dardir, and M. A. Mekewi, “High performance nature of biodegradable polymeric nanocomposites for oil-well drilling fluids,” *Egypt. J. Pet.*, 2015.
- [3] E. Haaland, G. Pettersen, and B. Tuntland, “Testing of Iron Oxides as Weight Materials for Drilling Muds,” *SPE J.*, no. 1, pp. 1–15, 1976.
- [4] P. N. Garay, *Pump Application Desk Book* (3rd ed.). Prentice Hall, 1996.
- [5] M. A. Rao, *Rheology of Fluid and Semisolid Foods: Principles and Applications* (2nd ed. Springer, 2007).
- [6] C. Tropea, A. L. . Yarin, and J. F. Foss, *Springer handbook of experimental fluid mechanics*. Springer, 2007.
- [7] E. C. Bingham, “An Investigation of the Laws of Plastic Flow,” *US Bureau of Standards Bulletin* 13. pp. 309–353, 1916.
- [8] M. Amanullah and M. Al-Tahini, Ashraf, “Nano-Technology- Its Significance in Smart Fluid Development for Oil and Gas Field Application,” in Paper SPE 126102 was presented at the SPE Saudi Arabia Section Technical Symposium and Exhibition, 2009.
- [9] K. P. Hoelscher, G. De Stefano, M. Riley, and S. Young, “Application of Nanotechnology in Drilling Fluids,” in Paper SPE 157031 was presented at the SPE International Oilfield Nanotechnology conference, 2012, no. June.
- [10] J. C. Baird and J. Y. Walz, “The effects of added nanoparticles on aqueous kaolinite suspensions. II. Rheological effects,” *J. Colloid Interface Sci.*, vol. 306, no. 2, pp. 411–420, 2007.
- [11] Lee. Jung-Kun, S. T., Son Y., T. Phouoc, S. X., D. Y., Martello, and K. Chyu., M., “Use of magnetic nanoparticles for smart drilling fluids,” in Paper AADE 2009NTCE-18-04 was presented at the National Technical Conference & Exhibition, New Orileans, 2009.
- [12] T. Huang, J. B. Crews, and G. Agrawal, “Nanoparticle Pseudocrosslinked Micellar Fluids : Optimal Solution for Fluid- Loss Control With Internal Breaking,” in Paper SPE 128067 was presented at the SPE International Symposium and Exhibition on Formation Damage Control, 2010.
- [13] R. Barati, “Application of nanoparticles as fluid loss control additives for hydraulic fracturing of tight and ultra-tight hydrocarbon-bearing formations,” *J. Nat. Gas Sci. Eng.*, vol. 27, pp. 1321–1327, 2014.
- [14] S. Agarwal, P. Tran, Y. Soong, D. Martello, and R. K. Gupta, “Flow Behavior of

Nanoparticle Stabilized Drilling Fluids and Effect of High Temperature Aging,” in Paper AADE-11-NTCE-3 was presented at the AADE National Technical Conference and Exhibition, 2011.

- [15] S. M. Javeri, Z. W. Haindade, and C. B. Jere, “Mitigating Loss Circulation and Differential Sticking Problems Using Silicon Nanoparticles,” in Paper SPE /IADC 145840 was presented at the SPE/IADC Middle East Drilling Technology Conference and Exhibition, 2011.
- [16] M. Amanullah, M. A. Al-Arfaj, and Z. Al-Abdullatif, “Preliminary Test Results of Nano-based Drilling Fluids for Oil and Gas Field Application,” in Paper SPE/IADC 139534 was presented at the SPE/IADC Drilling Conference and Exhibition, 2011.
- [17] P. Mcelfresh, C. Olguin, and D. Ector, “The Application of Nanoparticle Dispersions To Remove Paraffin and Polymer Filter Cake Damage,” in Paper SPE 151848 was presented at the SPE International Symposium and Exhibition on Formation Damage Control, 2012.
- [18] J. T. Srivatsa, M. B. Ziaya, and T. Tech, “An Experimental Investigation on use of Nanoparticles as Fluid Loss Additives in a Surfactant – Polymer Based Drilling Fluid,” in Paper IPTC 14952 was presented at the International Petroleum Technology Conference, 2012.
- [19] C. M. Jung, R. Zhang, and M. Sharma, “High-Performance Water-Based Mud Using Nanoparticles for Shale Reservoirs,” in Paper SPE 168799 was presented at the Unconventional Resources Technology Conference, 2013, no. 2004.
- [20] T. Sensoy, M. E. Chenevert, and M. M. Sharma, “Minimizing Water Invasion in Shale Using Nanoparticles,” in Paper SPE 124429 Was Presented at the SPE Annual Technical Conference, 2009, no. October.
- [21] J. Cai, M. E. Chenevert, M. M. Sharma, and J. Friedheim, “Decreasing Water Invasion Into Atoka Shale Using Nonmodified Silica Nanoparticles,” SPE Drill. Complet., vol. 27, no. 1, pp. 103–112, 2012.
- [22] G. Li, J. Zhang, H. Zhao, and Y. Hou, “Nanotechnology to Improve Sealing Ability of Drilling Fluids for Shale with Micro-cracks During Drilling,” in Paper SPE 156997 was presented at the SPE International Oilfield Nanotechnology conference, 2012.
- [23] J. Abdo and M. D. Haneef, “Nanoparticles : Promising Solution to Overcome Stern Drilling Problems Mechanical and Industrial Engineering Department,” NSTI-Nanotech, vol. 3, pp. 635–638, 2010.
- [24] J.-F. Berret, K. Yokota, and M. Morvan, “Interactions Between Polymers and Nanoparticles: Formation of ‘Supramicellar’ Hybrid Aggregates,” Soft Mater., vol. 2, no. 2–3, pp. 71–84, 2004.
- [25] M. F. Zakaria, M. Husein, and G. Hareland, “Novel Nanoparticle-Based Drilling

Fluid with Improved Characteristics,” in Paper SPE 156992 was presented at the SPE International Oilfield Nanotechnology Conference, 2012.

- [26] J. Nasser, A. Jesil, T. Mohiuddin, M. Al Ruqeshi, G. Devi, and S. Mohataram, “Experimental Investigation of Drilling Fluid Performance as Nanoparticles,” *World J. Nano Sci. Eng.*, vol. 57, no. 61, pp. 58–61, 2013.
- [27] J. Abdo and M. D. Haneef, “Clay nanoparticles modified drilling fluids of deep hydrocarbon wells,” *Appl. Clay Sci.*, vol. 86, pp. 76–82, 2013.
- [28] C. Vipulanandan and A. Mohammed, “Effect of nanoclay on the electrical resistivity and rheological properties of smart and sensing bentonite drilling muds,” *J. Pet. Sci. Eng.*, vol. 130, pp. 86–95, 2015.
- [29] A.-Y. A. S. and A. Z. Wagle V., “Using Nanoparticles to Formulate Sag-Resistant Invert Emulsion Drilling,” in Paper SPE/IADC 173004 was presented at the SPE/IADC Drilling conference and Exhibition, 2015.
- [30] A. S. Borisov, M. Husein, and G. Hareland, “A field application of nanoparticle-based invert emulsion drilling fluids,” *J. Nanoparticle Res.*, vol. 17, no. 8, pp. 340(1–13), 2015.
- [31] M. M. Barry, Y. Jung, J. K. Lee, T. X. Phuoc, and M. K. Chyu, “Fluid filtration and rheological properties of nanoparticle additive and intercalated clay hybrid bentonite drilling fluids,” *J. Pet. Sci. Eng.*, vol. 127, pp. 338–346, 2015.
- [32] C. Bose, G. A., F. B., and J. T. and B. R., “Nano-proppants for Fracture conductivity Improvement and fluid loss Reduction,” in Paper SPE 174037 was presented at the SPE Western Regional Meeting, 2015.
- [33] A. M. Shehata and H. A. Nasr-el-din, “Zeta Potential Measurements : Impact of Salinity on Sandstone Minerals,” in Paper SPE 173763 was presented at the SPE International Symposium on Oilfield Chemistry, 2015.
- [34] S. Kakadjian, F. Zamora, and J. Venditto, “Zeta Potential Altering System for Increased Fluid Recovery , Production , and Fines Control,” in Paper SPE 106112 was presented at the SPE International Symposium on Oilfield Chemistry, 2007.
- [35] M. Ahmadi, A. Habibi, P. Pourafshary, and S. Ayatollahi, “Zeta Potential Investigation and Mathematical Modeling of Nanoparticles Deposited on the Rock Surface to Reduce Fine Migration,” in Paper SPE 142633 was Presented at the SPE Middle East Oil and Gas, 2011.
- [36] R. Marsalek, “Particle size and Zeta Potential of ZnO,” *Procedia - Soc. Behav. Sci.*, vol. 9, pp. 13–17, 2014.
- [37] M. Schembre, J. and R. Kovscek, A., “Mechanism of Formation Damage at Elevated Temperature,” *J. Energy Resour. Technol.*, vol. 127, no. September 2005, pp. 171–180, 2005.

- [38] P. Moulin and H. Roques, "Zeta potential measurement of calcium carbonate," vol. 261, pp. 115–126, 2003.
- [39] Vernhet, "Bellon-Fontaine," *Phys.*, vol. 91, 1994.
- [40] A. Revil, P. A. Pezard, and Glover, P., W., J., "Streaming potential in porous media 1 . Theory of the zeta potential," vol. 104, pp. 21–31, 1999.
- [41] R. a. Shawabkeh, M. Al-Harthi, and S. M. Al-Ghamdi, "The Synthesis and Characterization of Microporous, High Surface Area Activated Carbon from Palm Seeds," *Energy Sources*, vol. 103, no. 36, pp. 93–103, 2014.
- [42] I. A. El-Monier and H. A. Nasr-El-Din, "An Al/Zr-Based Clay Stabilizer for High pH Applications," *J. Energy Resour. Technol.*, vol. 135, no. 2, pp. 1–7, 2013.
- [43] Center NBTC (Nanobiology), "Zeta Potential An Introduction in 30 Minutes," Technical Notes. 2003.
- [44] S. Salgin, U. Salgin, and S. Bahadir, "Zeta potentials and isoelectric points of biomolecules: The effects of ion types and ionic strengths," *Int. J. Electrochem. Sci.*, vol. 7, no. 12, pp. 12404–12414, 2012.
- [45] L. Pauling, *The Nature of the Chemical Bond*, Cornell Univ., 3rd ed. USA, 1960.
- [46] S. M. Elkatatny and H. A. Nasr-El-Din, "Efficiency of removing filter cake of water-based drill-in fluid using chelating agents utilizing a CT method," in *Society of Petroleum Engineers - SPE Deepwater Drilling and Completions Conference 2012*.
- [47] M. Mahmoud, H. Nasr-El-Din, C. De Wolf, and J. LePage, "Optimum Injection Rate of A New Chelate That Can Be Used To Stimulate Carbonate Reservoirs," *SPE J.*, vol. 16, no. 4, 2011.
- [48] M. A. Mahmoud, H. A. Nasr-El-Din, C. A. De Wolf, J. N. LePage, and J. H. Bemelaar, "Evaluation of a New Environmentally Friendly Chelating Agent for High-Temperature Applications," *SPE J.*, no. September, pp. 559–574, 2011.
- [49] A. A. Jones, "Charges on the Surfaces of Two Chlorites," *Clay Miner.*, vol. 16, pp. 347–359, 1981.
- [50] H. Tan, W. Skinner, and J. Addai-Mensah, "PH-mediated interfacial chemistry and particle interactions in aqueous chlorite dispersions," *Chem. Eng. Res. Des.*, vol. 91, no. 3, pp. 448–456, 2013.
- [51] J. Zhong, H. Æ. Yu, F. Zhang, and Æ. L. Yi, "Electrokinetic properties of barite nanoparticles suspensions in different electrolyte media," pp. 9611–9616, 2007.
- [52] M. Bizi, "Stability and flocculation of nanosilica by conventional organic polymer," *Nat. Sci.*, vol. 04, no. 06, pp. 372–385, 2012.
- [53] C. Cho, J. W. Holmes, and J. R. Barber, "Determination of the charge Density of Silica Sols," vol. 29, no. 197027, pp. 496–501, 1992.

- [54] D. G. V. S. Caratzoulas, "M. Tsapatsis, J Phys. Chem. B." p. 10429, 2005.
- [55] V. Nikolakis, "Curr. Opin Coll. Interf. Sci." p. 203, 2005.
- [56] T. Kuzniatsova, Y. Kim, K. Shqau, P. K. Dutta, and H. Verweij, "Zeta potential measurements of zeolite Y: Application in homogeneous deposition of particle coatings," Microporous Mesoporous Mater., vol. 103, no. 1–3, pp. 102–107, 2007.
- [57] A. M. Paiaman, M. K. G. Al-askari, B. Salmani, M. Masihi, and B. D. Alanazi, "Effect of Drilling Fluid Properties on Rate of Penetration," Nafta, vol. 60, no. 3, pp. 129–134, 2009.
- [58] S. Ronald, P., Bernhard, B., "Rheological Properties of High-Temperature Drilling Fluids," Master thesis, 1981.
- [59] R. Azar, J., J., and Samuel G., Drilling Engineering. United States of America: Library of Congress Cataloging-in Publication Data, 1937.
- [60] S. Besun, N, Ozgiiclii, B, Peker, "Shear-dependent rheological properties of starch / bentonite composite gels," no. 275, pp. 567–579, 1997.
- [61] S. N. Jaisankar, D. Samanta, and P. Saravanan, "Water based polymer nanoclays composite coating rheology for leather applications," no. Biles 1986, pp. 1–7, 2015.

Vitae

Name	: Fahd Saeed Alakbari
Nationality	: Yemeni
Date of Birth	: 8/13/1985
Email	: Alakbarifahd@gmail.com
Address	: Yemen-Mukalla
Phone	: 0507738092
Academic Background	: B.Sc. Petroleum Engineering, February, 2012 : Master of Science, Petroleum Engineering, King Fahd University of Petroleum and Minerals, CGPA 3.469/4.0, January, 2017.
Experience	: Researcher, King Fahd University of Petroleum & Minerals (2014-2017). - Drilling and completion techniques. - Drilling and completion fluid. - Drilling fluid properties. - Prediction of Bubble Point Pressure Using Artificial Intelligence (AI) Base Model (Paper conference SPE- 184208-MS).